Proceedings of the

8th International Symposium on Vibrations of Continuous Systems

Whistler, British Columbia, Canada
17-23 July 2011

Preface

The International Symposium on Vibrations of Continuous Systems is a forum for leading researchers from across the globe to meet with their colleagues and present both old and new ideas on the field. Each participant has been encouraged to either present results of recent research or to reflect on some aspect of the vibration of continuous systems which is particularly interesting, unexpected or unusual. This type of presentation is meant to encourage participants to draw on understanding obtained through many years of research in the field.

The location for the 8th Symposium is the Olympic village of Whistler in British Columbia. Nestled between Whistler and Blackcomb Mountains, this venue provides a spectacular backdrop and the opportunity to easily explore the mountains, lakes and rivers nearby.

This Proceedings contains short summaries of the presentations to be made at the Symposium as well as short biographical sketches of the authors.

Mark S. Ewing
General Chairman

Yoshi Narita
Editorial Chairman

Arthur Leissa
Honorary Chairman

Table of Contents

Presentation Summaries

Biosketches

Presentation Summaries

Applications of Steady-State Modal Data for a Piezoelectric Waveguide with a General Cross-Section

Hao Bai

Mechanical Engineering Department
Lakehead University
Thunder Bay, Ontario, Canada

Ertugrul Taciroglu and Stanley B. Dong

Civil and Environmental Engineering Department
University of California
Los Angeles, California, 90095-1593, USA

We are concerned with a prismatic cylinder of general cross-sectional shape as well as in its composition of any number of distinct piezoelectric materials. The materials comprising the cross-section are assumed to be perfectly bonded to each other at contiguous interfaces. The governing equations of motion are based on finite element modeling of the cross-section, but leaving the axial dependence and time undetermined at the outset; this method of derivation is known as *semi-analytical finite elements*. The spectral decomposition of the governing differential operator yields a complete set of modal data, that consist of all propagating modes as well as edge vibrations for the cylinder. Herein, we utilize these modal data (1) to study reflection of an incoming monochromatic wave reflections at the free end of a semi-infinitely long prismatic beam and (2) to construct a steady-state Green's function.

Governing Equations

The semi-analytical finite element equations of motion for free vibration are

$$\mathbf{K}_1\mathbf{V},_{zz} - \mathbf{K}_2\mathbf{V},_{z} - \mathbf{K}_3\mathbf{V} - \mathbf{M}\ddot{\mathbf{V}} = \mathbf{0} \tag{1}$$

where $\mathbf{M}$ - mass matrix obtained by assembly over the N elements of the finite element model of the cross-section, and $\mathbf{K}_i$ $(i = 1, 2, 3)$ - the assembled stiffness operators and $\mathbf{V}$ - assembled nodal displacement components (u, v, w) and electric potential ϕ. The $\mathbf{K}_i$ $(i = 1, 2, 3)$ and $\mathbf{M}$ matrices are formulated by modeling the behavior in the discretized cross-section by two-dimensional (x, y) interpolations leaving the axial dependence z and time t unspecified at the outset. We note that $\mathbf{M}$, $\mathbf{K}_1$ and $\mathbf{K}_3$ are symmetric, while $\mathbf{K}_2$ is antisymmetric.

Wavelike Solutions

Using $\mathbf{V} = \mathbf{V}_0 e^{i(\omega t + kz)}$ as the free vibration solution form in Eq. (1) gives

$$\left[-k^2\mathbf{K}_1\mathbf{V}_o - ik\mathbf{K}_2\mathbf{V}_0 - \mathbf{K}_3\mathbf{V}_0 + \omega^2\mathbf{M}\mathbf{V}_0\right]e^{i(\omega t+kz)} = 0 \tag{2}$$

As $e^{i(\omega t+kz)}$ is never zero for all z's and t's, the bracketed expression representing a two-parameter algebraic eigensystem must vanish. Depending on the choice of eigenparameter for this problem, data on either propagating waves or end modes are obtained.

Propagating Waves

Designating ω^2 as the eigenvalue and employing real k's gives a complex (hermitian) algebraic system for propagating waves. This hermitian system can be rendered real by doubling its size, i.e.,

$$\begin{bmatrix} \mathbf{K_3} + k^2\mathbf{K_1} & -k\mathbf{K_2} \\ k\mathbf{K_2} & \mathbf{K_3} + k^2\mathbf{K_1} \end{bmatrix} \begin{Bmatrix} \mathbf{V_0} \\ -i\mathbf{V_0} \end{Bmatrix} = \omega^2 \begin{bmatrix} \mathbf{M} & \cdot \\ \cdot & \mathbf{M} \end{bmatrix} \begin{Bmatrix} \mathbf{V_0} \\ -i\mathbf{V_0} \end{Bmatrix} \tag{3}$$

where real symmetric positive-definite (except for $k = 0$) matrices occur on both sides. Therefore, real ω_i's are anticipated.

End Modes

Opting for k as the eigenvalue, assigning real ω^2 and inverting $\mathbf{K}_1$ in the bracketed expression in Eq. (2) leads to

$$k^2\mathbf{V}_0 + ik\mathbf{K}_1^{-1}\mathbf{K}_2\mathbf{V}_0 + \mathbf{K}_1^{-1}\left(\mathbf{K}_3 - \omega^2\mathbf{M}\right)\mathbf{V}_0 = 0 \tag{4}$$

This complex eigenproblem can be converted to real form by first introducing $\gamma = ik$, defining $\mathbf{V}_1 = \gamma\mathbf{V}_0$ and then doubling its size.

$$\begin{bmatrix} \cdot & \mathbf{I} \\ \mathbf{K}_1^{-1}(\mathbf{K}_3 - \omega^2\mathbf{M}) & \mathbf{K}_1^{-1}\mathbf{K}_2 \end{bmatrix} \begin{Bmatrix} \mathbf{V}_0 \\ \mathbf{V}_1 \end{Bmatrix} = \gamma \begin{Bmatrix} \mathbf{V}_0 \\ \mathbf{V}_1 \end{Bmatrix} \tag{5}$$

This eigenproblem admits both real and complex conjugate eigenvalues describing what are called *end modes*, where their amplitudes regress exponentially or damped sinusoidally into its interior from the free end of a semi-infinitely long cylinder. Real eigenvalues γ's describe monotonic exponential decay, while complex eigenvalues γ's involve sinusoidal decay. The special case of γ being purely imaginary, so that the corresponding k is real, portrays a propagating wave and does not fit the description of an end mode; but they are part of the eigendata of system (5). Right- and left-handed eigenvectors ϕ_i's and ψ_i's, can be extracted from this system. They satisfy a bi-orthogonality relation.

Reflection of Monochromatic Waves at Free End of a Piezoelectric Beam

The end mode eigendata can be used to construct the reflected wave caused by a steady monochromatic wave impinging upon the free end of a semi-infinitely long piezoelectric beam. For an incident wave originating from $z = +\infty$, the reflected wave has the form

$$V_{refl}(z,t) = \sum_{n=1}^{N} a_n \phi_n e^{i(k_n z - \omega t)} \tag{6}$$

Using a sufficient number of end modes including all possible propagating waves for the reflected wave, it is possible to enforce traction-free conditions at the free end on a least-squares basis. Some examples will be given.

Steady-State Green's Function

Given a steady-state point load F at an arbitrary location (x_o, y_o, z_o), a Fourier transform of it in z gives $\bar{f}(x_o, y_o)$. The Green's function is found by some summation involving the aforementioned right eigenvectors together with an inverse Fourier transform. The solution is

$$V(z) = \frac{1}{2\pi} \sum_{n=1}^{2N} \int_{-\infty}^{+\infty} \frac{\psi_n^T \bar{f}}{B_n(k - k_n)} \phi_n e^{ikz} dk \tag{7}$$

For transformed variables independent of wave number k (i.e., the usual case), application of the Cauchy residue theorem yields the modal response. As the eigendata can be divided into two sets of waves, along the positive and negative z-direction, the solution can be written as

$$V(z) = i \sum_{k \in k_n^+} \frac{\psi_n^T \bar{f}}{B_n(k - k_n)} \phi_n e^{-ik_n z} + i \sum_{k \in k_n^-} \frac{\psi_n^T \bar{f}}{B_n(k - k_n)} \phi_n e^{ik_n z} \tag{8}$$

The convergence and accuracy of the summation was discussed for beams having different electric surface conditions. Both the mechanical load and electric charge are used as sources in this study.

Advances in dynamic stiffness plate elements for free vibration analysis of isotropic plates and stringer panels with mass and spring attachments

M. Boscolo, F. A. Fazzolari and J. R. Banerjee
School of Engineering and Mathematical Sciences, City University London, EC1V 0HB, UK

1 Introduction

Free vibration analysis of thin-walled structures plays an important role in aeronautical as well as naval and automobile design, amongst others. For instance, aircraft wings and fuselages are idealised as assemblies of thin skin reinforced by stringers. These structures are modelled as plate assemblies and often investigated by using the finite element method (FEM). One of the main advantages of using the FEM is that it can handle structures with complex geometry and the results generally converge to the exact ones with increasing number of elements. Nevertheless, FEM is an approximate method, requiring considerable computational power (e.g. analysis time, pre and post-processing time, storage requirement etc.) and modelling efforts. The accuracy of the FEM solution cannot be always guaranteed. This is particulary true for free vibration analysis at high frequencies. Although often overlooked, there is a much better method for free vibration analysis which is that of the dynamic stiffness method (DSM). The DSM gives exact results because the equations of motion are solved in closed analytical form when deriving the element properties. It should be noted that the DSM has been extensively developed for bars and beams at present [1, 2]. The extension of the DSM to plate elements is difficult, but indeed, very essential to model complex structures. Wittrick and Williams [3] are known to be the first who attempted the extension of DSM to plate elements. Their novel formulation is interesting and relies on extensive use of complex algebra. However, the effects of shear deformation and rotatory inertia were neglected in their analysis so that their DSM was entirely based on simple classical plate theory (CPT). They implemented their work in a computer program called VICONOPT [1, 3, 4] which has been extensively tested, validated and used for research both by the academia and the industry. The dynamic stiffness (DS) formulation for plates given by Wittrick and Williams [3, 4] is not suitable for analysing thick plates because of their CPT assumption. To circumvent this problem, Wittrick and Williams' work has recently been enhanced by the first and the third authors [5] of this paper as they included the important effects of shear deformation and rotatory inertia in their formulation. Also, during their investigation for in-plane free vibration, a special set of solutions for plates that was missed by Wittrick and Williams [1] was brought to light [6], illustrating significant results. In this paper, both the in plane and out of plane DS matrices using first order shear deformation theory (FSDT) are essentially assembled using necessary features such as element rotation, offset connection etc to carry out free vibration analysis of structures. For illustrative purposes, the free vibration analysis of a stringer panel is used as a classic example and the results are compared with those obtained from the FEM analysis through the application of NASTRAN. By carrying out a detailed parametric study, further results are presented to demonstrate the effects of spring and mass attachments on the free vibration characteristics of plates for different boundary conditions.

2 Theory

A general procedure for the dynamic stiffness formulation of a structural element can be summarised as follows: (i) Obtain the differential equations of motion and the natural boundary conditions for the problem by applying Hamilton's principle, (ii) Solve the differential equations in closed analytical form, (iii) Apply general boundary condition for forces and displacements at the chosen nodes, (iv) Eliminate the integration constants to relate the amplitudes of harmonically varying forces to the corresponding displacements. In general, when exact natural frequencies and mode shapes are sought through the use of analytical solutions, but without resorting to DSM, particular boundary conditions are applied and the frequency equation is obtained by eliminating the integration constants. This is termed as the classical method [7, 8] which is restricted to special cases. In the DSM development, general boundary conditions in algebraic form are applied, leading to a DS element which can be assembled in global coordinates to form the DS matrix of the complete structure. In essence, the global DS matrix contains implicity all the natural frequency information of the structure.

The out-of-plane DS matrix for a plate element with the effects of shear deformation and rotatory inertia obtained in [5] is combined with the inplane DS matrix [6] to give the following relationship:

$$\begin{bmatrix} \mathcal{N}_{xx_1} \\ \mathcal{N}_{xy_1} \\ \mathcal{Q}_{x_1} \\ \mathcal{M}_{xx_1} \\ \mathcal{M}_{xy_1} \\ \mathcal{N}_{xx_2} \\ \mathcal{N}_{xy_2} \\ \mathcal{Q}_{x_2} \\ \mathcal{M}_{xx_2} \\ \mathcal{M}_{xy_2} \end{bmatrix} = \begin{bmatrix} s_{nn} & s_{nl} & 0 & 0 & 0 & f_{nn} & f_{nl} & 0 & 0 & 0 \\ & s_{ll} & 0 & 0 & 0 & -f_{nl} & f_{ll} & 0 & 0 & 0 \\ & & s_{qq} & s_{qm} & s_{qt} & 0 & 0 & f_{qq} & f_{qm} & f_{qt} \\ & & & s_{mm} & s_{mt} & 0 & 0 & -f_{qm} & f_{mm} & f_{mt} \\ & & & & s_{tt} & 0 & 0 & f_{qt} & -f_{mt} & f_{tt} \\ & & & & & s_{nn} & -s_{nl} & 0 & 0 & 0 \\ & & & Symmetric & & & s_{tl} & 0 & 0 & 0 \\ & & & & & & & s_{qq} & -s_{qm} & s_{qt} \\ & & & & & & & & s_{mm} & -s_{mt} \\ & & & & & & & & & s_{tt} \end{bmatrix} \begin{bmatrix} U_1 \\ V_1 \\ W_1 \\ \Phi_{y_1} \\ \Phi_{x_1} \\ U_2 \\ V_3 \\ W_2 \\ \Phi_{y_2} \\ \Phi_{x_2} \end{bmatrix} \tag{1}$$

The sign conventions for forces and displacements are shown in Figure 1. The above DS element can be rotated and/or offset by using transformation matrices to assemble the global DS matrix of the final structure. (The assembly procedure in DSM is similar to that of the FEM.) Once the global DS matrix of the structure is formed, the best way to solve the eigen-value problem to yield natural frequencies, is to apply the Wittrick and Williams algorithm [9]. The mode shapes are then routinely computed by using the global DS matrix and setting the force vector to zero with a nodal displacements given an arbitrary value. Care must be exercised when deciding the arbitrarily chosen nodal displacement because mode shapes can be dominated by either in plane displacements or out of plane displacements.

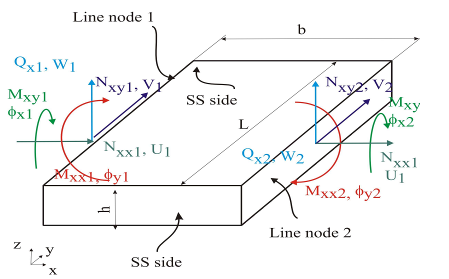

Figure 1: Edge conditions of the plate element and sign conventions

3 Preliminary results

The DSM developed in this paper has been used to carry out the free vibration analysis of a stringer panel which has a width $b = 1$ m, thickness $h = 0.002$ m and length $L = 1$ m. The stringer is located in the middle of the plate. The web of the stringer is 0.2 m high and its flange is 0.1 m long. The plate is made of aluminium with density $\rho = 2800$ kg/m^3, Young's modulus $E = 72$ GPa, and Poisson's ratio $\nu = 0.3$. A schematic view is shown in Figure 2. The first 8 natural frequencies were computed using the present theory and are compared with the results obtained by the FEM software NASTRAN using two different mesh sizes. These are shown in Table 1. The first and the fifth mode shapes are shown in Figure 3. The error in the FEM analysis is relatively small for all the natural frequencies except one. Increasing the number of elements increases the accuracy for most of the cases. Note that the FEM solution does not rapidly converge to the exact one in some cases. As can be seen in Table 1, the fifth mode shows comparatively larger error. It corresponds to a local mode of the flange, indicating that the FEM provides less accuracy in determining local modes.

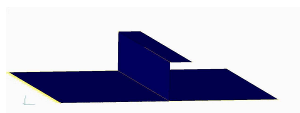

Figure 2: Stringer panel geometry

An exhaustive set of results is presented in the full paper which deals with spring and mass attachments at critical locations of a plate to illustrate their effects on its natural frequencies and mode shapes. Such a parametric study offers considerable benefits to the designers to solve frequency attenuation problem when avoidance of certain natural frequencies becomes necessary.

4 Concluding remarks

Table 1: First 8 natural frequencies for the stringer panel with 4 sides simply supported.

	DSM	FEM, NASTRAN			
		20 ×2 0 mm		5×5 mm	
Mode	ω, rad/s	ω, rad/s	error %	ω, rad/s	error %
1	856.47	852.10	-0.51	852.44	-0.47
2	1029.31	1027.11	-0.21	1027.76	-0.15
3	1295.22	1292.02	-0.25	1294.86	-0.03
4	1441.73	1437.99	-0.26	1441.84	0.01
5	1713.85	1635.20	-4.59	1631.24	-4.82
6	2027.19	2020.93	-0.31	2027.35	0.01
7	2140.81	2133.14	-0.36	2141.38	0.03
8	2554.86	2535.98	-0.74	2542.94	-0.47

By applying the DSM for plate elements based on the first order shear deformation theory, benchmark solutions for simple and complex structures are obtained. The DS results can be used as an aid to validate FEM and other approximate methods. The investigation has confirmed that the DSM is a much faster and more accurate analysis tool than the traditional FEM.

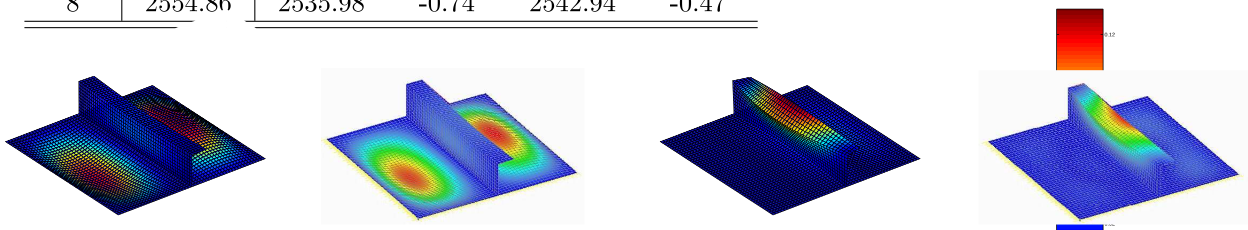

(a) Mode 1, DSM (b) Mode 1, FEM (c) Mode 5, DSM (d) Mode 5, FEM

Figure 3: Vibration mode comparison between DSM and FEM

References

[1] F. W. Williams and W. H. Wittrick. An automatic computational procedure for calculating natural frequencies of skeletal structures. *International Journal of Mechanical Sciences*, 12(9):781–791, 1970.

[2] J. R. Banerjee, C. W. Cheung, R. Morishima, M. Perera, and J. Njuguna. Free vibration of a three-layered sandwich beam using the dynamic stiffness method and experiment. *International Journal of Solids and Structures*, 44(22-23):7543–7563, 2007.

[3] W. H. Wittrick and F. W. Williams. Buckling and vibration of anisotropic or isotropic plate assemblies under combined loadings. *International Journal of Mechanical Sciences*, 16(4):209–239, 1974.

[4] F. W. Williams, D. Kennedy, R. Butler, and M. S. Anderson. VICONOPT: Program for exact vibration and buckling analysis or design of prismatic plate assemblies. *AIAA Journal*, 29:1927–1928, 1991.

[5] M. Boscolo and J. R. Banerjee. Dynamic stiffness elements and their applications for plates using first order shear deformation theory. *Computers and Structures*, 89:395–410, 2011.

[6] M. Boscolo and J. R. Banerjee. Dynamic stiffness method for exact inplane free vibration analysis of plates and plate assemblies. *Journal of Sound and Vibration*, 330(12):2928–2936, 2011.

[7] D.J. Gorman. Exact solutions for the free in-plane vibration of rectangular plates with two opposite edges simply supported. *Journal of Sound and Vibration*, 294(1-2):131 – 161, 2006.

[8] Y. F. Xing and B. Liu. New exact solutions for free vibrations of thin orthotropic rectangular plates. *Composite Structures*, 89(4):567–574, 2009.

[9] W. H. Wittrick and F. W. Williams. A general algorithm for computing natural frequencies of elastic structures. *Quarterly Journal of Mechanics and Applied Mathematics*, 24(3):263–284, 1970.

Three-dimensional natural frequency analysis of a piezoelectric plate by perturbation method

Piotr CUPIAŁ
Department of Process Control, Faculty of Mechanical Engineering and Robotics,
AGH University of Science and Technology, Kraków, Poland. Email: pcupial@agh.edu.pl

1. Introduction

The natural frequencies of a ceramic piezoelectric rectangular plate using three-dimensional formulation have been studied in Ref. [1]. In order to calculate the frequencies and the corresponding mode shapes, a set of coupled electromechanical governing equations has been solved there, under the corresponding mechanical and electrical boundary conditions. The present paper summarizes the use of a perturbation approach to the approximate calculation of a three-dimensional piezoelectric plate. A first-order perturbation solution is demonstrated to provide results that are accurate from the application point of view.

2. Formulation of the problem and the solution method

The governing equations of the free vibration of a three-dimensional piezoelectric plate have been discussed in Ref. [1]. They consist of four coupled equations with unknown displacements u_x, u_y, u_z and electrostatic potential ϕ. Assuming simply-supported boundary conditions along the four plate sides the solution is sought in the form:

$$\begin{Bmatrix} \bar{u}_x(\bar{x},\bar{y},\bar{z},\bar{t}) \\ \bar{u}_y(\bar{x},\bar{y},\bar{z},\bar{t}) \\ \bar{u}_z(\bar{x},\bar{y},\bar{z},\bar{t}) \\ \bar{\phi}(\bar{x},\bar{y},\bar{z},\bar{t}) \end{Bmatrix} = \begin{Bmatrix} X(\bar{z})\cos(m\pi\bar{x})\sin(n\pi\bar{y}) \\ Y(\bar{z})\sin(m\pi\bar{x})\cos(n\pi\bar{y}) \\ Z(\bar{z})\sin(m\pi\bar{x})\sin(n\pi\bar{y}) \\ \Phi(\bar{z})\sin(m\pi\bar{x})\sin(n\pi\bar{y}) \end{Bmatrix} \sin(\bar{\omega}\bar{t}). \tag{1}$$

The bar over a symbol stands for a non-dimensional quantity. Using the form of solution (1), the coupled equations of free vibration have the following form:

$$\begin{aligned}&(\bar{c}_{11}m^2\pi^2 + \bar{c}_{66}r^2n^2\pi^2)X(\bar{z}) - \bar{c}_{44}\xi^2X''(\bar{z}) + (\bar{c}_{12}+\bar{c}_{66})rmn\pi^2Y(\bar{z}) \\ &-(\bar{c}_{13}+\bar{c}_{44})\xi m\pi Z'(\bar{z}) - (\bar{e}_{15}+\bar{e}_{31})\xi m\pi\Phi'(\bar{z}) = \bar{\omega}^2X(\bar{z}),\end{aligned} \tag{2a}$$

$$\begin{aligned}&(\bar{c}_{12}+\bar{c}_{66})rmn\pi^2X(\bar{z}) + (\bar{c}_{66}m^2\pi^2 + \bar{c}_{11}r^2n^2\pi^2)Y(\bar{z}) - \bar{c}_{44}\xi^2Y''(\bar{z}) \\ &-(\bar{c}_{13}+\bar{c}_{44})r\xi n\pi Z'(\bar{z}) - (\bar{e}_{15}+\bar{e}_{31})\xi rn\pi\Phi'(\bar{z}) = \bar{\omega}^2Y(\bar{z}),\end{aligned} \tag{2b}$$

$$\begin{aligned}&(\bar{c}_{13}+\bar{c}_{44})\xi m\pi X'(\bar{z}) + (\bar{c}_{13}+\bar{c}_{44})\xi rn\pi Y'(\bar{z}) + \bar{c}_{44}(m^2\pi^2 + r^2n^2\pi^2)Z(\bar{z}) \\ &-\bar{c}_{33}\xi^2Z''(\bar{z}) + \bar{e}_{15}(m^2\pi^2 + r^2n^2\pi^2)\Phi(\bar{z}) = \bar{\omega}^2Z(\bar{z}),\end{aligned} \tag{2c}$$

$$\begin{aligned}&\xi^2\Phi''(\bar{z}) - \frac{\bar{\kappa}_{11}}{\bar{\kappa}_{33}}(m^2\pi^2 + r^2n^2\pi^2)\Phi(\bar{z}) = -\mu[(\bar{e}_{15}+\bar{e}_{31})\xi m\pi X'(\bar{z}) \\ &+(\bar{e}_{15}+\bar{e}_{31})r\xi n\pi Y'(\bar{z}) + \bar{e}_{15}(m^2\pi^2 + r^2n^2\pi^2)Z(\bar{z}) - \bar{e}_{33}\xi^2Z''(\bar{z})].\end{aligned} \tag{2d}$$

The non-dimensional quantities in Eqs. (1) and (2) are defined as follows:

$$
\begin{aligned}
&\bar{x}=\frac{x}{a},\quad \bar{y}=\frac{y}{b},\quad \bar{z}=\frac{z}{h},\quad \bar{u}_x=\frac{u_x}{h},\quad \bar{u}_y=\frac{u_y}{h},\quad \bar{u}_z=\frac{u_z}{h},\quad r=\frac{a}{b},\quad \xi=\frac{a}{h},\\
&\bar{c}_{11}=\frac{c_{11}}{c_{\mathrm{ref}}},\quad \bar{c}_{12}=\frac{c_{12}}{c_{\mathrm{ref}}},\quad \bar{c}_{13}=\frac{c_{13}}{c_{\mathrm{ref}}},\quad \bar{c}_{33}=\frac{c_{33}}{c_{\mathrm{ref}}},\quad \bar{c}_{44}=\frac{c_{44}}{c_{\mathrm{ref}}},\quad \bar{c}_{66}=\frac{c_{66}}{c_{\mathrm{ref}}},\\
&\bar{e}_{15}=\frac{e_{15}}{e_{\mathrm{ref}}},\quad \bar{e}_{31}=\frac{e_{31}}{e_{\mathrm{ref}}},\quad \bar{e}_{33}=\frac{e_{33}}{e_{\mathrm{ref}}},\quad \bar{\kappa}_{11}=\frac{\kappa_{11}c_{\mathrm{ref}}}{(e_{\mathrm{ref}})^2},\quad \bar{\kappa}_{33}=\frac{\kappa_{33}c_{\mathrm{ref}}}{(e_{\mathrm{ref}})^2},\\
&\bar{\phi}=\frac{\phi e_{\mathrm{ref}}}{h\,c_{\mathrm{ref}}},\quad \bar{\omega}=\omega a\sqrt{\frac{\rho}{c_{\mathrm{ref}}}},\quad \bar{t}=\frac{t}{a}\sqrt{\frac{c_{\mathrm{ref}}}{\rho}}.
\end{aligned}
\tag{3}
$$

The values of the material constants have been specified in Ref. [1], and the following reference values will be used: $c_{ref}=c_{11}, e_{ref}=e_{33}$. In addition, a small parameter $\mu=1/\bar{\kappa}_{33}$ enters Eq. (2d).

It is assumed that no surface tractions are applied to the plate faces and that the faces are electrically short-circuited, in which case the boundary conditions on the plate faces ($\bar{z}=0$ and $\bar{z}=1$) are written as follows:

$$
\begin{aligned}
&\xi X'(\bar{z})+m\pi Z(\bar{z})=0,\quad \xi Y'(\bar{z})+rn\pi Z(\bar{z})=0,\\
&-\bar{c}_{13}[m\pi X(\bar{z})+rn\pi Y(\bar{z})]+\bar{c}_{33}\xi Z'(\bar{z})+\bar{e}_{33}\xi\Phi'(\bar{z})=0,\quad \Phi(\bar{z})=0.
\end{aligned}
\tag{4}
$$

In order to transform the problem to a standard form used in perturbation analysis, a new function $\hat{Z}(\bar{z})$ is defined:

$$
Z(\bar{z})=\hat{Z}(\bar{z})+p(\bar{z}),\qquad p(\bar{z})=a_1\bar{z}+a_2\bar{z}^2+a_3\bar{z}^3,
\tag{5}
$$

where: $a_1=-\frac{\bar{e}_{33}}{\bar{c}_{33}}\Phi'(0),\quad a_2=\frac{\bar{e}_{33}}{\bar{c}_{33}}\left[2\Phi'(0)+\Phi'(1)\right],\quad a_3=-\frac{\bar{e}_{33}}{\bar{c}_{33}}\left[\Phi'(0)+\Phi'(1)\right].$

With this transformation, the electrostatic potential is removed from the third of boundary conditions (4), whereas the form of the remaining boundary conditions is unchanged. When expressed in terms of $\hat{Z}(\bar{z})$, the first three boundary conditions are those of an elastic plate without piezoelectric coupling. The governing equations, when expressed in terms of $\hat{Z}(\bar{z})$, contain the polynomial $p(\bar{z})$ and its derivatives up to the second order.

According to the perturbation method the functions $X(\bar{z}),Y(\bar{z}),\hat{Z}(\bar{z}),\Phi(\bar{z})$ are expanded in series of the small parameter μ:

$$
\begin{aligned}
&X(\bar{z})=X^{(0)}(\bar{z})+\mu X^{(1)}(\bar{z})+\ldots,\quad Y(\bar{z})=Y^{(0)}(\bar{z})+\mu Y^{(1)}(\bar{z})+\ldots\\
&\hat{Z}(\bar{z})=\hat{Z}^{(0)}(\bar{z})+\mu\hat{Z}^{(1)}(\bar{z})+\ldots,\quad \Phi(\bar{z})=\mu\Phi^{(1)}(\bar{z})+\mu^2\Phi^{(2)}(\bar{z})+\ldots\\
&p(\bar{z})=\mu p^{(1)}(\bar{z})+\mu^2 p^{(2)}(\bar{z})+\ldots
\end{aligned}
\tag{6}
$$

It is to be noted that the power series that defines $\Phi(\bar{z})$ begins with the first power of the small parameter μ, in consistency with Eq. (2d).

The zero-order approximation is obtained by solving the problem of the free vibration of an anisotropic elastic plate. In this way, the eigenvalues $\lambda_{mn}^{(0)} = (\overline{\omega}_{mn}^{(0)})^2$ are found together with the corresponding mode shapes. The first-order potential term $\Phi^{(1)}(\overline{z})$ is then obtained using the equation:

$$\xi^2 \Phi^{(1)''}(\overline{z}) - \frac{\overline{\kappa}_{11}}{\overline{\kappa}_{33}}(m^2\pi^2 + r^2 n^2 \pi^2)\Phi^{(1)}(\overline{z}) = -[(\overline{e}_{15} + \overline{e}_{31})\xi m\pi X^{(0)'}(\overline{z}) + (\overline{e}_{15} + \overline{e}_{31}) r\xi n\pi Y^{(0)'} + \overline{e}_{15}(m^2\pi^2 + r^2 n^2\pi^2)\hat{Z}^{(0)}(\overline{z}) - \overline{e}_{33}\xi^2 \hat{Z}^{(0)''}(\overline{z})]. \tag{7}$$

Having solved Eq. (7) for $\Phi^{(1)}(\overline{z})$, one can determine the first-order perturbation operator in Eqs. (2a-c). The eigenvalue including the first-order correction: $\lambda_{mn} \cong \lambda_{mn}^{(0)} + \mu\lambda_{mn}^{(1)}$ can be calculated by making direct use of the generalized eigenvalue problem perturbation formulas, discussed in Ref. [2].

3. Numerical results

By way of illustration, Table 1 shows the natural frequencies of an elastic plate (zero-order approximation). The results that include the first-order correction are shown in Table 2. For comparison, exact values taken from Ref. [1], obtained using the coupled electromechanical solution, are shown in Table 2 in parentheses. By including the first-order correction, the relative error is reduced from about –11% (zero-order approximation) to about –1.5%, for the material constants typical of PZT4, for which $\mu = 0.2579$. Considerable increase in accuracy can therefore be achieved using first-order perturbation analysis. Higher order perturbation terms are being studied now using the above approach.

Table1: Lowest non-dimensional circular frequencies of a rectangular plate with $r = a/b = 2$ and $\xi = a/h = 100$. The case of elastic plate without electromechanical coupling (zero-order aproximation).

m \ n	1	2	3
1	$\overline{\omega}_{11}^{(0)} = 0.1144$	$\overline{\omega}_{12}^{(0)} = 0.3887$	$\overline{\omega}_{13}^{(0)} = 0.8430$
2	$\overline{\omega}_{21}^{(0)} = 0.1828$	$\overline{\omega}_{22}^{(0)} = 0.4564$	$\overline{\omega}_{23}^{(0)} = 0.9101$
3	$\overline{\omega}_{31}^{(0)} = 0.2969$	$\overline{\omega}_{32}^{(0)} = 0.5695$	$\overline{\omega}_{33}^{(0)} = 1.022$

Table 2: First-order perturbation solution. Exact values after Ref. [1] are given in parentheses.

m \ n	1	2	3
1	$\overline{\omega}_{11} = 0.1266$ (0.1287)	$\overline{\omega}_{12} = 0.4301$ (0.4368)	$\overline{\omega}_{13} = 0.9331$ (0.9476)
2	$\overline{\omega}_{21} = 0.2023$ (0.2056)	$\overline{\omega}_{22} = 0.5052$ (0.5132)	$\overline{\omega}_{23} = 1.008$ (1.023)
3	$\overline{\omega}_{31} = 0.3286$ (0.3338)	$\overline{\omega}_{32} = 0.6306$ (0.6405)	$\overline{\omega}_{33} = 1.132$ (1.149)

References

1. Cupiał P., Three-dimensional natural vibration analysis and energy considerations for a piezoelectric rectangular plate, *Journal of Sound and Vibration*, 283, 2005, 1093-1113.
2. Kato T., *Perturbation Theory for Linear Operators*, Springer-Verlag, Berlin, 1966.

Free vibration of laminated plates by a variable-kinematic Chebyshev-Ritz method

Lorenzo Dozio
Department of Aerospace Engineering, Politecnico di Milano, Italy

Erasmo Carrera
Department of Aeronautics and Space Engineering, Politecnico di Torino, Italy

Introduction. Laminated composite plates are widely used as structural components in many engineering applications. They are typically characterized by higher shear and normal flexibility than traditional isotropic plates and exhibit the so-called zig-zag form of displacement field in the thickness direction. Such properties, along with high degrees of orthotropy and moderate thickness-to-length ratios, put great difficulties in achieving accurate description of their mechanical behavior using classical plate theories. A considerable effort was thus made to derive refined 2-D modeling of multilayered structures, ranging from higher-order equivalent single layer (ESL) theories to layer-wise (LW) formulations [1]. At the same time related techniques that were suitable for computer implementation have been developed. In this context, a powerful approach, referred as Carrera's unified formulation (CUF), was introduced by the second author in the mid-nineties of the last century. It is a formal technique permitting to handle in an unified manner an infinite number of 2-D displacement-based or mixed ESL and LW axiomatic plate and shell theories with variable kinematic properties. CUF was successfully implemented to obtain Navier-type analytical solutions and finite element results for bending, buckling and vibration problems of transversely anisotropic structures.

Present study. Attention is focused in this study on extending CUF to the Ritz method for free vibration analysis of straight-sided quadrilateral laminated plates having an arbitrary combination of free, clamped and simply supported boundary conditions. It is widely recognized that the Ritz method has a high spectral accuracy and converge faster than local methods such as finite elements. Therefore, it can provide reliable upper-bound benchmark vibration results and can be quite suitable during preliminary design studies and/or parametric analyses. Contrary to all previous Ritz-based formulations relying on axiomatic plate models with a *fixed* kinematic theory, the present approach allows to generate arbitrarily accurate Ritz solutions from a large variety of higher-order ESL and LW theories by properly expanding so-called *Ritz fundamental nuclei* of the plate mass and stiffness matrices. The Ritz fundamental nuclei are invariant with respect to the order of theory and thus no *ad hoc* theoretical development and software coding is needed when the order is changed. Chebyshev polynomials multiplied by boundary functions are used here as admissible functions. The combination of formalism of CUF and Ritz expansion based on Chebyshev polynomials has been denoted as variable-kinematic Chebyshev-Ritz method.

Mathematical modeling. A general quadrilateral flat laminated plate of uniform thickness h and N_l orthotropic layers is considered. For generality and convenience, the formulation is expressed in dimensionless form. Thus, the actual quadrilateral plate in the $x-y$ physical domain is mapped into a square plate in the computational $\xi-\eta$ domain ($-1 \leq \xi, \eta \leq 1$). The constitutive equations of a generic layer k are written as:

$$\boldsymbol{\sigma}_p^k = \mathbf{C}_{pp}^k \boldsymbol{\epsilon}_p^k + \mathbf{C}_{pn}^k \boldsymbol{\epsilon}_n^k \qquad \boldsymbol{\sigma}_n^k = \mathbf{C}_{np}^k \boldsymbol{\epsilon}_p^k + \mathbf{C}_{nn}^k \boldsymbol{\epsilon}_n^k \tag{1}$$

where $\boldsymbol{\sigma}$ and $\boldsymbol{\epsilon}$ are the stresses and strains, split into in-plane (p) and out-of-plane (n) components, and matrices $\mathbf{C}$ contain the elastic coefficients. According to CUF and assuming harmonic motion with circular frequency ω, the displacement vector for each k-th lamina is expressed through an indicial notation over τ as follows:

$$\mathbf{u}^k(\xi, \eta, z, t) = F_\tau(z) \hat{\mathbf{u}}_\tau^k(\xi, \eta) e^{j\omega t} \tag{2}$$

where $\tau = t, r, b,\ r = 2, \ldots, N-1,\ F_\tau(z)$ are assumed thickness functions and N is the order of the theory. Note that in Eq. (2) the summation convention for repeated indices is implied. Strains are linearly related to displacements according to the following relations:

$$\boldsymbol{\epsilon}_\mathrm{p}^k = F_\tau(z) \mathbf{D}_\mathrm{p} \hat{\mathbf{u}}_\tau^k(\xi, \eta) e^{j\omega t} \qquad \boldsymbol{\epsilon}_\mathrm{n}^k = F_\tau(z) \mathbf{D}_\mathrm{n} \hat{\mathbf{u}}_\tau^k(\xi, \eta) e^{j\omega t} + F_{\tau,z}(z) \hat{\mathbf{u}}_\tau^k(\xi, \eta) e^{j\omega t} \tag{3}$$

where $\mathbf{D}_p$ and $\mathbf{D}_n$ are matrices of differential operators. Following the standard Ritz procedure and introducing another indicial notation over i, the components of the displacement amplitude vector $\hat{\mathbf{u}}_\tau^k(\xi, \eta)$ are approximated by sets of two-dimensional finite series as follows:

$$\hat{\mathbf{u}}_\tau^k(\xi, \eta) = \boldsymbol{\Phi}_{\tau i}(\xi, \eta) \mathbf{c}_{\tau i}^k \tag{4}$$

in which $i = 1, \ldots, M$ and $\boldsymbol{\Phi}_{\tau i}$ is a 3×3 diagonal matrix whose elements $\phi_{\alpha\tau i}(\xi, \eta)$ $(\alpha = u, v, w)$ are given by the product of a two-dimensional polynomial $p_i(\xi, \eta)$ and a boundary-compliant function $\phi_{\alpha\tau}^b(\xi, \eta)$ such that

$$\phi_{\alpha\tau i}(\xi, \eta) = \phi_{\alpha\tau}^b(\xi, \eta) p_i(\xi, \eta) = \phi_{\alpha\tau}^b(\xi, \eta) p_q(\xi) p_r(\eta) \tag{5}$$

$p_s(\chi) = \cos\left[(s-1)\arccos(\chi)\right]$, $(s = 1, 2, \ldots, P; \chi = \xi, \eta)$, is the 1-D s-th Chebyshev polynomial and the indices i, q and r are related by the following expression: $i = P(q-1)+r$. Using the above quantities, the maximum strain energy U_max and the maximum kinetic energy T_max of the plate vibrating harmonically are given by

$$U_\mathrm{max} = \frac{1}{2} \sum_{k=1}^{N_l} \mathbf{c}_{\tau i}^{k\mathrm{T}} \mathbf{K}_{k\tau sij} \mathbf{c}_{sj}^k \qquad T_\mathrm{max} = \frac{1}{2} \omega^2 \sum_{k=1}^{N_l} \mathbf{c}_{\tau i}^{k\mathrm{T}} \mathbf{M}_{k\tau sij} \mathbf{c}_{sj}^k \tag{6}$$

where

$$\begin{aligned}
\mathbf{K}_{k\tau sij} = \iint_{-1}^{+1} & \Big\{ \left(\mathbf{D}_p \boldsymbol{\Phi}_{\tau i}\right)^\mathrm{T} \left[E_{\tau s}^k \mathbf{C}_{pp}^k \left(\mathbf{D}_p \boldsymbol{\Phi}_{sj}\right) + E_{\tau s}^k \mathbf{C}_{pn}^k \left(\mathbf{D}_n \boldsymbol{\Phi}_{sj}\right) + E_{\tau s_{,z}}^k \mathbf{C}_{pn}^k \boldsymbol{\Phi}_{sj} \right] \\
& + \left(\mathbf{D}_n \boldsymbol{\Phi}_{\tau i}\right)^\mathrm{T} \left[E_{\tau s}^k \mathbf{C}_{np}^k \left(\mathbf{D}_p \boldsymbol{\Phi}_{sj}\right) + E_{\tau s}^k \mathbf{C}_{nn}^k \left(\mathbf{D}_n \boldsymbol{\Phi}_{sj}\right) + E_{\tau s_{,z}}^k \mathbf{C}_{nn}^k \boldsymbol{\Phi}_{sj} \right] \\
& + \boldsymbol{\Phi}_{\tau i}^\mathrm{T} \left[E_{\tau_{,z} s}^k \mathbf{C}_{np}^k \left(\mathbf{D}_p \boldsymbol{\Phi}_{sj}\right) + E_{\tau_{,z} s}^k \mathbf{C}_{nn}^k \left(\mathbf{D}_n \boldsymbol{\Phi}_{sj}\right) + E_{\tau_{,z} s_{,z}}^k \mathbf{C}_{nn}^k \boldsymbol{\Phi}_{sj} \right] \Big\} |\mathbf{J}| d\xi d\eta
\end{aligned} \tag{7}$$

$$\mathbf{M}_{k\tau sij} = \iint_{-1}^{+1} \boldsymbol{\Phi}_{\tau i}^\mathrm{T} E_{\tau s}^k \rho^k \boldsymbol{\Phi}_{sj} |\mathbf{J}| d\xi d\eta \tag{8}$$

are 3×3 matrices representing the *Ritz fundamental nuclei* of the formulation. In Eqs. (7,8) $|\mathbf{J}|$ is the determinant of the Jacobian matrix of the transformation and the following layer integrals are introduced: $E_{\tau s}^k = \int_k F_\tau F_s dz$, $E_{\tau s_{,z}}^k = \int_k F_\tau F_{s,z} dz$, $E_{\tau_{,z} s}^k = \int_k F_{\tau,z} F_s dz$, $E_{\tau_{,z} s_{,z}}^k = \int_k F_{\tau,z} F_{s,z} dz$. The global stiffness $\mathbf{K}$ and mass $\mathbf{M}$ matrix of the plate are obtained by first expanding at a layer level the fundamental nuclei through variation of the indices τ and s. The corresponding matrices at multilayer level are assembled according to the used variable descriptions. In the ESL case these matrices are simply summed, whereas LW models require continuity of displacement variables at the

Table 1: Comparison of the first four frequency parameters $\lambda = \omega h\sqrt{\rho^1/E_2^1}$ corresponding to some lower-order modes of a square simply-supported cross-ply $[0/90^o]$ plate with $h/b = 0.1$.

Mode (m,n)	Theory	1	2	3	4
(1,1)	Exact [2]	0.06027	0.52994	0.58275	1.23675
	ED6	0.06041	0.53404	0.58406	1.23887
	LD3	0.06027	0.52994	0.58275	1.23684
(1,2)(2,1)	Exact [2]	0.14539	0.62352	0.95652	1.23891
	ED6	0.14609	0.62470	0.96396	1.23980
	LD3	0.14539	0.62352	0.95653	1.23901
(2,2)	Exact [2]	0.20229	0.95796	1.03000	1.23958
	ED6	0.20344	0.96443	1.03280	1.24092
	LD3	0.20229	0.95796	1.03001	1.23969

Table 2: Comparison of the first eight frequency parameters $\lambda = \omega b^2/\pi^2 h\sqrt{\rho^1/E_2^1}$ for clamped anti-symmetric angle-ply $[45^o/-45^o/45^o/-45^o]$ rhombic composite laminates with $h/a = 0.1$.

Skew angle	Theory	Mode							
		1	2	3	4	5	6	7	8
30^o	Ref. [3]	2.6325	3.9549	4.7125	5.2107	6.3577	6.4954	6.9760	7.7176
	FSDT	2.7415	4.1217	4.9126	5.4393	6.6178	6.7834	7.2749	8.0387
	ED3	2.6332	3.9555	4.7116	5.2082	6.3554	6.4892	6.9684	7.7069
	LD2	2.5864	3.8889	4.6365	5.1223	6.2625	6.3891	6.8693	7.6034
45^o	Ref. [3]	3.3015	4.6290	5.8423	6.0039	7.0792	7.7269	8.2726	8.9874
	FSDT	3.4429	4.8218	6.0844	6.2411	7.3679	8.0201	8.6065	9.3235
	ED3	3.3029	4.6297	5.8393	6.0027	7.0710	7.7221	8.2560	8.9741
	LD2	3.2463	4.5577	5.7535	5.9219	6.9747	7.6256	8.1521	8.8731

interface. Finally, resulting matrices are expanded by varying the indices i, j related to the Ritz expansion. Matrices $\mathbf{K}$ and $\mathbf{M}$ have dimensions $3M(N+1) \times 3M(N+1)$ for ESL models and $[3(N+1)N_l - 3(N_l-1)]M \times [3(N+1)N_l - 3(N_l-1)]M$ for LW models. The extremization of the energy functional $\Pi = U_{\max} - T_{\max}$ with respect to the coefficients $\mathbf{c}_{\tau i}^k$ yields a standard generalized eigenvalue problem.

Results. Two preliminary results are here presented to show the applicability of the method. A square simply-supported cross-ply $[0/90^o]$ plate with thickness-to-length ratio 0.1 is first considered in Table 1. Ritz solutions obtained with a sixth-order ESL theory (ED6) and a third-order layer-wise theory (LD3) are compared against exact solutions from [2] for the first four frequency parameters $\lambda = \omega h\sqrt{\rho^1/E_2^1}$ corresponding to lower-order modes (1,1), (1,2)=(2,1) and (2,2). It is seen that very good agreement is obtained with LW models. A second example is shown in Table 2, where the first eight non-dimensional frequencies of clamped angle-ply $[45^o/-45^o/45^o/-45^o]$ rhombic composite laminates with $h/a = 0.1$ and two skew angles are presented. Numerical values computed from first-order shear deformation theory (FSDT), a third-order ESL theory (ED3) and a second-order layer-wise theory (LD2) are compared with finite element results from [3]. ED3 solutions agree with reference values. It is seen that more accurate results are obtained using a LW model.

References

[1] E. Carrera, Theories and finite elements for multilayered, anisotropic, composite plates and shells, *Archives of Computational Methods in Engineering*, 9 (2002), 87-140.

[2] W.Q. Chen, C.F. Lue, 3D free vibration analysis of cross-ply laminated plates with one pair of opposite edges simply supported, *Composite Structures*, 69 (2005), 77-87.

[3] A.K. Garg, R.K. Khare, T. Kant, Free vibration of skew fiber-reinforced composite and sandwich laminates using a shear deformable finite element model, *Journal of Sandwich Structures and Materials*, 8 (2006), 33-52.

On When Oscillatory Response of a Structural Element is Not Modal Response

Mark S. Ewing, Associate Professor
Himanshu Dande, Graduate Research Assistant
University of Kansas Aerospace Engineering

For a single degree of freedom oscillator, the concept of physical damping beyond the "critical damping" value is characterized by "overdamped" response behavior. For free vibration, this overdamped response to an initial disturbance results in no oscillatory behavior—which is the basic requirement of "vibration". For forced response, very high damping (even at levels somewhat less than critical damping) results in response levels less than the static (zero frequency) deflection, with no response "amplification" near the undamped natural frequency.

For continuous systems, the concept of overdamped response is more difficult to describe. Indeed, for continuous systems, the physics of vibration is in one way entirely different than for a single degree of freedom oscillator. That is, ***free*** vibration of structural elements can be described as the constructive interference of wave motion from a disturbance and the reflection of such wave motion from structural boundaries. If the damping is too great, however, traveling waves will dissipate before getting to a boundary. With no reflection, there is no modal response.

A heavily damped plate subjected to an impulsive excitation in the interior will sound "dead"—high frequency components of response are damped out before reflection, and only a low frequency "thud" survives as vibration—there is no "ringing". The same plate subjected to oscillatory excitation responds similarly: lower frequency "modes" may respond, but higher frequency modes cannot, because there is no reflection from boundaries to "set up" the higher frequency modes.

Recent experiments aimed at discovering the limits of applicability of damping estimation algorithms have brought to light some interesting behavior of plates as well as an explanation of when damping estimation fails ***in terms of*** the existence of true vibration.

Taking a viewpoint from room acoustics, a parallel with structural response within a closed domain (a structure or structural element) is made. Near a point source of sound—in the "near field"—the response an "ear" hears is dominated by the source. Far from the sound source—in the "far field"—the response is dominated by the reflections from the room walls. Therefore, in the far field, the state of sound is called a "reverberant field". At any given frequency, the degree of coherency is totally due to the geometry of the room and, when the coherency is high—at an essentially infinite number of natural frequencies—the response is manifested as acoustic modes of the room. In the case of structural vibration, for low levels of damping, nearly the entire structural element is in the reverberant field with respect to excitation at a point. At natural frequencies, the entire structural element responds in the natural modes of vibration.

Using statistical energy analysis, an estimate of the "radius of the near field" in a plate may be made by noting when the near field kinetic energy equals the kinetic energy in the far field. Lyon and DeJong have reported this radius to be:

$$r_D = \frac{\omega \eta M}{2\pi\rho c_g}$$

Here, ω is the radial frequency, η is the loss factor, M is the plate mass, ρ is the density and c_g is the group velocity in the plate.

In the reverberant field, the ***causal*** relationships on which modal analysis and modal testing are based exist. However, inside the near field, the response is ***not*** representative of the whole structure; rather, it is dependent on the local excitation, and not significantly dependent on the reflection of flexural waves from the boundaries. As such, damping estimation using the normal input-output (causal) relationships inside the near field—such as force-to-displacement frequency response functions—must fail. For high levels of damping, then, damping estimation algorithms based on input-output relationships including the popular, Impulse Response Decay Method (IRDM), modal curve-fitting and half-power bandwidth techniques must fail. Only output-only techniques such as the Random Decrement Method ***can*** work. In a recent study, the responses of three plates with loss factors 0.001 (0.1%), 0.01 (1%) and 0.1 (10%), subjected to a random force at a single point were *simulated* with a finite element model (although a continuous system model could have been used as easily). The resulting responses at up to 16 points on the plate were used to estimate the loss factor using the IRDM. The loss factor estimations for the two lower loss factors nearly perfectly matched the model loss factors. But, for the plate model with a 10% loss factor, serious errors occurred, especially at high frequencies, as shown, below, regardless of the number of responses used. Presumably, the problem was that many of the response points were inside the near field. [All estimations using the Random Decrement Method resulted in a match with the model loss factors.]

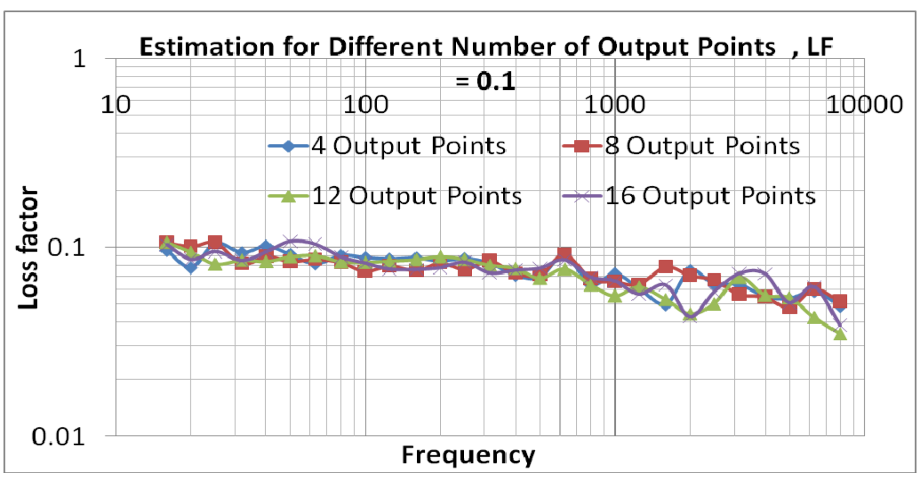

To shed some light on this, a steel plate completely treated with constrained layer damping has been subjected to sinusoidal mechanical excitation at a point to demonstrate the existence of the near- and far-fields observable in a highly-damped plate. The velocities of 4800 points on the plate were recorded using a scanning laser vibrometer.

Plots of the resulting kinetic energy of the plate are shown below. On these plots, a circle with radius predicted by the equation above (using estimates of the loss factor) is also shown, giving an indication of the close agreement between theory and experiment. Clearly, the radius of the near field decreases with frequency: higher frequency oscillations damp out in a shorter distance.

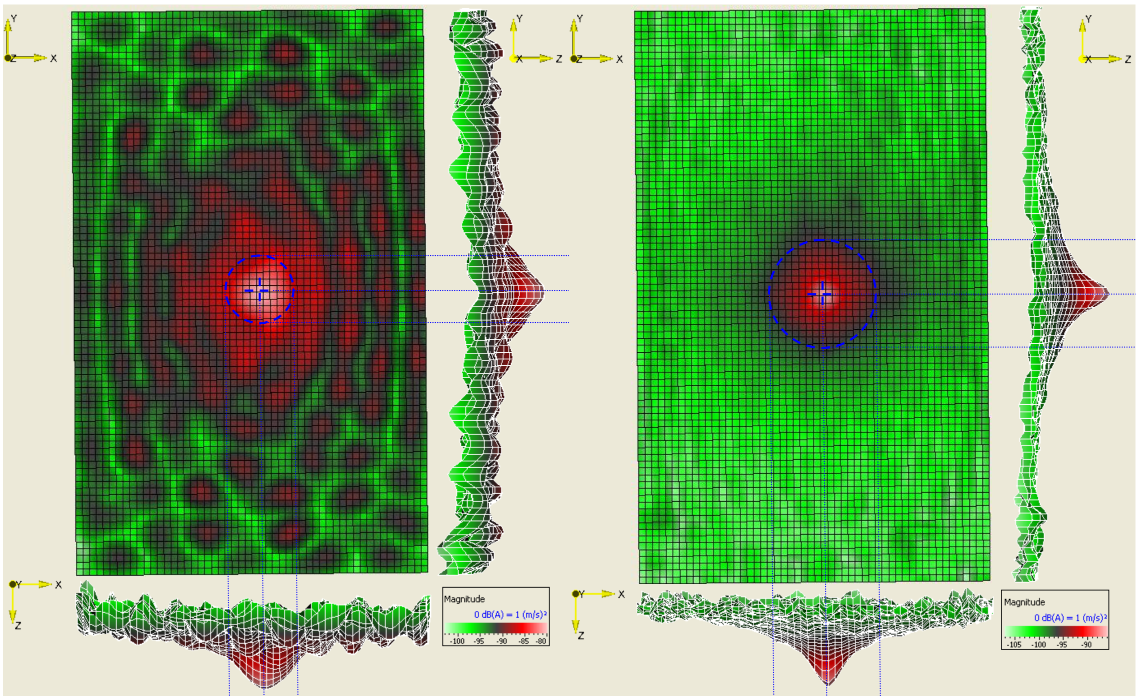

f = 1000 Hz, η = 0.08
r_D = 8.772 in.

f = 4000 Hz, η = 0.0625
r_D = 13.71 in.

The bottom line for damping estimation is that if one uses input-output relationships based on response outside the near field, accurate estimates result, because the input-output relationships are valid. If responses within the near field are used, the response is far greater than the input-output relationship would predict. Therefore, damping is underestimated: high response equals low damping. So, to carefully estimate structural damping, one must use an output-only-based algorithm or only use output measurements ***outside*** the near field. *Another* bottom line is that the observations made here were enabled by proper schooling in the vibrations of continuous systems ***and*** the duality of free vibrations with wave motion in a closed domain.

References

Lyon, R.H., and DeJong, R.G., *Theory and Application of Statistical Energy Analysis*, 2nd Edition, R H Lyon Group, 1998.

Ewing, M. S., Dande, H., and Vatti, K., "Validation of Panel Damping Loss Factor Estimation Algorithms Using a Computational Model", Proceedings, 50th AIAA Structures, Structural Dynamics and Materials Conference, Palm Springs, CA, May 2009.

Study on Vibration Design of Laminated Fibrous Composite Plates Reinforced by Short Fibers and Curvilinear Fibers

Shinya HONDA*[1] and Yoshihiro NARITA*[2]

*[1] Corresponding Author, Faculty of Engineering, Hokkaido University,
N13W8, Kita-ku, Sapporo, Hokkaido, 060-8628, Japan, honda@eng.hokudai.ac.jp
*[2] Hokkaido University, ynarita@eng.hokudai.ac.jp

1. Introduction

The present paper focuses on locally anisotropic structures which are often part of natural compounds. Natural compounds have local anisotropic properties distributed optimally throughout the compound to perform more effectively than homogenously anisotropic materials. It may then be hypothesized that if local anisotropy can be exploited in structural design, it would be possible to design more effective engineering structures. To realize local anisotropy with curvilinear fibers, fiber reinforced composites would be highly appropriate, especially with an innovative method that has recently been developed to produce composites with curvilinear fibers. The method is termed automated tow-placement technology [1]. An optimum curvilinear fiber shape is developed under continuous constraints on the fiber orientations, where the fiber shapes are expressed as projections of contour lines on a cubic polynomial surface. The results show that plates with curvilinear fibers result in higher fundamental frequencies than plates with parallel fibers.

2. Fiber shape expression and optimization problem

Curvilinearly shaped fibers are defined by projected contour lines of a cubic polynomial function $f(x,y)$ here, as

$$\begin{aligned} f(x,y) = c_{00} + c_{10}x + c_{01}y + c_{20}x^2 + c_{11}xy + c_{02}y^2 \\ + c_{30}x^3 + c_{21}x^2y + c_{12}xy^2 + c_{03}y^3 \end{aligned} \tag{1}$$

where c_{ij} (i, j = 0, 1, 2, 3) are shape coefficients which determine the surface shape. An example of a surface and the corresponding curves is shown in Fig. 1(a) and (b).

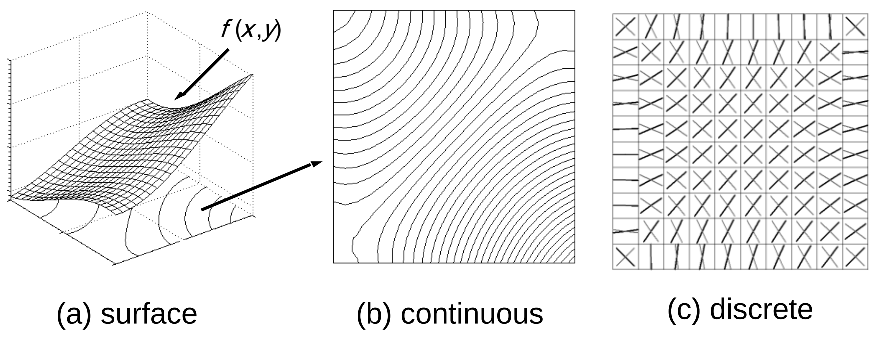

Fig. 1 Examples of (a) surface, (b) continuous fibers, and (c) discrete fiber orientations.

The originally developed FEA code to accept curvilinear fiber shapes is employed to calculate natural frequencies of the present composite plate. The FEA is performed with an isoparametric eight-node plane element based on the first-order shear deformation theory (FSDT) [2] to enable an analysis of the variously shaped plates. In the FEA, continuous fibers are discretized and the fiber orientation angles for each element are calculated using the co-ordinates of the center of the element by

$$\theta(x_c, y_c) = \tan^{-1}(-\frac{\partial f / \partial x}{\partial f / \partial y})\bigg|_{x=x_c, y=y_c} \qquad \text{(when } \partial f / \partial y = 0,\ \theta = 90^\circ\text{)} \tag{2}$$

where (x_c, y_c) are the co-ordinates of the center of the element. The angles are in the same direction as the tangents to the surfaces in the horizontal plane, and assume straight fibers and a constant volume fraction in the element but different angles for each element (Fig. 1(c)). It is possible to describe different shapes of surfaces and curvilinear fibers by varying the values of the shape coefficients c_{ij}.

The present problem limits plates to symmetric K-angle-ply laminates $[(\pm\theta)_{K/4}]$s where the "+layer" means that the layer has fiber shapes determined in the optimization problem, and the "–layer" is the layer with fiber shapes symmetric to the "+layer" with respect to the horizontal line and becomes $-\theta$ in Eq. (2). Thus it is sufficient to design one layer in this problem formulation. The objective is maximizing the fundamental frequency Ω_1, and the corresponding shape coefficients c_{ij} for the optimum fiber shapes are the design variables. This problem can be stated as

$$\begin{aligned} &\text{Maximize} : \Omega_1 \\ &\text{Design variables} : c_{10}, c_{01}, c_{20}, c_{11}, c_{02}, c_{30}, c_{21}, c_{12}, c_{03} \\ &\text{Subject to} : -1 \le c_{ij} \le 1 \quad (i, j = 0, 1, 2, 3) \end{aligned} \tag{3}$$

The increment of c_{ij} is 0.1 in the range from -1 to 1, and there are 21 possible values for each shape coefficient. These values were determined by previous numerical experiments. As an optimizer, simple genetic algorithm (SGA) method is used with the two point crossover, mutation, and elitist tactics.

3. Numerical results

Figure 2 shows optimized results for the four boundary conditions, with letters showing the states of the edges: F for Free, S for simply supported, and C for clamped edges, and the letter P represents a point support in the counterclockwise direction starting from the left edge of the plate. They present a simply supported plate (Ex. 1 SSSS), a fully clamped plate (Ex. 2 CCCC), a plate with unsymmetrical boundary conditions including two free edges (Ex. 3 CSFF), and a plate with a point support at the free corner of CSFF (Ex. 4 CSF(P)F). Only the "+ layer" is shown as overlapping views would make it difficult to find fiber continuity in Fig. 2.

Plots of the fundamental frequencies of the plates here and conventional plates are presented in Fig. 3. The typical lay-up configurations, $[(0^\circ)_4]$s, $[(0^\circ/90^\circ)_2]$s, $[(\pm 60^\circ)_2]$s, $[(\pm 45^\circ)_2]$s and $[(\pm 15^\circ)_2]$s, are shown in Fig. 3 for comparison. Except for the purely simply supported plates (Ex. 1), the plates with curvilinear fibers result in higher frequencies than all conventional plates with typical lay-ups. Even in the case of Ex. 1, the result is very similar frequencies to the plates with parallel fibers. This is because the optimum fiber shapes for Ex. 1 show quite similar shapes to $[(\pm 45^{\circ})_2]s$, this establishes that parallel fibers have advantages over curvilinear fibers for simply supported plate. However, the other boundary conditions give clearly curved fiber shapes and higher fundamental frequencies than the parallel fibers.

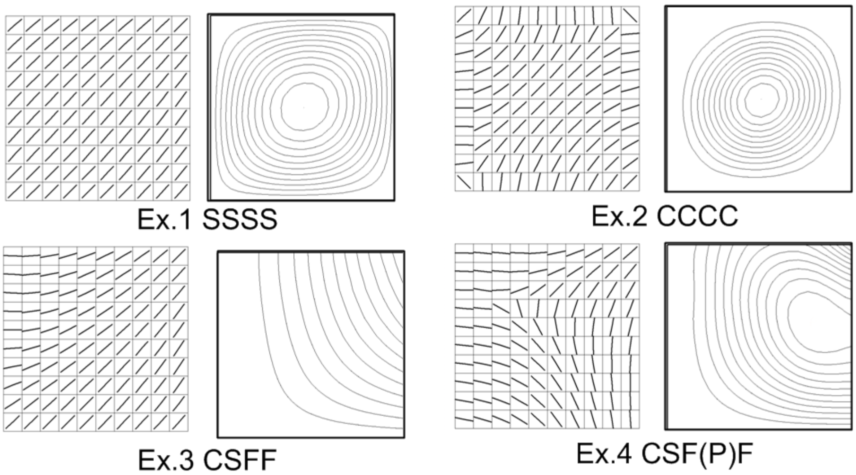

Fig. 2 Optimum curvilinear fiber shapes (+ layer) for the four examples of the plates and the corresponding vibration modes.

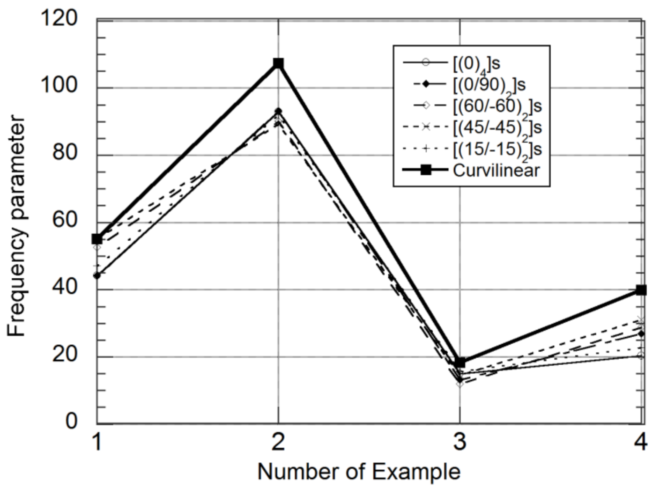

Fig. 3 Frequencies for the present plates with optimum curvilinear fibers and conventional plate with parallel fibers.

Reference

[1] Lopes C. S., Gürdal Z., and Camanho P. P., Variable-stiffness composite panels: Buckling and first-ply failure improvements over straight-fibre laminates, *Computers & Structures* Vol. 86 (2008), pp. 897-907

[2] Reddy J. N., Mechanics of laminated composite plates theory and analysis, CRC Press, Inc., 1997

Three dimensional vibration analyses of cracked rectangular FGM plates

C. S. Huang, K. P. Wang, and P. J. Yang
Department of Civil Engineering, National Chiao Tung University, Hsinchu, Taiwan

INTRODUCTION

Laminated composite materials are prevalent in engineering systems, particularly in aeronautical vehicles and aerospace structures. However, the abrupt change in material properties across the interface between material layers can cause large interlaminar stresses even some delaminations. Functionally graded materials (FGMs) are found to overcome these adverse interlamination stress and delamination effects associated with conventional laminated composite builds. Material properties of FGMs vary continuously by gradually changing the volume fraction of constituent material properties. FGMs have been extensively explored in the last two decades along a variety of interdisciplinary fronts, including electronics, chemistry, optics, biomedicine, aeronautical and mechanical engineering.

A novel examination of the three-dimensional (3-D) vibrations of rectangular FGM plates having cracks is summarized. Employing 3-D theory of elasticity and a variational Ritz methodology, new hybrid series of mathematically complete orthogonal polynomials and crack functions as the assumed displacement fields are proposed to enhance the convergence of numerical solutions for vibration frequencies of a cracked rectangular FGM plate. The proposed admissible hybrid series properly describe the $\vartheta(1/\sqrt{r})$ 3-D stress singularities at the terminus edge front of the crack, allowing for displacement discontinuities across the crack sufficient to explain the most general 3-D "mixed modes" of local crack-edge deformation and stress fields typically seen in fracture mechanics. The correctness and validity of the vibration analysis are confirmed through comprehensive convergence studies and comparisons with published results for homogeneous and FGM rectangular plates with cracks based on various plate theories. The locally effective material properties are estimated by a simple power law and the effects of the volume fraction on the frequencies are investigated. Frequency data, mode shapes and nodal patterns are shown for FGM rectangular plates having cracks with varying crack size effects implying flaw-size influence in FGM plate vibration, including crack length ratios, crack positions, and crack inclination angles (α).

METHODOLOGY AND RESULTS

Consider a cracked rectangular FGM plate as shown in Fig. 1. An appropriately enhanced Ritz procedure proposed herein yields accurate solutions of cracked FGM plate vibrations with the accuracy and efficiency of the approximate solutions largely depending on the appropriate choice of admissible functions for the three displacement components, $U_i(x, y, z)$. A hybrid series of mathematically complete admissible orthogonal polynomials and newly-developed crack functions accounting for stress singularities at the front of the crack, while permitting displacement discontinuities across the crack, are used to approximate each of $U_i(x, y, z)$. The displacement amplitude functions are expressed as

$$U_i = \hat{U}_{ip} + \hat{U}_{ic}$$

where $\hat{U}_{ip}$ is an assumed finite series of mathematically complete polynomials; and $\hat{U}_{ic}$ is an assumed finite series of crack functions, supplementing the assumed polynomial series, $\hat{U}_{ip}$, to appropriately describe the essential singular stresses at the crack front and displacement discontinuities across the crack.

Orthogonal polynomials are adopted to expand $\hat{U}_{ip}$ as

$$\hat{U}_{ip}(x,y,z) = f_i(z)\sum_{l=1}^{N_{iz}}\sum_{j=1}^{N_{ix}}\sum_{k=1}^{N_{iy}} A_{jkl}^{(i)} P_j^{(i)}(x) Q_k^{(i)}(y) z^{l\text{-}1} \quad (i=1,\ 2,\ 3),$$

where $P_j^{(i)}(x)$ and $Q_k^{(i)}(y)$ are orthogonal polynomials in the x and y directions, respectively, and are generated by using a standard Gram-Schmidt orthogonalization process. They satisfy the geometric boundary conditions along the four side faces of a rectangular plate.

To enhance the convergence accuracy of the proposed Ritz procedure due to the presence of a crack, stress singularities at the front of the crack and displacement discontinuities across the crack are considered in constructing admissible crack functions, $\hat{U}_{ic}$. For a plate with a side crack, $\hat{U}_{ic}$ is expressed as

$$\hat{U}_{ic}(r,\theta,z) = g_i(x,y,z)\sum_{l=1}^{N_{iz}}\sum_{n=1}^{\bar{N}_i}\sum_{m=0}^{n}[B_{nml}^{(i)} r^{(2n-1)/2}\cos\frac{2m+1}{2}\theta + C_{nml}^{(i)} r^{(2n-1)/2}\sin\frac{2m+1}{2}\theta\ ]\, z^{l\text{-}1}$$

where $g_i(x,y,z)$ (i =1, 2, 3) are boundary functions to satisfy the geometric boundary conditions for U_i on the plate faces. For a plate with an internal crack, $\hat{U}_{ic}$ is expressed as

$$\hat{U}_{ic}(r_1,r_2,\theta_1,\theta_2) = g_i(x,y,z)\sum_{l=1}^{N_{iz}}\ \{\sum_{n=1}^{\bar{N}_i}\sum_{m=0}^{n} B_{nml}^{(i)}\, r_1^{(2n-1)/2}\cos\frac{2m+1}{2}\theta_1 + \tilde{B}_{nml}^{(i)}\, r_2^{(2n-1)/2}\cos\frac{2m+1}{2}\theta_2 +$$
$$C_{nml}^{(i)}\, r_2^{\beta}\sin^2(\theta_2/2)\, r_1^{(2n-1)/2}\sin\frac{2m+1}{2}\theta_1 + \tilde{C}_{nml}^{(i)}\, r_1^{\beta}\sin^2(\theta_1/2)\, r_2^{(2n-1)/2}\sin\frac{2m+1}{2}\theta_2\}z^{l-1}$$

Table 1 contrasts $\omega(b^2/h)\sqrt{\rho/E}$ obtained by various theories for SSSS homogeneous cracked square plates with horizontal side cracks (α = 0°) having various length ratios (d/a) and positioned at c_y/b = 0.5. As expected, the differences between the frequencies of very thin plates (h/b = 0.002) obtained based on the classical thin plate theory and Mindlin plate theory are negligible, and both are consistent with the present 3-D elasticity-based solutions up to at least three significant figures. For the thin (h/b = 0.05) and moderately thick (h/b = 0.1) plates, the $\omega(b^2/h)\sqrt{\rho/E}$ solutions based on the classical thin plate theory are considerably stiffer than the solutions based on Mindlin plate theory and present 3-D elasticity theory, especially for moderately thick plates (h/b = 0.1) and for the higher modes. The solutions based on Mindlin plate theory are slightly over-correcting in reducing the classical thin plate theory solutions for transverse shear effects, and the Mindlin plate theory solutions are smaller than the present 3-D elasticity-based solutions. Percentage differences between the shear deformable Mindlin $\omega(b^2/h)\sqrt{\rho/E}$ solutions and the present 3-D solutions are less than 1%. Generally speaking, this 1% difference does not significantly increase with increasing crack length ratio (d/a).

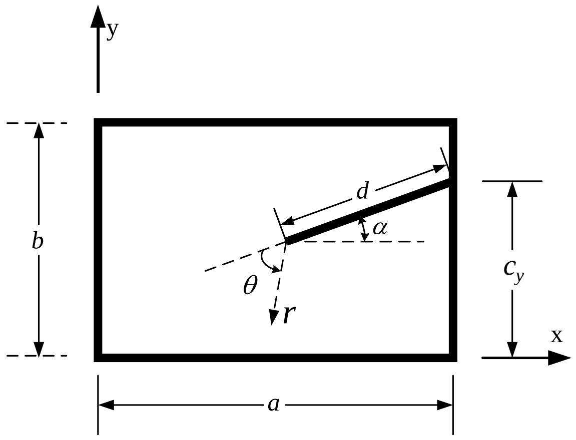

(a)Top view of a plate with a side crack

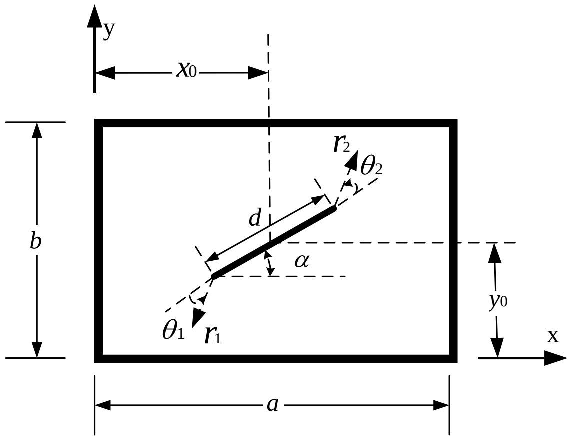

(b)Top view of a plate with an internal crack

Fig. 1 A rectangular functionally graded material (FGM) plate having a crack showing position coordinates, crack length, and crack orientation

Table 1. Comparisons of $\omega(b^2/h)\sqrt{\rho/E}$ predicted by various theories for homogeneous cracked, SSSS square plates with different thickness ratios (h/b = 0.002, 0.05, 0.1)

d/a	h/b	Mode 1	2	3	4	5
0.2	0.002	[5.961]	[14.89]	[14.93]	[23.84]	[29.62]
		(5.961)	(14.89)	(14.92)	(23.84)	(29.62)
		{5.961}	{14.88}	{14.93}	{23.84}	{29.62}
	0.05	[5.961]	[14.89]	[14.93]	[23.84]	[29.62]
		(5.900)	(14.54)	(14.55)	(22.91)	(28.29)
		{5.905}	{14.56}	{14.57}	{22.95}	{28.35}
	0.1	[5.961]	[14.89]	[14.93]	[23.84]	[29.62]
		(5.750)	(13.66)	(13.69)	(20.87)	(25.41)
		{5.758}	{13.72}	{13.74}	{20.99}	{25.57}
0.4	0.002	[5.810]	[14.46]	[14.60]	[21.57]	[27.91]
		(5.810)	(14.46)	(14.60)	(21.56)	(27.91)
		{5.810}	{14.47}	{14.60}	{21.57}	{27.91}
	0.05	[5.810]	[14.46]	[14.60]	[21.57]	[27.91]
		(5.725)	(13.90)	(14.23)	(20.48)	(26.49)
		{5.730}	{13.92}	{14.25}	{20.54}	{26.55}
	0.1	[5.810]	[14.46]	[14.60]	[21.57]	[27.91]
		(5.562)	(12.84)	(13.39)	(18.54)	(23.83)
		{5.572}	{12.90}	{13.43}	{18.66}	{23.97}

Note: [ ]: classical thin plate theory; ( ): Mindlin plate theory; { }: present 3-D elasticity-based solution

Linear and Nonlinear Frequency Characteristics of Rotating Discs

Stanley G. Hutton and Ramin M. H. Khorosany
Department of Mechanical Engineering, University of British Columbia
Vancouver B.C., Canada V6T 1Z4
huttonstan@gmail.com

Consideration of the linear vibration characteristics of unconstrained rotating thin disc leads to the important concept of "critical speeds". These critical rotational speeds are of interest because they correspond to the situation where a natural frequency of the rotating disc, as measured by a stationary observer, is zero. Such speeds correspond physically to the speeds at which a travelling circumferential wave, of shape corresponding to the mode shape of the natural frequency being considered, travel around the disc in the absence of applied forces. At such speeds, according to linear theory, the blade may respond as a space fixed stationary wave and an applied dc force may induce a resonant condition in the disc response. Thus, in general, linear theory predicts that for rotating discs, with low levels of damping, large responses may be encountered in the region of the critical speeds. However, large response invalidates the predictions of linear theory which has neglected the nonlinear stiffness produced by the effect of in-plane forces.

In the present work experimental studies were conducted in order to measure the frequency response characteristics of rotating discs both in an idling mode as well as when subjected to a lateral force. The applied lateral forces (produced by an air jet) were such as to produce displacements large enough that non linear geometric effects were important in determining the disc frequencies.

This paper presents the results of these experiments and compares them with analytical predictions based upon equations developed using Von Karman plate theory. The results show that in the case of finite disc displacements the frequency characteristics are significantly different to the linear case. In particular no critical speeds exist in the case of finite displacements.

The pertinent characteristics of linear theory predictions can be illustrated by reference to Figure 1. This Figure plots the relationship between disc natural frequency, as measured by a space fixed observer, and disc rotational speed for a steel disc of outer dia. 17", inner dia. 6" and plate thickness 0.050". The disc is assumed to be axi-symmetric; clamped at its inner radius; and free at its outer radius.

Inspection of this Figure shows that at zero speed the disc has natural frequencies at approximately 52, 52 and 61Hz. Where it can be shown that these frequencies correspond to mode shapes (0,1), (0,0) and (0,2). Where the notation (M, N) means the mode has M nodal circles and N nodal diameters. Further, the disc has three lowest critical speeds of approximately 2400; 2700; and 2850rpm.At each of these speeds the linear analysis predicts that the disc has a natural frequency of 0 Hz, whence a static force will produce a standing wave response.

At speeds other than zero it may be seen that each nodal diameter mode has two frequencies, one corresponding to a backward travelling wave and one corresponding to a forward travelling wave. A critical speed occurs when the disc speed equals the speed at which a nodal diameter mode freely travels around the disc.

Figure 2 shows the same plot as for Figure 1 but for the case where the disc is acted upon by a space fixed spring of stiffness 20lb/in. In this case the symmetry of the system is destroyed and at zero speed the natural frequency of every nodal diameter mode is split into two. In one case a nodal diameter passes through the location of the spring, and thus the frequency is the same as without the spring (and corresponds to the minimum frequency that the system can adopt), and in the other case the nodal diameters are such that the spring is at an anti-node giving rise to the maximum frequency that the system can adopt.

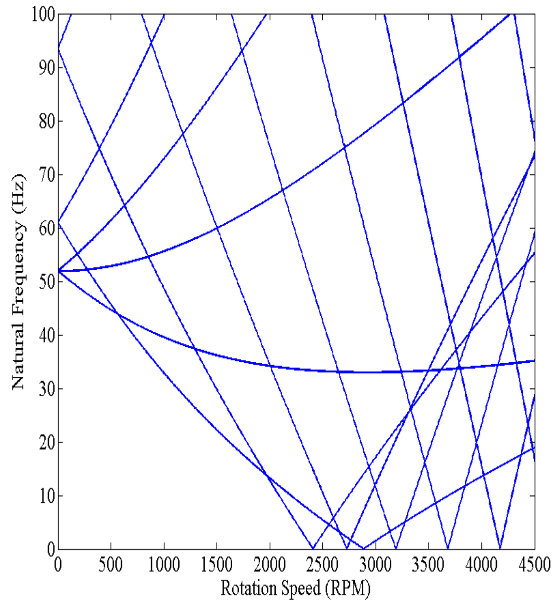

Figure 1 Computed Variation of Natural Frequency with Speed for Symmetric Unconstrained Clamped Disc (Linear)

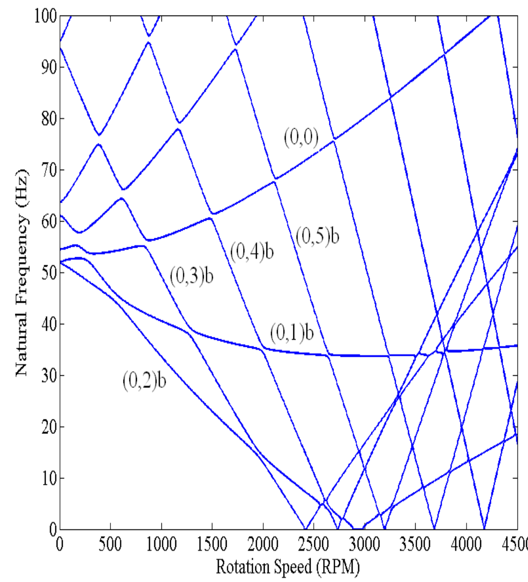

Figure 2 Computed Variation of Natural Frequency with Speed for a Spring Constrained Clamped Disc (k=20 lbf/in)

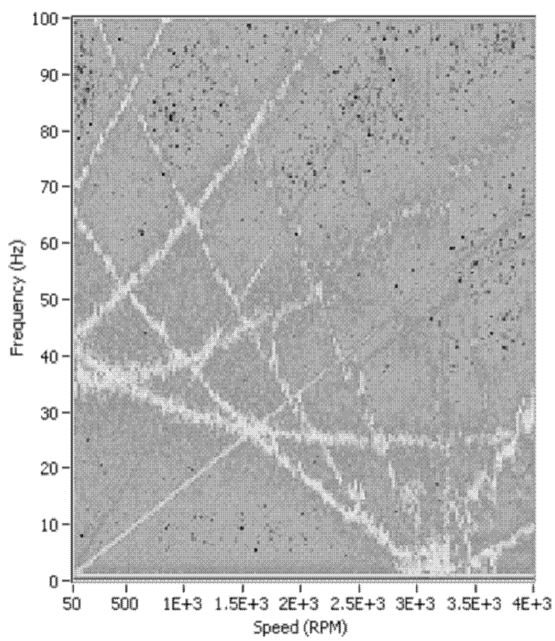

Figure 3 Experimental Frequency Speed Map -Clamped Disc Idling Response

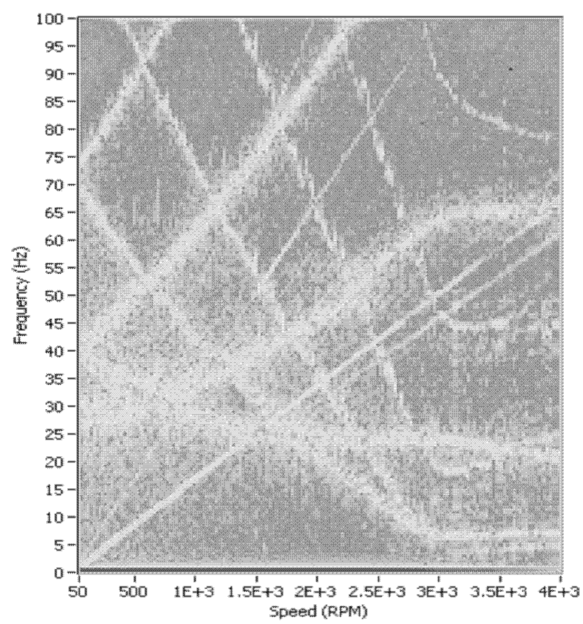

Figure 4 Experimental Frequency Speed Map -Clamped Disc Response to Air Jet Excitation

EXPERIMENTAL RESULTS

Figures 3 and 4 show the results of the experimental run-up tests from dc to 4,000rpm, for the disc considered.

In Figure 3 the excitation is low level broadband and in Figure 4 an air jet is applied to the rim of the disc of sufficient magnitude for non-linear effects to be significant.

From Figure 4 it may be seen that the nonlinear behaviour is significantly different to the linear behaviour contained in Figure 3. In particular, the critical speed characteristic evident in the linear response is missing in the nonlinear experimental results. As may be seen in Fig 4 the frequencies corresponding to the backward travelling waves do not continue to reduce until they have zero value. Instead, in the region of the linear critical speed, these frequencies level off and maintain a constant level as speed is further increased. In this case no reflected waves are evident. Further investigations indicate that at the frequency lock-in speeds a standing wave develops.

ANALYTICAL PREDICTIONS

Linear Results

In the case of the clamped inner boundary condition, the agreement between the predicted linear frequencies at zero speed (Figure 1) and the measured values in Figure 3 is not so good. Further tests on free-free discs give better agreement. The reason for the difference between the measurements and the prediction is likely due to the inaccuracy of modeling the inner clamped boundary condition. The mathematical model assumes perfect fixity with a zero slope. In practice the clamping plate used in this case would not have provided full fixity and some degree of rotation would likely have occurred.

Nonlinear Results

Results of the nonlinear analysis will be presented at the conference.

ACKNOWLEDGEMENTS

This work was supported by funding from NSERC Canada, and FPInnovations , Forintek Division, Canada.

REFERENCES

[1] Hutton , S.G., Chonan, S. and Lehmann, B.F., 1987, "Dynamic response of a guided circular saw," Journal of Sound and vibration, 112, pp. 527-539.
[2] Jen-San Chen and Hsu, C.-M., 1997, "Forced response of a spinning disc under space-fixed couples," Journal of Sound and Vibration, 206, pp. 627-639.
[3]Nowinski, J.L., 1964, "Nonlinear transverse vibrations of a spinning disc," Journal of Applied Mechanics, 31, pp. 72-78.
[4] Jen-San Chen, 2001, "On the Internal Resonance of a Spinning Disc Under Space-Fixed Pulsating Edge Loads, Journal of Applied Mechanics," 68, pp. 854-859.
[5] Raman, A. and Mote, C.D., 2001 "Experimental studies on the non-linear oscillations of imperfect circular discs spinning near critical speed," International Journal of Non-Linear Mechanics, 36, pp. 291-305.
[6] Raman ,A., Hansen , M. H. and Mote, C.D., 2002, "A Note on the Post-Flutter Dynamics of a Rotating Disc," Journal of Applied Mechanics, 69, pp. 864-866 .
[7] Nayfeh, A.H., 2000, "Nonlinear interactions: Analytical, Computational, and Experimental Methods," Wiley, New York.

On the bipenalty method: why is it advantageous to add stiffness and mass

Sinniah Ilanko[1] and Luis E. Monterrubio[2]

[1]School of Engineering, The University of Waikato, Hamilton, New Zealand.

Email: ilanko@waikato.ac.nz

[2]Department of Structural Engineering, University of California, San Diego , 9500 Gilman Drive, Mail Code 0085, La Jolla, CA 92093-0085, USA, Email: lemonterrubiosalaza@ucsd.edu

In a recent paper, Askes et al [1] proposed the simultaneous use of stiffness and inertia of large magnitude to model constraints in time domain analysis. From a frequency domain perspective, as stiffness and inertia have opposite effects on the natural frequencies, this seems counter-intuitive. With increasing stiffness, the natural frequencies either increase or remain unchanged, whereas the opposite is true for inertia. However, it can be shown, through very simple illustrative examples, that the natural frequencies and modes of continuous systems can be found in this way, and that there are advantages in using both stiffness and mass simultaneously.

The "artificial stiffness" method of Courant [2] has gone through some changes recently, thanks to some debate generated at the first ISVCS [3]. At this symposium, Ilanko proposed the use of masses, instead of stiffness, as a way to model constraints, so that true upperbound solutions to frequencies could be obtained using the Rayleigh-Ritz Method. However, with large masses, introduction of very low frequencies with modes which violate the constraints and the difficulty in selling the idea of enforcing continuity conditions with large masses that vibrated at the differential velocity of the connecting points, shifted the focus on a different strategy using "negative stiffness" instead of mass [4,5]. It may be worth noting here, that the idea of using negative stiffness occurred to the Lead Author, as a result of what he learnt from a mistake in the sign of a mass term in his PhD research [6,7]. The switching of the sign did not affect the results for the limiting case of a very large mass used as a test in verifying the accuracy of the computer program. This pointed to the fact that if the mass is sufficiently large as to prevent the motion of a point, then the sign of the mass (whether it is right or wrong) will have no effect on the frequencies. Using positive and negative stiffness, it is possible to determine and control any error due to violation of the constraints, but it is necessary to ensure that the magnitude of the stiffness is greater than the highest magnitude of the critical penalty stiffness values associated with negative stiffness. Subsequently, the legitimacy of using positive and negative mass to modelling constraints was established for frequency analysis and it was also used successfully in time domain analysis [8-10]. However, it has been found that when using inertial type penalty parameters, while the higher modes converge well even with very small penalty masses, the magnitude of inertial penalty needed to enforce constraints at lower modes can cause numerical problems for some very high modes [11, 12]. The most recently introduced bipenalty method, which has been developed for time domain analysis, seems to offer a solution that addresses all the problems listed above. By using both stiffness and mass at two carefully tuned combinations, it is possible to obtain bounded results for the natural frequencies of constrained system.

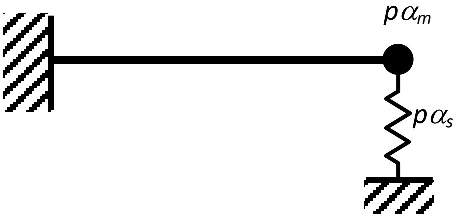

Fig 1. Cantilever with spring-mass restraint

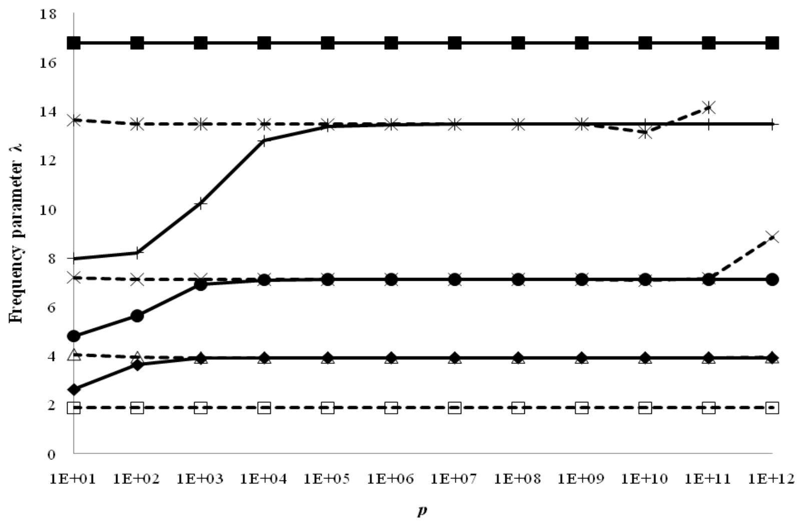

Figure 2. Frequency parameter λ vs penalty parameter $\log_{10} p$ for the propped

Fig. 1 shows an Euler-Bernoulli beam of length *L*, flexural rigidity *EI* and mass per unit length *m*, clamped at the left end and attached to a spring and mass at the right end. The stiffness of the spring is $p\alpha_s$ as where $\alpha_s = EI/L^3$ and *p* is the penalty parameter. The magnitude of mass is $p\alpha_m$ where $\alpha_m = \alpha_s/r$. The ratio *r* is the tuning ratio that changes the relative dominance of stiffness and mass. If *r* is very small then the system behaves as if it is inertially penalised and if *r* is very large it behaves like an elastically penalised system. With a four term assumed displacement of the form $f = \sum_{i=1}^{4} a_i x^{i+1}$ in a Rayleigh-Ritz method, results were generated for various values for the tuning ratio *r*. Figure 2 shows the variation of the non-dimensional frequency parameter of the beam $\lambda = L\left(m\omega^2/(EI)\right)^{1/4}$ with the penalty parameter *p* for two special cases. The solid line shows the results for a stiffness dominated penalised system with $r = \omega_4^2$, and the dotted lines shows the results for an inertia dominated case with $r = \omega_1^2$, where ω_i is the ith frequency of the cantilever beam (unconstrained at the right end). It may be seen that the three natural frequencies of the propped cantilever are approached from opposite directions by the natural frequencies of the penalised system with the two different tuning ratios. The highest frequency of the stiffness dominated system and the lowest frequency of the inertia dominated system remain unchanged; these are in fact equal to the highest and lowest frequencies of the constrained system, respectively. The way to tune the penalty parameter and the reasons for this behaviour will be presented at the symposium.

References

1. Askes, H., Caramés-Saddler, M. & Rodríguez-Ferran, A. 2010 Bipenalty method for time domain computational dynamics. *Proc. R. Soc. A* **466**, pp 1389-1408. (doi:10:1098/rspa.2009.0350).

2. Courant, R. 1943 Variational methods for the solution of problems of equilibrium and vibration. *Bulletin of the American Mathematical Society* **49**, 1-23.

3. Ilanko, S, 1997, On the application of Rayleigh's Principle and the Ritz method - Some Points to Ponder, Proceedings of the International Symposium on Vibrations of Continuous Systems, Colorado, pp 27-8.

4. Ilanko, S. & Dickinson, S.M. 1999 Asymptotic modelling of rigid boundaries and connections in the Rayleigh-Ritz Method. *Journal of Sound and Vibration* **219**, 370-378.

5. Ilanko, S. 2002a Existence of natural frequencies of systems with imaginary restraints and their convergence in asymptotic modeling. *Journal of Sound and Vibration* **255**, 883-898.

6. Ilanko, S and Dickinson, S.M., 1994, Corrigendum: The vibration and post-buckling of geometrically imperfect, simply supported, rectangular plates under uni-axial loading, part I: Theoretical approach; part II: Experimental investigation (S. Ilanko and S. M. Dickinson 1987 Journal of Sound and Vibration **118**, 313-351), *Journal of Sound and Vibration* **139,** 519-521

7. Ilanko, S, 1985, Vibration behaviour of in-plane loaded rectangular plates with initial geometrical imperfections, PhD Thesis, The University of Western Ontario, Canada.

8. Ilanko, S. 2005, Introducing the use of positive and negative inertial functions in asymptotic modeling. *Proc. R. Soc. A* **461**, 2545–2562.

9. Williams, F.W. & Ilanko, S. 2006 The use of the reciprocals of positive and negative inertial functions in asymptotic modelling. *Proc. R. Soc. A* **462**, 1909-1915.

10. Hetherington, J. & Askes, H. 2009 Penalty methods for time domain computational dynamics based on positive and negative inertia. *Computers and Structures* **87**, 1474-1482.

11. Monterrubio, L.E. 2009 The use of positive and negative penalty functions in solving constrained optimization problems and partial differential equations. PhD Thesis, University of Waikato.

12. Monterrubio, L.E. 2009 Free vibration of shallow shells using the Rayleigh–Ritz method and penalty parameters. *Proc. of the Inst. of Mech. Eng., Part C* 223, 2041-2983.

VIBRATION OF DAMAGED STRUCTURES USING A HYBRID CONTINUOUS AND FINITE ELEMENT MODEL

David Kennedy and Reja E. Rabbi
Cardiff School of Engineering, Cardiff University, Cardiff CF24 3AA, UK

Finite element analysis [1] has become the most widely used method in structural dynamics. Location of the natural frequencies of free vibration entails the solution of the linear eigenproblem

$$\left(\mathbf{K}-\omega^2\mathbf{M}\right)\mathbf{D}=\mathbf{0} \tag{1}$$

where ω is the circular frequency and $\mathbf{D}$ is the vector of nodal displacement amplitudes. The static stiffness matrix $\mathbf{K}$ and mass matrix $\mathbf{M}$ are found by integration of expressions involving shape functions which are assumed to represent the internal displacements between the nodes of each element. Such discretisation approximations may lead to inaccuracies, particularly when finding higher natural frequencies.

In contrast, an exact dynamic stiffness matrix $\tilde{\mathbf{K}}(\omega)$ can often be found by direct solution of the governing differential equations, resulting in the continuous transcendental eigenproblem

$$\tilde{\mathbf{K}}(\omega)\tilde{\mathbf{D}}=\mathbf{0} \tag{2}$$

which may be solved using the Wittrick-Williams algorithm [2]. The absence of discretisation approximations means that nodes are only required at joints of the structures, resulting in smaller problems and guaranteed accuracy for any natural frequency. This approach has been successfully applied to the vibration, buckling and postbuckling analysis and optimum design of prismatic assemblies of rectangular plates made from metals and laminated composite materials [3]. The structure and its loading are assumed to be invariant in the longitudinal (x) direction. The further assumption that the vibration or buckling mode $\tilde{\mathbf{D}}$ varies sinusoidally in the x direction satisfies simply supported end conditions for orthotropic structures with no shear load [4]. Otherwise a series of modes $\tilde{\mathbf{D}}_m$ with sinusoidal half-wavelengths λ_m and dynamic stiffness matrices $\tilde{\mathbf{K}}_m(\omega)$ $(m=1,2,3,\ldots)$ is coupled using Lagrangian multipliers to enforce the end conditions and optional attachments to transverse supporting structures [5].

Figure 1 shows a rectangular plate $OABC$ with an embedded damaged region $pqrs$. The damage might be delamination in a composite plate, but could be generalised to any region of modified stiffness, e.g. a cutout or patch. Uniform damage extending over the whole length of the plate is easily modelled by modifying the stiffness of the strip $PQRS$ [6], while approximate smeared stiffnesses for $PQRS$ have been derived [7] which take account of the longitudinal position of $pqrs$.

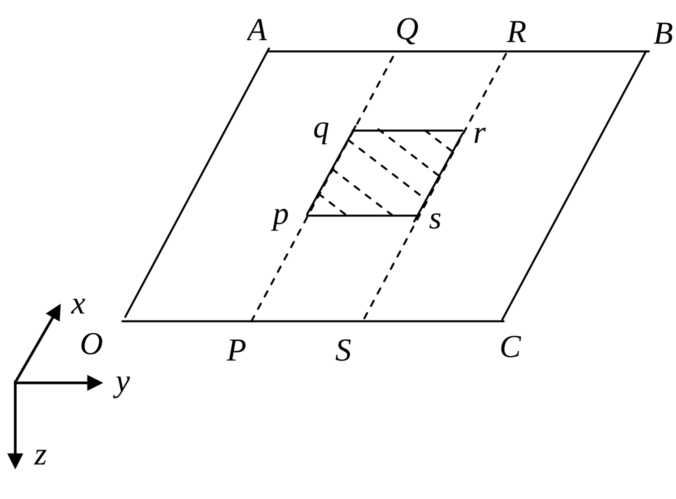

Figure 1. Rectangular plate $OABC$ containing an embedded damaged region $pqrs$.

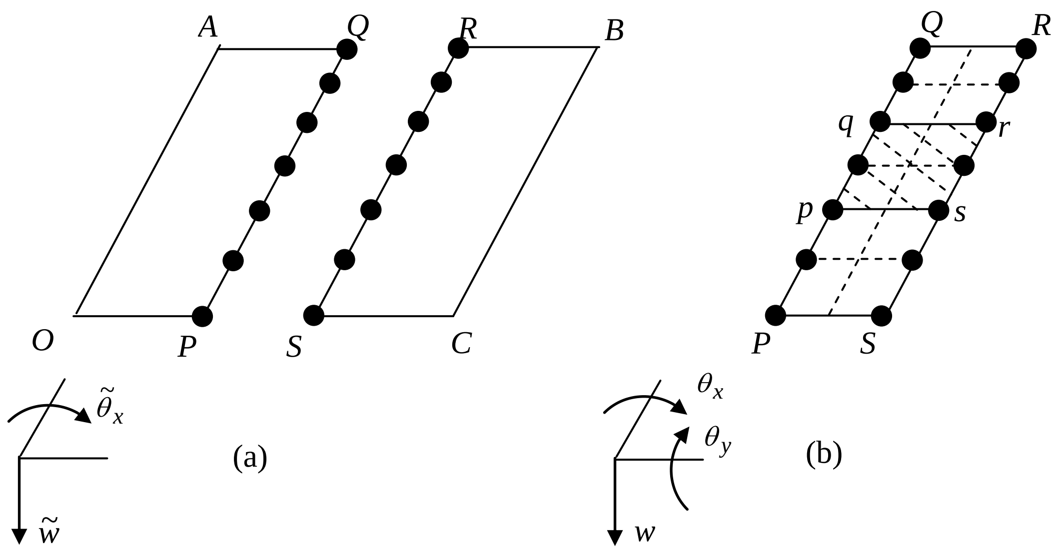

Figure 2. Hybrid (a) continuous and (b) finite element model for rectangular plate $OABC$ containing an embedded damaged region $pqrs$.

A new hybrid model is shown in Figure 2. For simplicity, classical plate theory is assumed and in-plane displacements are ignored. The undamaged, prismatic regions $OAQP$ and $SRBC$ are together modelled continuously with dynamic stiffness matrices $\tilde{\mathbf{K}}_m(\omega)$ relating the lateral displacements $\tilde{w}$ and rotations $\tilde{\theta}_x$ at the four (line) nodes $\{OA, PQ, SR, CB\}$ to the corresponding perturbation forces. (Because of the assumptions made, the rotation $\tilde{\theta}_y$ about the y axis is given by $\partial\tilde{w}/\partial x$.) The remaining region $PQRS$ is not prismatic and is modelled using finite elements, with static stiffness matrix $\mathbf{K}$ and mass matrix $\mathbf{M}$. Rectangular elements are used, each having 12 degrees of freedom, namely w, θ_x and θ_y at each of four corner nodes, and employing appropriate polynomial shape functions [1]. The continuous and finite element models are coupled using Lagrangian multipliers to enforce the constraints

$$w = \tilde{w}\ ; \qquad \theta_x = \tilde{\theta}_x\ ; \qquad \theta_y = \partial\tilde{w}/\partial x \tag{3}$$

at the locations denoted by solid circles along the boundaries PQ and SR.

Minimisation of potential energy [5] gives the transcendental eigenproblem

$$\begin{bmatrix} \tilde{\mathbf{K}}_1(\omega) & & & & & \mathbf{e}_1^{\mathrm{H}} \\ & \tilde{\mathbf{K}}_2(\omega) & & & & \mathbf{e}_2^{\mathrm{H}} \\ & & \tilde{\mathbf{K}}_3(\omega) & & & \mathbf{e}_3^{\mathrm{H}} \\ & & & \cdots & & \vdots \\ & & & & (\mathbf{K}-\omega^2\mathbf{M}) & \mathbf{f}^{\mathrm{T}} \\ \mathbf{e}_1 & \mathbf{e}_2 & \mathbf{e}_3 & \cdots & \mathbf{f} & \mathbf{0} \end{bmatrix} \begin{bmatrix} \tilde{\mathbf{D}}_1 \\ \tilde{\mathbf{D}}_2 \\ \tilde{\mathbf{D}}_3 \\ \vdots \\ \mathbf{D} \\ \mathbf{P}_{\mathrm{L}} \end{bmatrix} = \mathbf{0} \tag{4}$$

where $\{\mathbf{e}_m\}$ $(m = 1, 2, 3, \ldots)$ and $\mathbf{f}$ contain the coefficients of the constraint equations; $\mathbf{P}_{\mathrm{L}}$ is the vector of Lagrangian multipliers; T denotes transpose and H denotes Hermitian transpose. The Wittrick-Williams algorithm [5] gives the number of natural frequencies below a trial value of ω as

$$J(\omega)=\sum_m\left[J_{0m}(\omega)+s\{\tilde{\mathbf{K}}_m(\omega)\}\right]+s\left\{\left(\mathbf{K}-\omega^2\mathbf{M}\right)\right\}+s\{\mathbf{R}\}-r \tag{5}$$

Here $s\{\}$ denotes the sign count of a matrix, i.e. the number of negative leading diagonal elements of the upper triangular matrix obtained by standard Gaussian elimination; $J_{0m}(\omega)$ is the total number of member fixed-end natural frequencies with half-wavelength λ_m lying below ω;

$$\mathbf{R}=-\sum_m \mathbf{e}_m\left[\tilde{\mathbf{K}}_m(\omega)\right]^{-1}\mathbf{e}_m^{\mathrm{H}}-\mathbf{f}\left(\mathbf{K}-\omega^2\mathbf{M}\right)^{-1}\mathbf{f}^{\mathrm{T}} \tag{6}$$

and r is the order of $\mathbf{R}$. It is assumed that there are no fixed-end natural frequencies of the individual finite elements below the largest frequency of interest.

Proof of concept is demonstrated by the excellent convergence in Table 1, which shows non-dimensional fundamental natural frequencies of a simply supported beam of length $3L$ and mass per unit length μ. The beam is divided into three portions of equal length L; the flexural rigidity is EI in the two outer portions (which are modelled continuously) and $(1-\alpha)EI$ in the central portion (which is modelled using either n =1 or 2 finite elements, or continuously to provide an exact comparator). Here the continuous and finite element models can be combined into a single dynamic stiffness matrix, so the Lagrangian multiplier formulation of equation (4) is not required. Numerical results using Lagrangian multipliers to model damaged plates will be presented at the Symposium.

References

[1] Zienkiewicz OC, Taylor RL. *The Finite Element Method*. Butterworth-Heinemann, Oxford, 2000.

[2] Williams FW, Wittrick WH. An automatic computational procedure for calculating natural frequencies of skeletal structures. *International Journal of Mechanical Sciences* 12(9):781–791, 1970.

[3] Kennedy D, Featherston CA. Exact strip analysis and optimum design of aerospace structures. *The Aeronautical Journal* 114(1158):505-512, 2010.

[4] Wittrick WH, Williams FW. Buckling and vibration of anisotropic or isotropic plate assemblies under combined loadings. *International Journal of Mechanical Sciences* 16(4):209-239, 1974.

[5] Anderson MS, Williams FW, Wright CJ. Buckling and vibration of any prismatic assembly of shear and compression loaded anisotropic plates with an arbitrary supporting structure. *International Journal of Mechanical Sciences* 25(8):585-596, 1983.

[6] Damghani M, Featherston CA, Kennedy D. Critical buckling of delaminated composite plates using exact stiffness analysis. *Proceedings of 9th International Conference on Computational Structures Technology*, Athens, CST.209:1-14, 2008.

[7] Damghani M, Kennedy D, Featherston CA. Global buckling behaviour of composite plates containing embedded rectangular delaminations using exact stiffness analysis. *Proceedings of CEAS European Air and Space Conference*, Manchester 1-15, 2009.

Table 1. Non-dimensional fundamental natural frequencies $\omega\sqrt{\mu L^4/EI}$ of a damaged beam.

Damage parameter α	0.0	0.1	0.2	0.3	0.4	0.5
Continuous + FE $(n=1)$	1.09721	1.06191	1.02220	0.97711	0.92531	0.86488
Continuous + FE $(n=2)$	1.09666	1.06133	1.02159	0.97648	0.92465	0.86421
Continuous	1.09662	1.06129	1.02156	0.97644	0.92461	0.86417

Frequency Response Analysis of a Rectangular Plate Subjected to Point Force by Using Transfer Matrix Method

Kotaro ISHIGURI*, Yukinori KOBAYASHI**, Yohei HOSHINO and Takanori EMARU
Graduate School of Engineering, Hokkaido University
N13W8, Kita-ku, Sapporo-shi, Hokkaido, 060-8628, Japan

1. Introduction

This paper presents a numerical method to investigate the frequency response of a rectangular plate. When we use the transfer matrix method (TMM) to calculate frequency response of plates, exciting force is limited to a line force and applicable object is also restricted. To expand the range of application of the TMM, we propose a method to calculate modal parameters from free vibration analysis by using the TMM. Modal mass is calculated by numerical integration from modal vectors. We have applied this method to calculate the response of plates subjected to a point force. Comparing the results obtained from the proposed method and finite element method, characteristics of the frequency response of both methods agree with each other. Calculation process of the proposed method has an advantage of computational efficiency.

2. Transfer matrix method for a rectangular plate

We can employ the TMM to solve vibration problems of the rectangular plate that is simply-supported along a pair of opposite edges. Figure 1 shows a rectangular plate and the coordinate system. We assume that the edges x=0 and x=L_a are simply-supported in this paper. Considering free vibration problem and employing the method of separation of variables for out-of-plane displacement w as $w = L_a \overline{w} \sin(m\pi x / L_a)$. $\overline{w}$ is the nondimensional displacement and m is half-wave number in x direction. Introducing nondimensional coordinate $\eta = y / L_a$ and employing the method of separation of variables for other variables in the same manner, governing equation of the plate is expressed as the state equation

$$\frac{d}{d\eta}\{\mathbf{z}(\eta)\} = [\mathbf{U}]\{\mathbf{z}(\eta)\}, \tag{1}$$

where $\{\mathbf{z}(\eta)\}$ is the state vector that consists of variables expressing displacement, slope, moment and shear force, and [**U**] is the constant matrix determined by using frequency, material parameters of the plate and the half-wave number m.

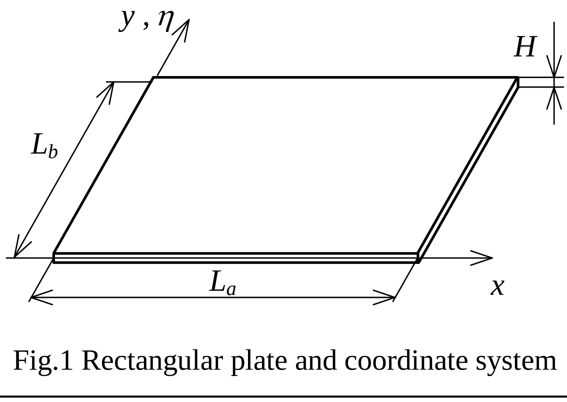

Fig.1 Rectangular plate and coordinate system

*First author currently belongs to Railway Technical Research Institute at Tokyo, Japan.
**Corresponding author: kobay@eng.hokudai.ac.jp

The state vector $\{\mathbf{z}(\eta)\}$ can be expressed as $\{\mathbf{z}(\eta)\}=[\mathbf{T}(\eta)]\{\mathbf{z}(0)\}$ by using the transfer matrix $[\mathbf{T}(\eta)]$ of the plate. Substituting this relationship into Eq. (1), the following equation can be obtained

$$\frac{d}{d\eta}[\mathbf{T}(\eta)] = [\mathbf{U}][\mathbf{T}(\eta)]\,. \tag{2}$$

The matrix $[\mathbf{T}(\eta)]$ is obtained by integrating Eq. (2) numerically with the starting value $[\mathbf{T}(0)]=[\ \mathbf{I}\ ]$ (identity matrix). Considering boundary conditions along edges y=0, L_b, we can derive the frequency equations and obtain natural frequencies and modal vectors.

3. Modal parameters

In this section, we calculate the modal mass by using the vibration modes obtained by the TMM for the plate. We specify the half wave number m in x direction for the TMM. The vibration mode obtained by the TMM expresses the displacement distribution in y direction.

Displacement $w(x,y,t)$ of the plate is expressed as

$$w(x,y,t)=\sum_{j}^{\infty} X_j(x)Y_j(y)q_j(t)\,, \tag{3}$$

where $X_j(x)$ and $Y_j(y)$ are eigenfunctions and $q_j(t)$ is time function. Modal mass m_i is obtained by

$$m_i=\rho H\int_0^{L_a}\int_0^{L_b} X_i^2(x)Y_i^2(y)dxdy=\rho H\left(\int_0^{L_a} X_i^2(x)\ dx\right)\left(\int_0^{L_b} Y_i^2(y)\ dy\right), \tag{4}$$

where ρ and H are the density and thickness of the plate, respectively. Trapezoidal integration is applied to calculate the integrations with number of divisions n_a in x direction and n_b in y direction as follows:

$$\int_0^{L_a} X_i^2(x)dx=\frac{L_a}{n_a}\sum_{k=1}^{n_a}\left(\frac{X_{k+1}^2+X_k^2}{2}\right), \tag{5}$$

$$\int_0^{L_b} Y_i^2(y)dy=\frac{L_b}{n_b}\sum_{k=1}^{n_b}\left(\frac{Y_{k+1}^2+Y_k^2}{2}\right). \tag{6}$$

Function $X_i(x)$ is the sinusoidal function in the TMM, and then we can simplify the integration as follows:

$$\int_0^{L_a} X_i^2(x)dx=\int_0^{L_a}\sin^2(m\pi x/L_a)dx\quad (m=1,2,3\cdots)\,. \tag{7}$$

Modal rigidity is obtained by

$$k_i=\omega_i^2\,m_i\,. \tag{8}$$

Once we calculate eigenvalues and eigenfunctions from the free vibration analysis, responses of the forced vibration are calculated by using modal parameters.

Equation of motion under normalized coordinate system $\boldsymbol{\delta}$ is expressed as

$$\mathbf{m}\ddot{\boldsymbol{\delta}}+\mathbf{c}\dot{\boldsymbol{\delta}}+\mathbf{k}\boldsymbol{\delta}=\mathbf{f}\,, \tag{9}$$

where **m, c, k** are matrices of modal mass, modal damping and modal rigidity, respectively. External force vector **f** is obtained as follows,

$$\mathbf{f}=\boldsymbol{\Phi}^T\,\mathbf{F}e^{j\omega t}\,,\quad \boldsymbol{\Phi}=[\boldsymbol{\Phi}_1,\boldsymbol{\Phi}_2,\boldsymbol{\Phi}_3,\cdots\boldsymbol{\Phi}_n]\,, \tag{10}$$

where **F** is the external force vector under the physical coordinate system, ω is frequency of the external force and $\mathbf{\Phi}$ is the modal matrix that is composed of modal vector $\mathbf{\Phi}_i$. We can specify the applied position of the external force by using the point of division of the transfer matrix. Substituting Eq. (10) into Eq. (9), i-th element of displacement vector can be obtained as

$$\delta_i = \frac{\mathbf{\Phi}^T \mathbf{F}}{m_i} \cdot \frac{1}{-\omega^2 + j\omega\alpha_i + \omega_i^2}, \tag{11}$$

where ω_i is i-th natural frequency and α_i is coefficient of i-th modal damping. Response vector on physical coordinate is obtained by

$$\mathbf{X} = \mathbf{\Phi}\boldsymbol{\delta}. \tag{12}$$

4. Simulation and discussion

Figure 2 shows convergence characteristics of natural frequencies of the plate simply-supported along all edges. Dimensions of the plate are L_a=0.3 m, L_b=0.2 m, H = 5.0×10^{-4} m. It seems enough accurate if we use more than 50 divisions.

Figure 3 shows dimensions and excitation positions E_1 and E_2 of a rectangular plate. We can specify the arbitrary position in x direction because the displacement in x direction is expressed by using sinusoidal function. Figure 4 and 5 show resonant responses of the plate subjected to a point force of 0.1N at black dot with each natural frequency. Numbers in the parentheses denote the half-wave number in x and y directions of the corresponding mode shape of vibration. In the cases of (1, 2) and (2, 1) modes of Fig.5, any vibration is not excited on the plate because the exciting point E_2 is on the nodal line of each mode.

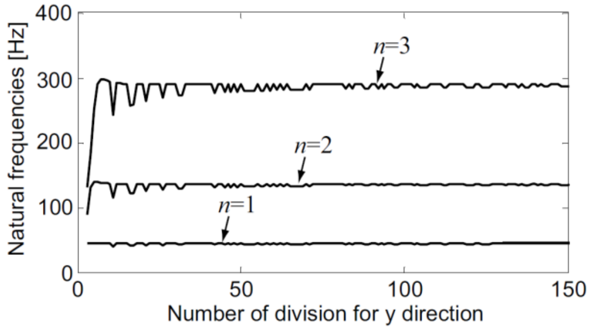

Fig.2 Convergence characteristics of natural frequencies (SSSS, m=1)

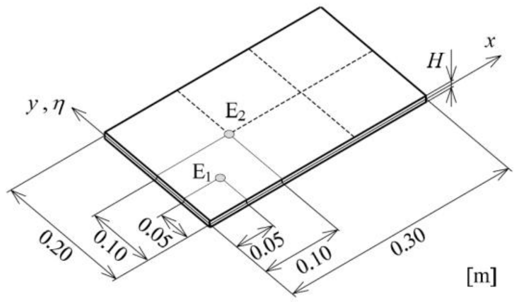

Fig.3 Excitation positions of the rectangular plate

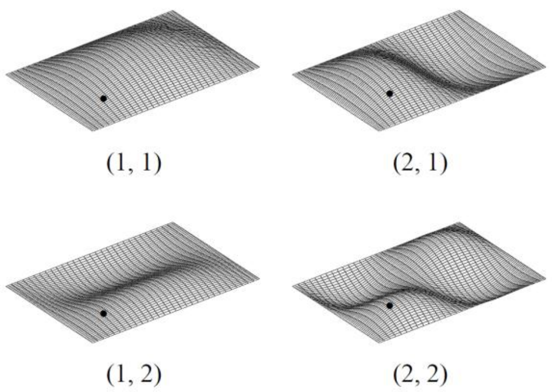

Fig.4 Resonant responses of simply-supported rectangular plate (SSSS, E_1)

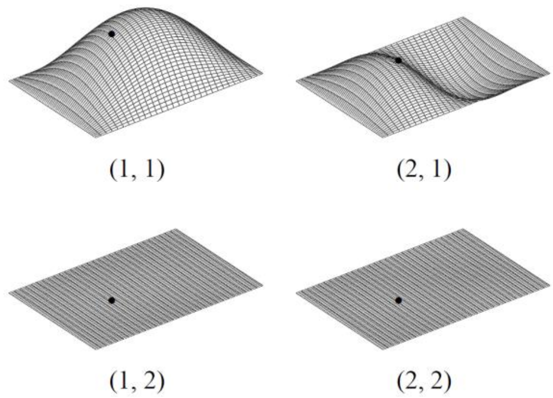

Fig.5 Resonant responses of simply-supported rectangular plate (SSSS, E_2)

Two Interesting Reminiscences

Arthur Leissa
Fort Collins, Colorado, USA

The writer was the advisor of 40 Ph.D. students and 20 M. Sc. students on their dissertations and theses, most of them dealing with vibrations of continuous systems. Below he is reminiscing about two of them that yielded particularly interesting results.

Nonlinear Free Vibrations of Taut Strings

In the study of vibrations of continuous systems or, for that matter, a mathematics course in Fourier series and boundary value problems, the problem of the transverse free vibration of a taut string of length L is often first considered. There it is assumed that the tension in the string is sufficiently large that it remains constant during the vibration. But if the string vibrates with a significant amplitude, the tension does change. How much does this affect the vibration?

This problem was taken up by Kirchhoff {1} more than a century ago. He derived the following equation of transverse motion for the string:

$$\left[T_0 + \frac{EA}{2L}\int_0^L \left(\frac{\partial w}{\partial x}\right)^2 dx\right]\frac{\partial^2 w}{\partial x^2} = \rho\,\frac{\partial^2 w}{\partial t^2} \qquad (1)$$

Here T_0 is now the string tension in its equilibrium position and the second term in the brackets is the tension increase due to transverse displacement averaged over the length of the string. The integro-differential equation (1) is nonlinear, and appears formidable. However a variable separable form of solution is possible, and it is exact. Assume that

$$w(x,t) = \phi(t)\sin\frac{m\pi x}{L} \qquad (2)$$

Substituting (2) into (1) yields

$$\phi'' + \frac{T_0}{\rho}\left(\frac{m\pi}{L}\right)^2\phi + EA\left(\frac{m\pi}{L}\right)^4\phi^3 = 0$$

This nonlinear ordinary differential equation in ϕ is the well known Duffing equation for a single d.o.f. system having a hard spring, and has an exact solution in terms of elliptic integrals.

A more general analysis has been carried out [2, 3], assuming an elastic string, but does not assume small slopes, and includes longitudinal motion along with the transverse. This resulted in two highly nonlinear, coupled equations in the two displacement components. Accurate numerical solutions were obtained by means of a form of the Galerkin method using incremental time steps and finite differences. Table 1 presents the ratio of the fundamental frequency obtained from the two types of nonlinear analysis described above to that from linear analysis for a variety of nondimensional amplitudes (δ/L) and of initial equilibrium strains (ϵ_0). From these results it is clear that the classical, linear solution is reasonably accurate only under very restricted conditions.

Table 1. Ratio (ω/ω_L) of nonlinear to linear frequencies.

$\frac{\delta}{L}$	ϵ_o	Coupled, large slope equations	Kirchhoff Eq. (2.137)
	10^{-1}	1.050	1.001
	10^{-2}	1.014	1.009
0.01	10^{-3}	1.089	1.088
	10^{-4}	1.673	1.673
	10^{-5}	4.324	4.331
	10^{-1}	1.073	1.023
	10^{-2}	1.213	1.207
0.05	10^{-3}	2.335	2.338
	10^{-4}	6.718	6.732
	10^{-5}	21.02	21.07
	10^{-1}	1.142	1.148
	10^{-2}	1.674	1.673
0.10	10^{-3}	4.298	4.331
	10^{-4}	13.23	13.35
	10^{-5}	41.73	42.10
	10^{-1}	1.366	1.314
	10^{-2}	2.785	2.850
0.20	10^{-3}	8.208	8.479
	10^{-4}	25.76	26.64
	10^{-5}	81.40	84.17
	10^{-1}	1.896	1.966
	10^{-2}	4.844	5.420
0.40	10^{-3}	14.87	16.86
	10^{-4}	46.76	53.24
	10^{-5}	*	168.3

Vibrations of Rectangular Membranes Subjected to Shear and Nonuniform Tensile Stresses

In the classical problem of transverse vibration of a membrane it is assumed that the boundary is stretched all around by uniform, static tensile stress. But what if the tensile stress is not uniform? Or if shear stresses also exist along the boundary? The equation of transverse free vibrations for this is

$$\frac{\partial}{\partial x}\left(\sigma_x \frac{\partial w}{\partial x}\right) + \frac{\partial}{\partial y}\left(\sigma_y \frac{\partial w}{\partial y}\right) + \frac{\partial}{\partial x}\left(\tau_{xy} \frac{\partial w}{\partial y}\right) + \frac{\partial}{\partial y}\left(\tau_{xy} \frac{\partial w}{\partial x}\right) = \rho \frac{\partial^2 w}{\partial t^2}$$

where, in addition to the static stresses shown, w is the transverse displacement and is the membrane mass density per unit area. This equation has no exact solution which would satisfy meaningful boundary conditions (e.g., w = 0) all around. But accurate results have been obtained by the very well known Ritz method [4, 5]. The transverse displacement is taken simply as

$$W(x,y) = \sum_{m=1}^{M} \sum_{n=1}^{N} A_{mn} \sin\frac{m\pi x}{a} \sin\frac{n\pi y}{b}$$

This set of functions is not only mathematically complete (guaranteeing upper bound convergence to the exact frequencies as sufficient terms are taken), but are orthogonal with each other (which simplifies the calculations). Fig. 1 shows nondimensional frequencies ($\omega a\sqrt{\rho/\sigma_x}$) and nodal patterns for a square membrane stretched by uniform tension all around, plus added uniform, inplane shear stress. It is seen that most (but not all) of the membrane frequencies are decreased by the addition of shear stress, and that severely distorted nodal patterns arise when the shear stress becomes large.

Fig. 1. Contour plots and nondimensional membrane frequencies for biaxial tension with added shear.

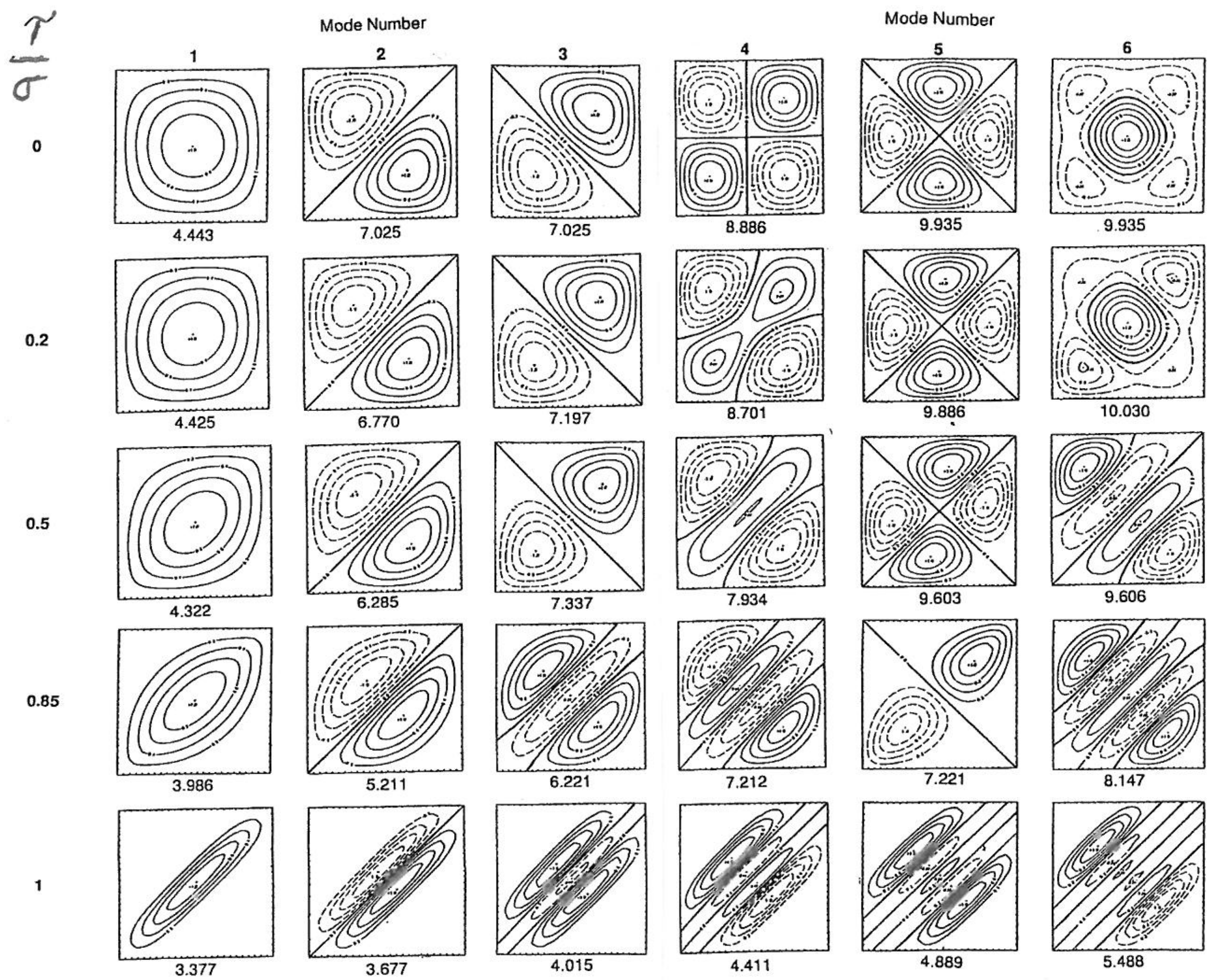

References

1. Kirchhoff, G. Vorlesungen uber Mathematische Physik: Mechanik. Leipzig, 1876
2. Saad, A,M. Nonlinear free vibration analysis of strings by the Galerkin method, Ph. D dissertation, Ohio State University, 1992.
3. Leissa, A. W. and Saad, A. M. Large amplitude vibrations of strings, J. Appl. Mech., Vol. 61, pp. 296-301, 1994.
4. Ghamat-Rezaei, A. Vibrations of a rectangular membrane subjected to non-uniform loading, M.Sc. thesis, Ohio State University, 1988.
5 Leissa, A. W. and Ghamat-Rezaei, A. Vibrations of rectangular membranes subjected to shear and nonuniform tensile stresses, J. Acoust. Soc. Amer., Vol. 88, No. 1, pp. 231-238, 1990.

Approach of a Mode Shape Function to Analyses on Nonlinear Vibrations of a Stepped Beam

Ken-ichi NAGAI, Shinichi MARUYAMA, Katsuya ISHIGAMI and Ryusuke KOBAYASHI
Department of Mechanical System Engineering, Graduate School of Engineering,
Gunma University, 1-5-1 Tenjin-cho, Kiryu, Gunma 376-8515, JAPAN, kennagai@gunma-u.ac.jp

1. Introduction Recently, technology of a micro electro-mechanical system (MEMS) has been developed drastically. Micro devices such as an acceleration pickup and an optical scanner are widely utilized. These devices are composed with elements of thin elastic structures. The elements have complicated shape with discontinuous cross section like a stepped beam or combined configuration of beam and plate. Dynamical responses of the elements are excited by an external force. Clear and large-amplitude responses of the elements are required. It is of practical importance to analyze nonlinear responses of beam and plate.

Introducing the mode shape function, which has been proposed by the senior author, analytical procedure is presented on nonlinear vibrations of a stepped beam. The stepped beam is divided into a few segments with different cross sections. The mode shape function is expressed with the product of truncated power series and trigonometric functions. The function is infinitely differentiable function of class C^∞ with the coordinate variable. The function satisfies the boundary conditions and continuity conditions with higher derivatives at connecting points of the segments of the stepped beam. First, linear natural frequencies and corresponding modes of vibration of the stepped beam are calculated with the similar procedure of the finite element analysis. Based on the coordinate functions of linear combination of the vibration modes and applying the Galerkin procedure, the nonlinear governing equations of the stepped beam is reduced to the nonlinear ordinary differential equations of motion in a multiple-degree-of-freedom system.

2. Mode Shape Function The authors have analyzed nonlinear vibrations of beams and arches(1),(2) with linear geometrical boundary conditions, of which ends are simply-supported or clamped. In the analyses, the non-dimensional deflection of the beams $\hat{w}(\xi,\tau)$ are assumed with the linear combinations of the mode shape function $\zeta_i(\xi)$ as follows:

$$\hat{w}(\xi,\tau)=\sum_j \hat{b}_j(\tau)\zeta_j(\xi),\quad \zeta_j(\xi)=e_j(\xi)f_j(\xi),\quad (j=1,2,3,...) \tag{1}$$

$$e_j(\xi)=\cos(j-1)\pi\xi,\quad f_j(\xi)=\sum_{k=1}^{5}c_{jk}\xi^{k-1},\quad (\xi=0\sim 1) \tag{2}$$

where ξ, τ and $\hat{b}_j(\tau)$ are the non-dimensional coordinate of the beam, the time and unknown time function. In the above equation, the trigonometric function $e_j(\xi)$ can set the number of nodes corresponding to the order of vibration mode j. The coefficients c_{jk} in the truncated power series $f_j(\xi)$ are chosen to satisfy the both geometrical and dynamical boundary conditions.

Moreover, the mode shape function has been also applied to a vibration of a cantilevered beam(3) and to nonlinear vibrations of beams with nonlinear dynamical boundary conditions, e.g., a post-buckled cantilevered beam of which free end is constrained by a stretched string(4). Furthermore, the nonlinear vibrations of a post-buckled L-shaped beam were analyzed(5). In these analyses, the trigonometric function $e_j(\xi)$ in the mode shape function is modified as follow:

$$e_j(\xi)=\cos p_{1j}\pi\xi+q_j\sin p_{2j}\pi\xi,\quad f_j(\xi)=\sum_{k=1}^{5}c_{jk}\xi^{k-1} \tag{3}$$

where the coefficients p_{1j}, p_{2j} and q_j are appropriately chosen to set the location of nodes. Based on the mode shape function, ordinary linear/nonlinear differential equations of motion in a multiple-degree-of-freedom system are derived by the modified Galerkin procedure.

3. Analytical Procedure To analyze nonlinear vibrations of a stepped beam, as shown in Fig.1, in which cross section changes discontinuously at several positions, the beam is divided into *N* segments. To obtain accurate results, assumed function should be infinitely differentiable and satisfies the continuity conditions of deflection, gradient, bending moment and shearing force at the boundary of neighboring segments. The deflection in each segment is assumed with the mode shape function. The deflection in the whole region of the beam is expressed with the global coordinate as:

$$\hat{w}(\xi,\tau) = \sum_j \hat{b}_j(\tau) Z_j(\xi), \quad (j = 1,2,3,...), \quad (\xi = 0 \sim 1) \tag{4}$$

where, $Z_j(\xi)$ denotes the coordinate functions composed with the mode shape function as:

$$Z_j(\xi) = \sum_{n=1}^{N} \zeta_{jn}(\xi_n) R(\xi, \xi_{[n-1]}, \xi_{[n]}), \quad \xi_n = d_n[\xi - (\xi_{[n-1]} + \xi_{[n]})/2], \quad d_n = (\xi_{[n]} - \xi_{[n-1]})^{-1} \tag{5 a,b}$$

$$\zeta_{jn}(\xi_n) = \sum_p \sum_q c_{njpq} (2\xi_n)^{q-1} \cos(p-1)\pi(\xi_n + 1/2), \quad (p = 1,2, q = 1,...4) \tag{5 c}$$

The function, $\zeta_{jn}(\xi_n)$ is the mode shape function of the j–th mode defined by the local coordinate in the n–th segment ξ_n from $\xi_n = -1/2$ to $\xi_n = 1/2$. The symbol c_{njpq} is the unknown coefficients. The function $R(\xi, \xi_{[n-1]}, \xi_{[n]})$ implies the rectangular window within the n–th segment from $\xi_{[n-1]}$ to $\xi_{[n]}$ in the global coordinate. The nonlinear governing equations of the stepped beam, neglecting the axial inertial force, are shown with the Hamilton's principle as:

$$\begin{aligned}\int_{\tau_0}^{\tau_1} \sum_{n=1}^{N} \Bigg\{ \int_{\xi_n=-1/2}^{\xi_n=1/2} \Bigg[\frac{1}{d_n} \bar{\rho}_n \bar{A}_n A_n(\xi_n) \hat{w}_{,\tau\tau} - d_n \hat{m}_{xn,\xi_n\xi_n} - d_n(\hat{n}_x \hat{w}_{,\xi_n})_{,\xi_n} \\ - \frac{1}{d_n} \bar{\rho}_n \bar{A}_n A_n(\xi_n)\left(p_s + p_d \cos\omega\tau\right) \Bigg] \delta\hat{w} d\xi_n + \left[\hat{q}_{xn}\delta\hat{w}\right]_{-1/2}^{1/2} - \left[d_n \hat{m}_{xn} \delta\hat{w}_{,\xi_n}\right]_{-1/2}^{1/2} \Bigg\} d\tau = 0\end{aligned} \tag{6 a}$$

$$\begin{aligned}\hat{n}_x &= \kappa \left\{ u_e + \sum_{m=1}^{N} \int_{\xi_m=-1/2}^{\xi_m=1/2} \frac{d_m}{2} (\hat{w}_{,\xi_m}{}^2 - w_{0,\xi_m}{}^2) d\xi_m \right\} \\ \kappa &= \left\{ \sum_{m=1}^{N} \frac{1}{d_m \bar{E}_m \bar{A}_m \gamma_m} \right\}^{-1}, \quad \gamma_m = \left\{ \int_{-1/2}^{1/2} A_m(\xi_m)^{-1} d\xi_m \right\}^{-1}\end{aligned} \tag{6 b}$$

$$\hat{m}_{xn} = -d_n^2 \bar{E}_n \bar{I}_n I_n(\xi_n)\left(\hat{w}_{,\xi_n\xi_n} - w_{0,\xi_n\xi_n}\right), \quad \hat{q}_{xn} = d_n \hat{m}_{xn,\xi_n} + d_n \hat{n}_x \hat{w}_{,\xi_n} \tag{6 c,d}$$

In Eq. (6 a), from the first to forth terms correspond to the inertia force, the restoring force, the lateral force due to the axial force $\hat{n}_x$ and the external force, respectively. Eq. (6 b) denotes the axial force which includes the nonlinear terms of deflection $\hat{w}_{,\xi_m}{}^2$ and initial axial displacement u_e of a beam end. The symbol w_0 implies the initial lateral deflection of the beam. Eqs. (6 c) and (6 d) denote the bending moment $\hat{m}_{xn}$ and the restoring force, respectively.

Based on the linearized governing equation (6 a), the modes of linear vibration are determined. Choosing deflection, gradient, bending moment and shearing force at the both ends of the segment as the unknown variables, the unknown coefficients $c_{njpq}, (p = 1,2, q = 1,...4)$ in the mode shape function Eq. (5 c) are expressed with unknown eight variables in one segment. Following to a similar manner of the finite element procedure, the modes of linear vibration are determined.

The vibration modes composed by the mode shape functions in each segment are used as the coordinate functions $Z_j(\xi)$ in the nonlinear governing equations for static deflections $\bar{w}(\xi)$ and dynamic responses $\tilde{w}(\xi,\tau) = w(\xi,\tau) - \bar{w}(\xi)$. It is noteworthy that number of coordinate functions in the nonlinear analysis can be drastically decreased compared with the degrees of freedom in the foregoing calculation of linear vibration modes.

$$\left[\bar{w}(\xi), \tilde{w}(\xi, \tau)\right] = \sum_j \left[\bar{b}_j, \tilde{b}_i(\tau)\right] Z_j(\xi) \tag{7}$$

Applying the Galerkin procedure to the static equilibrium equation of the beam, the following simultaneous nonlinear cubic equations in terms of $\bar{b}_j$ are obtained as follows.

$$\sum_j \hat{C}_{ij} \bar{b}_j + \sum_j \sum_k \sum_l \hat{E}_{ijkl} \bar{b}_j \bar{b}_k \bar{b}_l - \hat{F}_i - p_s \hat{G}_i = 0, \quad (i,j,k,l = 1,2,...) \tag{8}$$

The equation of motion in terms of the dynamic response $\tilde{w}(\xi,\tau)$ is also transformed to ordinary differential equations in multiple-degree-of-freedom system. Furthermore, the ordinary differential equations are transformed to the standard form in terms of normal coordinates $b_j(\tau)$ corresponding to the linear natural modes of vibration $\tilde{\zeta}_j(\xi)$ at the static equilibrium position of the stepped beam as follows.

$$b_{i,\tau\tau} + 2\varepsilon_i\omega_i b_{i,\tau} + \omega_i^2 b_i + \sum_j\sum_k D_{ijk}b_jb_k + \sum_j\sum_k\sum_l E_{ijkl}b_jb_kb_l - G_ip_d\cos\omega\tau = 0 \qquad (9)$$

Dynamic responses are calculated with the harmonic balance method or the numerical integration. The foregoing analysis can be named as the nonlinear finite segment analysis (NLFSA).

4. Results and Conclusion Table 1 shows the convergence of the non-dimensional natural frequencies of a uniform beam simply-supported at both ends. The results divided into two segments of the beam agree well with the exact results to fourth modes of vibration. Figs. 2 and 3 show the natural frequency and the corresponding modes of vibration of a stepped beam with a rectangular cross section. The thickness h_2 of the beam within the region from $\xi = 0.4$ to $\xi = 0.6$ is changed compared with uniform thickness h_1. As the thickness h_2 is increased, the natural frequencies increase first, and then decreases related to the increase in the mass and the bending rigidity of the beam. Fig.4 shows the nonlinear steady-state response of stepped beams clamped at both ends. The frequency response curves correspond to the characteristics of restoring force of a hardening spring. As the thickness h_2 is increased, the frequency response curve approaches slightly to that of linear case because of the drastic increase in the mass of the stepped beam.

References

1) Nagai, K., Nagaya, K., Takeda, S. and Arai, N.: A Free Vibration of Beams Carrying a Concentrated Mass under Distributed Axial Forces, *Transaction of the JSME, Ser. C*, Vol. 54 No. 497, pp.39-46, (1988). (in Japanese)
2) Maruyama, S., Nagai, K., Yamaguchi, T. and Hoshi, K.: Contribution of Multiple Vibration Modes to Chaotic Vibrations of a Post-buckled Beam with an Axial Elastic Constraint, *Journal of System Design and Dynamics*, Vol. 2 No. 3, pp.738-749, (2008).
3) Nagai, K.: A Mode Shape Function Approach to Vibrations of Beams with Variable Cross Section, *Proc. of Asia-Pacific Vibration Conference*, pp.1452-1457, (1993).
4) Maruyama, S., Nagai, K., Muto, K. and Yamaguchi, T.: Chaotic Vibrations on a Coupled Vibrating System of a Post-Buckled Cantilevered Beam and Axial Vibrating Body Connected with a Stretched String, *Proc. of ASME 2009 IDETC & CIE* (CD-ROM), DETC2009-87230, (2009).
5) Onozato, N,. Nagai, K., Maruyama, S. and Yamaguchi, T.: Analysis on Chaotic Vibrations of a post-buckled L-shaped Beam with an Axial Constraint, *Proc. 13th Conference on Nonlinear Vibrations, Dynamics and Multibody Systems* (CD-ROM), Session No.2-2, (2010).

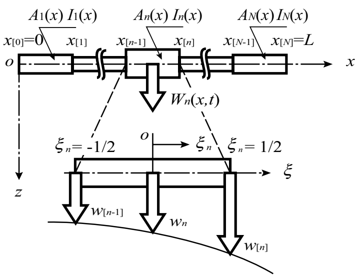

Fig. 1 Dynamical model of a stepped beam

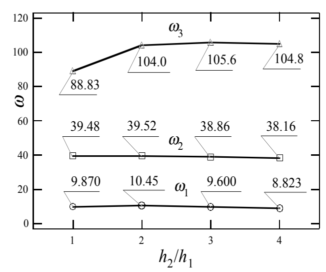

Fig. 2 Natural frequencies of a stepped beam (simply-supported)

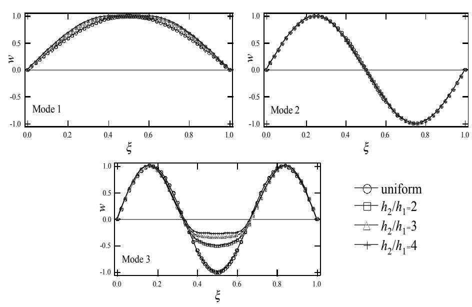

Fig. 3 Linear vibration modes of a stepped beam (simply-supported)

Table 1 Natural frequencies of a uniform beam simply-supported at both ends

number of segments	natural frequency				
	ω_1	ω_2	ω_3	ω_4	ω_5
1	9.8696	39.477	90.214	148.44	…..
2	9.8696	39.478	88.826	157.91	247.34
3	9.8696	39.478	88.826	157.91	246.74
4	9.8696	39.478	88.826	157.91	246.74
Exact solution	9.8696	39.478	88.826	157.91	246.74

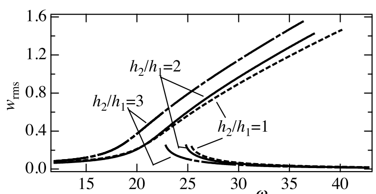

Fig. 4 Nonlinear frequency response curves of a stepped beam (clamped)

Vibration Optimization of Composite Laminated Shallow Shells with respect to Surface Shapes and Lay-ups

Yoshihiro NARITA, Shinya HONDA, Takeru KATO* and Daisuke NARITA**

Faculty of Engineering, Hokkaido University,
N13W8, Kita-ku, Sapporo, Hokkaido, 060-8628, Japan, ynarita@eng.hokudai.ac.jp
*graduate student, Hokkaido University, **Hokkaido Automotive Engineering College

1. Introduction

Free vibration of laminated composite shallow shells with variable surface shapes and lay-up configurations is analyzed. The semi-analytical Ritz solution is used in a simple genetic algorithm to optimize the frequency with respect to surface shapes and lay-ups. The shell shape is defined by a cubic polynomial and this makes it possible to express the shell shape with variable curvature radii by varying the value of coefficient in each term. The coefficient and the lay-up configuration of the laminated shell are directly employed as design variables, and constraints are imposed on the coefficients and curvature radii to keep the present shells being shallow. In numerical examples, the present analysis gives results to agree well with experimental and finite element analysis results. It is demonstrated that the obtained optimum solutions result in higher fundamental frequencies than the shells with typical shapes and lay-up configurations.

2. Analysis of laminated shallow shells with variable curvature

The Ritz method is used to obtain the natural frequencies of the shell with variable curvature. For a shell geometry shown in Fig.1, the surface geometry is expressed [1] by a cubic polynomial as

$$\phi(x,y) = c_{20}x^2 + c_{11}xy + c_{02}y^2 + c_{30}x^3 + c_{21}x^2y + c_{12}xy^2 + c_{03}y^3 \qquad (1)$$

where c_{pa} (p, q = 0, 1, 2, 3) are coefficients to determine the surface geometry. Under the assumption that the slope of surface changes moderately, i.e. $(\partial\square/\partial x)^2 = (\partial\square/\partial y)^2 = 0$, then the curvature is given by

$$\frac{1}{R_x} = 2(c_{20} + 3c_{30}x + c_{21}y),\ \frac{1}{R_y} = 2(c_{02} + c_{12}x + 3c_{03}y),\ \frac{1}{R_{xy}} = c_{11} + 2c_{21}x + 2c_{12}y \qquad (2)$$

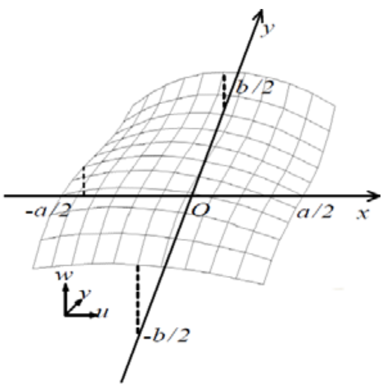

Fig. 1 The coordinate systems $O-xyz$ for the present shell.

In applying the Ritz method, one has to formulate the strain and kinetic energies, and the strain energy is given by

$$V = V_s + V_{bs} + V_b \tag{3}$$

where V_s is the energy due to stretching motion, V_{bs} is to coupling motion between stretching and bending and V_b is to bending motion [2]. After applying the minimizing procedure, one gets a frequency equation as

$$\left(\begin{bmatrix} k_{11} & k_{12} & k_{13} \\ k_{12} & k_{22} & k_{21} \\ k_{13} & k_{21} & k_{33} \end{bmatrix} - \Omega^2 \begin{bmatrix} m_{11} & 0 & 0 \\ 0 & m_{22} & 0 \\ 0 & 0 & m_{33} \end{bmatrix} \right) \begin{Bmatrix} P_{ij} \\ Q_{kl} \\ R_{st} \end{Bmatrix} = 0 \tag{4}$$

where k_{ij} and m_{ij} (i, j = 1, 2, 3) are elements of the stiffness and mass matrices, and P_{ij}, Q_{kl} and R_{st} are undetermined coefficients which appear in displacement functions. Solving the eigenvalue problem, the eigenvalue gives values of natural frequencies in non-dimensional form $\Omega = \omega a^2(\rho / D_0)^{1/2}$ with $D_0 = E_2 h^3/12(1 - \nu_{12}\nu_{21})$ being a reference stiffness.

3. Optimum design for the maximum fundamental frequency by a genetic algorithm

The design variables are taken as the coefficients c_{pa} (p, q = 0, 1, 2, 3) to represent the surface geometry and the fiber orientation angles θ_i (i = 1, 2, 3, 4) to represent the angles for upper (or lower) half layers of symmetrically laminated eight-layer shells. The object function is the fundamental frequency to be maximized. Then the optimization problem is formulated as

$$\begin{aligned} &\text{Maximizing}: \quad \Omega_1 \\ &\text{Design variable}: \quad c_{pq}\,(p, q = 0,1,2,3),\ \ \theta_i\,(i = 1,2,3,4) \\ &\text{Subject to}: \quad -0.20 \le c_{pq} \le 0.20,\ -0.5 \le \frac{1}{R_x}, \frac{1}{R_y}, \frac{1}{R_{xy}} \le 0.5, \\ &\qquad\qquad\quad -90° < \theta_i \le 90° \end{aligned} \tag{5}$$

The optimization is made by using a simple Genetic Algorithm [3]. A gene of an individual (parameters of curvature and fiber angle) is represented by binary digits, and the parents are chosen by a roulette method. An elite tactics is used to suppress divergence of optimum solutions, and violation of the shallow shell theory is avoided by imposing the penalty on the object function.

4. Numerical results

In numerical examples, the material constants for a typical CFRP material are used as

E_1 = 138 [GPa], E_2 = 8.96 [GPa], G_{12} = 7.1 [GPa], ν_{12} = 0.30

An aspect ratio is taken as a / b = 1.0 (square planform), and the thickness is a value of relatively thin as h / a = 0.01. The notation for boundary conditions is given by a set of four capital letters of F (free), S (simple support) and C (clamp), starting from left-hand-side edge. This notation is introduced so that the image of the plate boundary condition is directly applicable, and therefore the in-plane boundary conditions of F and C are totally free and constrained, respectively. The S2 type condition is applied to S. Twelve different combinations are considered.

Figure 2 shows four examples CCCC, SSSS, FSFS and CFFF, chosen from the twelve sets of boundary conditions in the numerical study, on the optimum surface shapes and lay-up designs. In (a) totally clamped case (CCCC), the surface shape presents a part of sphere, and the lay-up is given by [1st (outer most) layer/ 2nd layer/ 3rd layer/ 4th (inner most) layer]$_s$= [15/-75/60/-30]$_s$. It is noted that the first and second layers cross perpendicular each other, and likewise between the third and fourth layers. A similar surface shape is found for (b) SSSS, and it is suggested that the uniform boundaries, i.e. CCCC and SSSS, tend to give spherical surface as the optimum shape.

In conclusion for the shells of square planform, when a pair of opposite edges is supported in (c) FSFS, the optimum shape becomes hyperbolic paraboloidal shape. In this case, the first and second layers take 90 degree (perpendicular to the simply supported edges) and inner third and fourth layers take different angles, unlike the flat plate with optimum angles all being 90 degree. It is also seen that in (d) CFFF, the optimum shape is similar to the hyperbolic paraboloidal shape. As for the experiment, the results will be presented in the oral presentation.

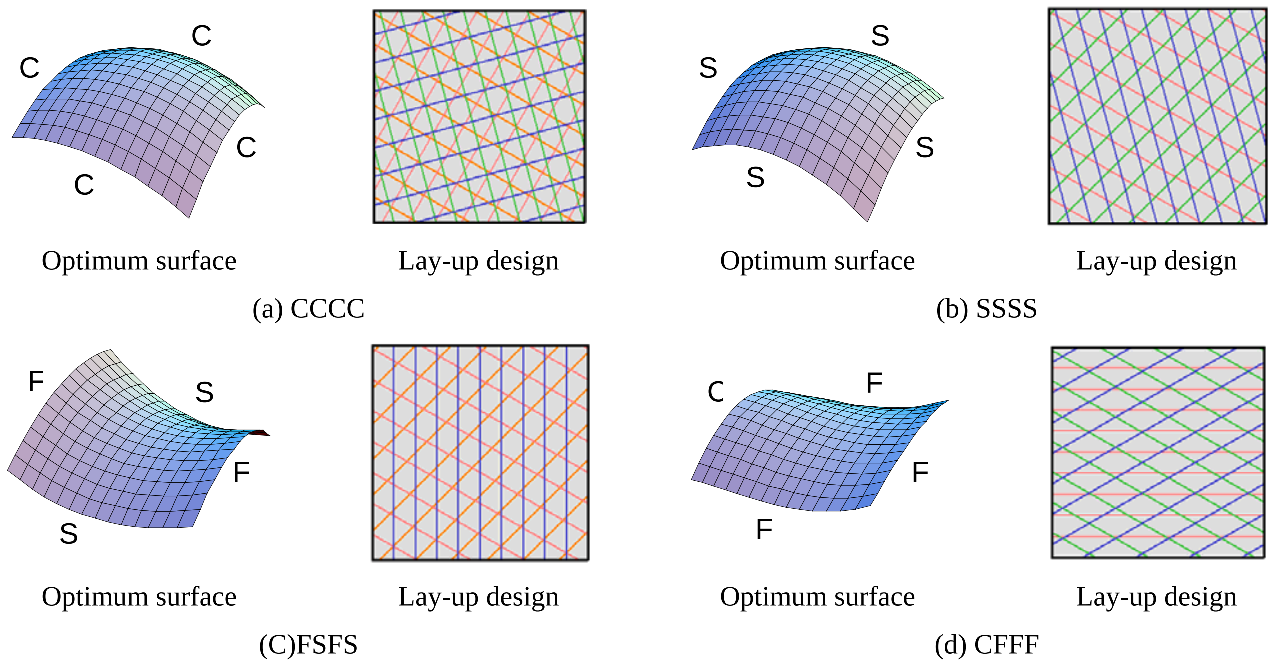

Fig. 2 The optimum surface shapes and lay-up configurations for (a) CCCC, (b)SSSS, (c)FSFS and (d) CFFF of shallow square shells with symmetric 8-layers.

References

(1) Narita, Y. and Narita, D., Free Vibration of Shallow Shells with General Surfaces Expressed in Cubic Polyonomial Function, *Proceedings of the Sixth International Symposium on Vibrations of Continuous Systems*, (2007.7), Squaw Valley, California, USA.

(2) Narita, Y., Robinson, P., Maximizing the fundamental frequency of laminated cylindrical panels using layerwise optimization, *International Journal of Mechanical Sciences*, Vol.48, (2006), pp.1516-1524.

(3) Narita, Y., Itoh, M., Zhao, X., Optimal design by genetic algorithm for maximum fundamental frequency of laminated shallow shells, *Advanced Composite Letters*, Vol.5, (1996), pp.21-24.

Nonlinear dynamics of cylindrical shells: nonlinear modal coupling and energy diffusion

Francesco Pellicano

Dipartimento di Ingegneria Meccanica e Civile, Univ. di Modena e Reggio Emilia, Modena, Italy

Abstract.

The goal of this paper is to investigate and explain complex dynamic phenomena arising in circular cylindrical shells under base excitation. The experiment consists of a shell connected with a rigid body on the top and a base excitation. A violent resonant phenomenon is experimentally observed when a harmonic base excitation is close to the resonance of the first axisymmetric mode: saturation, energy spreading from low to high frequencies and nonstationarity are observed. A theoretical model is developed to reproduce the phenomenon; the model takes into account geometric shell nonlinearities and the interaction with an electrodynamic shaker, which provides the base excitation.

Introduction

Nowadays several commercial software allows to carry out static, stability and vibration analyses; however, regarding the shell dynamics, such kind of analyses are generally reliable in the linear filed, i.e. very small deformations. Problems like global stability, post-critical behaviours and nonlinear vibrations cannot yet be accurately analyzed with commercial software; on such fields there is need of further development of computational models.

The problem under investigation was studied on linear basis in Ref. [1], where a new method, based on the nonlinear Sanders Koiter theory, was developed. Among the others, the method showed good accuracy also in the case of a shell connected with a rigid body; this method is the starting point for the model developed in the present research.

A work strictly related with the present paper is due to Mallon et. al [2], they studied circular cylindrical shells made of orthotropic material, the Donnell's nonlinear shallow shell theory was used with a multimode expansion for discretization (PDE to ODE). They presented also experimental results. The theoretical model considered also the shaker-shell interaction (it is to note that one of the first works concerning the interaction between an electromechanical shaker and a mechanical system is due to Krasnopol'skaya [3]). No good quantitative match between theory and experiments was found: saturation phenomena, beating and chaos were found numerically. However, this can be considered a seminal work due to the intuition that some complex phenomena can be due to the shaker shell interaction.

In the present paper, experiments are carried out on a circular cylindrical shell, made of a polymeric material (P.E.T.) and clamped at the base by gluing its bottom to a rigid support. The axis of the cylinder is vertical and a rigid disk is connected to the shell top end. Nonlinear phenomena are investigated by exciting the shell using a shaking table and a sine excitation, the base excitation induces a vertical motion of the top disk that causes axial loads due to inertia forces. Such axial loads generally give rise to axial-symmetric deformations; however, in some conditions it is observed experimentally that a violent resonant phenomenon takes place, with a strong energy transfer from low to high frequencies and huge amplitude of vibration. Moreover, an interesting saturation phenomenon is observed: the response of the top disk was completely flat as the excitation frequency was changed around the first axisymmetric mode resonance.

A semi-analytical approach is proposed for reproducing experimental results and giving a deeper interpretation of the observed phenomena. The model considers nonlinear Sanders-Koiter theory for the shell and the modelling of the interaction with the shaker. Comparisons between experiments and numerical results show a good behaviour of the model, numerical analyses furnish useful explanations about the instability phenomena that are observed experimentally.

Experimental results

The system under investigation is described in Figure 1; a circular cylindrical shell, made of a polymeric material (P.E.T.), is clamped at the base by gluing its bottom to a rigid support (a disk that is rigidly bolted to a shaker, such disk is technically called "fixture"); the connection is on the lateral surface of the shell, in order to increase the gluing surface, see Figure 1. A similar connection is carried out on the shell top; in this case the shell is connected to a disk made of aluminium alloy, such disk is not externally constrained; therefore, it induces a rigid body motion to the top shell end.

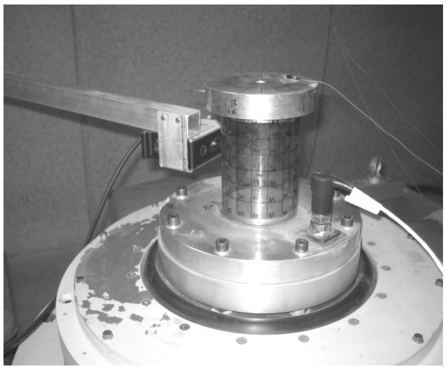

Figure 1. Experimental setup.

Material characteristics are directly measured with specific tests (Young modulus E and mass density ρ) or found in literature (Poisson ratio ν).

The material parameters of the shell are the following: $= 1366\frac{\text{kg}}{m^3}$; $\nu = 0.4$; $E = 46\times10^8\,\frac{\text{N}}{\text{m}^2}$; the mass of the top disk is 0.82kg. The geometrical parameters are: mean radius $R = 43.88 \times 10^{-3}$m, shell length $L = 96 \times 10^{-3}$m, shell thickness $h = 0.25 \times 10^{-3}$m, $\frac{R}{h} = 176$, $\frac{L}{R} = 2.19$.

The fixture is bolted to a high power shaker (LDS V806, 13000N peak force, 100g maximum acceleration, 300kg payload, 1-3000Hz band frequency); such shaker is used to excite the shell from the base.

Figures 2a-d represent the amplitudes of vibration in terms of acceleration (base and top disk vibration) or displacement (measured on the lateral surface of the shell, the vertical position is on the middle): during experiments the input voltage was sinusoidal ($v(t)=v_0\sin(2\pi\ f\ t)$, v_0=0.07V) and the frequency was moved step by step. Figure 2a shows that the maximum excitation (base motion) is between 8 and 14 g; from such data one can guess that there is a strong interaction between the shaker and the shell-disk; it is worthwhile to remember that the shaker control is open loop.

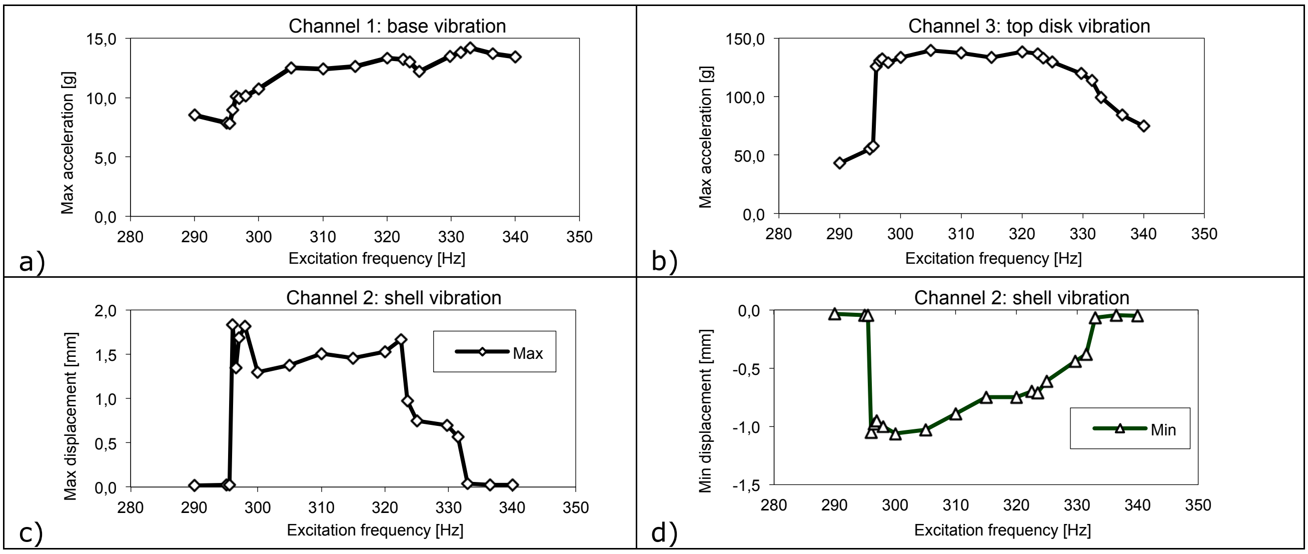

Figure 2. Experimental results, harmonic excitation, amplitude of vibrations: a) base excitation amplitude (acceleration [g]), b) top disk amplitude (acceleration [g]), c) response on the shell mid-span (displacement [mm], positive inward), d) minimum response of the shell mid-span (displacement [mm], negative outward.

The top disk vibration (Fig. 2b) increases as the first axisymmetric mode resonance is approached, from 333 Hz to 320 Hz the slope of the curve changes, when the excitation frequency is less than 322 Hz the top disk vibration amplitude remains flat up to 295 Hz; below such frequency the top disk response amplitude drops down.

Figure 2c shows the maximum amplitude of vibration (positive for inward shell deflection). For excitation frequencies higher than 333 Hz the shell vibration is small. Reducing the excitation frequency below 333Hz, the shell vibration amplitude suddenly grow up, at 331.5 Hz the amplitude is 0.57 mm, the increment is 1325%; such huge increment takes place in a narrow frequency band, i.e. from 333 Hz to 331.4 Hz (about 0.5% frequency variation); these data show that a new dynamic phenomenon appears suddenly. Another jump in the shell response is observed from 325 Hz to 320 Hz. Reducing the excitation frequency to 300 Hz does not cause a big changing in the response, which remains almost flat; from 300 Hz to 296 Hz.

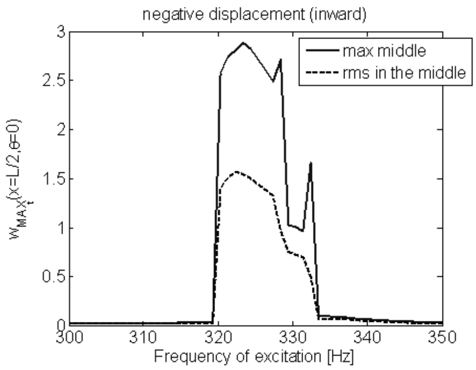

Figure 3. Amplitude frequency diagrams, numerical simulations, backward frequency sweep, shell vibration (mm). inward (negative) displacement and RMS(w)

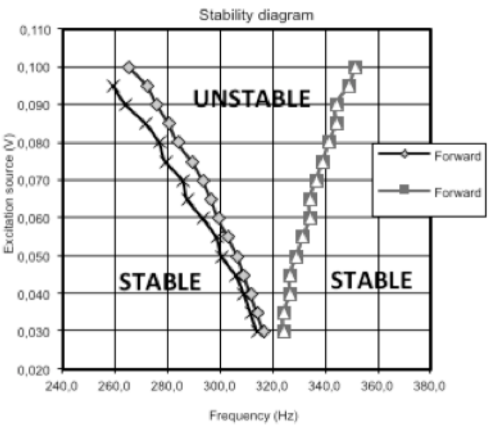

Figure 4. Stability diagram: experiments

Figure 2d shows the behaviour of the minimum shell vibration (negative means outward deflection).

Figure 3 shows results of simulations carried out considering an input voltage equal to 0.09V, this value is larger than the excitation used during the experiments (0.07V); however, below such value the numerical model did not detect any dynamic instability. Simulations

are carried out by decreasing the excitation frequency. The behavior is coherent with the experimental results (see Figure 2c), the numerical model overestimates the amplitude of vibration (experiments give 1.8mm max inward vibration) and underestimates the frequency range for which the instability
Figure 4 shows that the boundaries are almost straight lines starting from 320 Hz, they behave similarly to the classical Ince-Strutt diagrams referred to the instability regions of the Mathieu equation, which is the paradigm for problems with time varying coefficients (parametric excitation). For such reason, the region where huge vibrations take place is named here "instability region". Figure 4 suggests that the present phenomenon can be correlated to large in-plane loads, which are generated on the shell when the first axisymmetric mode undergoes to the resonance; such loads induce a parametric excitation on the shell like modes, which are high frequency modes, this is an explanation of the energy transfer from low to high frequency. The left and right boundaries of Figure 4 should theoretically touch each other at the bottom, depending on the damping; however, it was impossible to find experimentally such minimum.

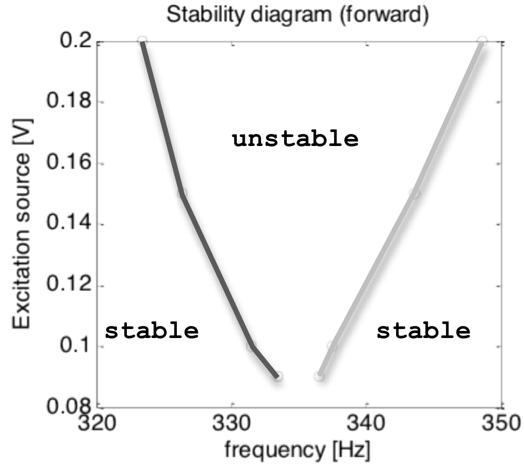

Figure 5. Stability diagram:

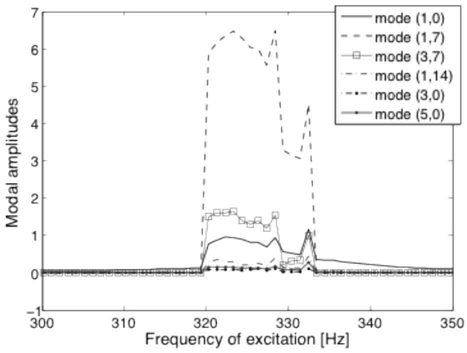

Figure 6. Modal amplitudes of the radial displacement w, amplitude frequency diagrams, numerical simulations, excitation source 0.09V.

Figure 5 shows the stability boundaries obtained numerically by varying both the excitation source voltage and frequency; the boundaries are coherent with experiments, this is a further confirmation that the instability is due to a parametric resonance. The boundaries, obtained by increasing the excitation frequency (forward), are quite similar to the experimental boundaries; numerical boundaries are moved up with respect to the experiments, i.e. for the same excitation voltage the experimental instability region is wider. Backward boundaries are not presented for the sake of brevity.
Figure 6 shows the modal amplitudes referred to the radial, this figure clarifies that, outside the instability region the sole active mode is the first axisymmetric one (mode m=1, n=0), with an almost negligible contribution of mode (5,0). When the instability takes place, the mode (1,7) is excited and absorbs the most of the vibration energy, mode (1,0) is still excited in such region, but it seems to be driven by the resonant mode (1,7); the third mode, that is strongly excited, is the mode (3,7), it is driven by the cubic nonlinearities of the system; the other modes are scarcely excited. The analysis of the mode components clarifies the energy transfer mechanism occurring during the dynamic instability: the energy inlet is provided at low frequency (close to the resonance of mode (1,0)), when the instability takes place there is an energy transfer to the high frequency mode (1,7) (the frequency of such mode is 793Hz).

Conclusions

Experiments clearly show a strong nonlinear phenomenon appearing when the first axisymmetric mode is excited: the phenomenon leads to large amplitude of vibrations in a wide range of frequencies, it appears extremely dangerous as it can lead to the collapse of the shell; moreover, it appears suddenly both increasing and decreasing the excitation frequency and is extremely violent.
The theoretical model shows satisfactory agreement with experiments and clarifies the energy transfer mechanism from low frequency axisymmetric modes and high frequency asymmetric modes, confirming the conjecture arising by the experimental data analysis. The instability type is not yet clarified, time responses show no sub-harmonic response, therefore it seems that the instability regions is the secondary one. Once the model will be completely set and the agreement with experiments will be fully satisfactory, a deeper bifurcation analysis will be carried out to have a complete clarification.

References

[1] Pellicano, F., 2007. Vibrations of circular cylindrical shells: theory and experiments. J. of Sound and Vibration, 303, 154–170.
[2] Mallon, N.J., Fey R.H.B., and Nijmeijer, H., 2008. Dyn. stab. of a thin cyl. shell with top mass subjected to harmonic base-acc. Int. J. of Solids and Structures, 45(6), 1587-1613.
[3] Krasnopol'skaya, T. S., 1976. Self-excitations by an electrodynamic vibrator. Kiev State University, transl. Prikladnaya Mekhanika, 13(2), 108-113.

Tracking of Eigenfrequencies of Vibrating Beams by Phase-Locked Loops

Wolfgang Seemann, Dominik Kern, Tobias Brack

Chair for Engineering Mechanics (ITM), Karlsruhe Institute of Technology (KIT), Germany

Abstract

Resonance excitation, the worst case for civil engineers, is of interest for mechanical engineers, as this can lead to an improved efficiency in some applications. The eigenfrequencies can be calculated from the material and geometrical parameters, however there is some uncertainty and they may vary with time. Thus a controller that adapts to the varying eigenfrequency is very attractive. Since the phase difference between excitation and response is an indicator for resonances, a Phase-Locked Loop (PLL) appears as an appropriate approach. With some modifications of the conventional PLL from radio electronics it is possible to track varying eigenfrequencies fast and robust in simulation and experiment. There are two categories of applications for resonance tracking: as actuator to obtain maximum power transmission and as sensor to extract information about the mechanical systems in terms of its mass-, damping-, stiffness- distribution or its boundary conditions. Typical structural models are continua with an infinite number of eigenfrequencies in contrast to concentrated parameter models with only one Degree of Freedom (1-DoF) and consequently only one eigenfrequency. The tracking of higher modes should also be taken into consideration, as it has potential for optimization, such as certain mode combinations in ultrasonic motors.

As an example a clamped-clamped beam is investigated that is excited in its second eigenfrequency. There are two reasons for modeling the beam. First the Frequency Response Function (FRF) should be calculated to characterize resonances and secondly a state space model has to be built for further simulations. The beam including its actuation and sensing with Macro Fibre Composites (MFCs) is modeled according to the Bernoulli-Euler theory in consideration of prestress and outer damping [1,2]. The FRF is found by a harmonic ansatz and gives the transfer function between actuator moment (input) and sensor charge (output). It allows the finding of a good sensor location to excite a certain mode, while blinding out others. Further it reveals that a change of the prestress distinctly shifts the resonance peaks and the corresponding characteristic phase differences. These characteristic phase differences are 90° for all modes. Thus the approach is a modified PLL to perform the tracking. The conventional PLL [3] consists of a phase detector, a low-pass filter and a Voltage Controlled Oscillator (VCO). It is widely spread for the frequency demodulation in radio receivers, where it follows the frequency leaving a certain phase difference as controller offset. In terms of control theory it corresponds to a proportional controller. In order to follow the phase exactly with zero phase deviation, the proportional controller needs to be enhanced by an integral term, i.e. the phase must be controlled by a PI-controller as shown in Fig. 1. A key component is the phase detector. The choice is made for the Phase-Frequency-Detector (PFD), because it has a phase difference detection range from $-2\pi \ldots +2\pi$ and it has a theoretically infinite pull-in range.

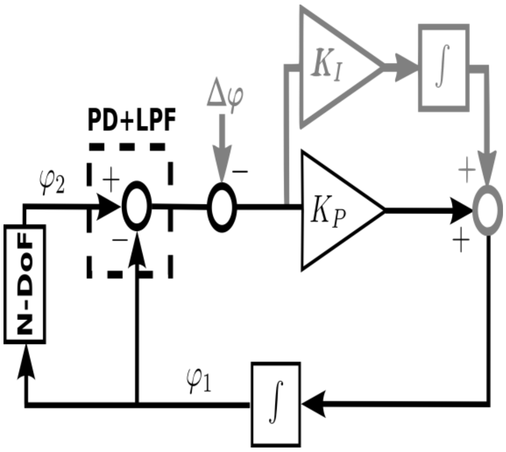

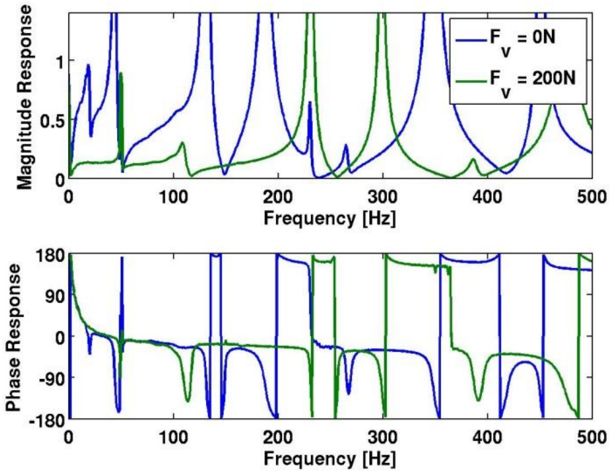

Fig.1: Structure of the PLL, modifications are marked grey

Fig.2: Experimentally measured FRF of the beam unstressed (blue) and prestressed (green)

The parameters of the low-pass filter and the controller are determined by simulations. There the PLL is combined with a state space model of the beam, which is formulated by a Galerkin scheme using the eigenfunctions of the homogeneous solution as trial functions. Both beam model and PLL components are linear systems, however the closed loop is a nonlinear control system due to the conversion between harmonic signals of the beam bending and phase signals inside the PLL.

The experimental setup consists of a clamped-clamped beam made of spring steel. One clamp is fixed while the other has a translational degree, which can be set either by a thread drive in order to increase the prestress continuously or by a weight dropping for a step change. The piezoelectric transducers (MFC type) are bonded on front and back surface at a location that excites the second mode strongly and the third not. At first the FRF was captured. It is shown in Fig. 2. It confirms the predictions from the simulation, Note, the phase range is periodic -π…+π. Finally the tracking of continuous and step changes of the beam's eigenfrequency was carried out. By inspection of the step response it was found that the closed loop can be approximated as a linear system of third order. This approximation turned out to be very helpful for fine-tuning of the controller parameters.

Acknowledgement This work was supported by the Priority Program No.1156 "Adaptronics in Tooling Machines" of the German Research Foundation (DFG).

References

[1] P. Hagedorn*, A. DasGupta, Vibrations and Waves in Continuous Mechanical Systems* (2007), p.150.

[2] A. Preumont*, Vibration Control of Active Structures 2. Edition* (2002), p. 51.

[3] R. Best, *Phase-Locked Loops 6. Edition* (2007), p. 20

Extensional and flexural modes of vibration of single layer graphene sheets by lattice structure and continuum plate theories

A. V. Singh and S. Arghavan
Department of Mechanical & Materials Engineering,
The University of Western Ontario, London ON N6A 5B9, Canada.
E-mail: avsingh@uwo.ca

Introduction. Novoselov and his colleagues [1,2] very recently demonstrated for the first time that a two dimensional free standing carbon structure can exist with stable atomic structure. It was termed as graphene and showed great potential for many future applications in nano-composites due to exceptionally superior mechanical, thermal and electrical properties. A graphene sheet is made of carbon atoms which are tightly packed into a 2D array of hexagonal cells and held together by covalent bond between adjacent carbon atoms. This molecular structure, therefore, allows to treat graphene as a plane lattice structure with honeycomb cells. Each side of a hexagonal cell represents the covalent bond between the carbon atoms and provides structural strength to keep atoms from getting apart. Each carbon atom in the analysis is considered as a nodal point at which the mass is assumed to be concentrated. Also, six degrees of freedom are assigned to each node. These correspond to three displacement and three rotation components about the Cartesian axes. A frame element joining two carbon atoms has axial, bending and torsional stiffness properties [3]. Studies based on this approach have been made and reported in the literature by a large number of researchers [3-6]. This paper deals with the free vibration analysis of various shaped graphene sheets by the lattice structure method and keeping this method as the basis, an equivalent continuum plate method of analysis is suggested.

Methods of Analysis. The geometric and material properties of the covalent bond suitably converted into engineering parameters are found in the literature. The followings are adopted in this study.

> Length representing the covalent bond L = 1.42 Å, circular cross sectional area A = 1.68794 Å^2, moment of inertia I = 0.22682 Å^4, Young's modulus $E = 5.488\times10^{-8}$ N Å^{-2}, shear modulus $G = 8.711\times10^{-9}$ N Å^{-2}, and the mass of the carbon atom $m_c = 1.9943\times10^{-26}$ Kg.

The stiffness matrix of each 3D frame element is created in the element coordinate system first and then transformed into the structure coordinate system to obtain the assembled matrix [**K**] for the graphene sheet. To create the assembled mass matrix [**M**], the mass of the carbon atom is lumped at the displacement degrees of freedom of the nodes. In this manner, the equations: $\mathbf{K}\,\mathbf{x}=\mathbf{F}$ for the static analysis and $\mathbf{M}\,\ddot{\mathbf{x}}+\mathbf{K}\,\mathbf{x}=\mathbf{F}$ for the dynamic analysis are deduced. Here **x** and **F** are the displacement and force vectors respectively. The over-dot represents differentiation with respect to time. A graphene is seen as lattice structure with voids throughout in each cell. This makes the lattice structure modeling method extremely desirable for very accurate results. Results from such analyses exhibit astounding similarity between graphene and continuous membrane (or plate) in overall static and vibrational behaviors. The drawback found in the lattice structure modeling is that a huge amount of computer capitals is required to produce accurate results even for a very small size graphene. With this into consideration, a simplified equivalent continuum plate modeling method is proposed in the following.

In the present research, first the static analysis is performed on the lattice structure model of the rectangular graphene sheets with length a and width b. Using the displacement under the load, the overall Young's moduli are calculated using classical closed form equations and also numerical solutions depending upon the shape of graphene sheets. This procedure is carried out separately for in and out of plane loading conditions. For the in-plane condition, the graphene is fixed at one edge and subjected to an axial load P on the opposite edge. This load P is equally divided to nodes. The displacement u_0 at the loaded edge is found from the lattice structure method and then used along with thickness h = 3.4 Å in $E = Pa/u_0 bh$ to obtain the value of E. Similarly, the lattice structure model of the rectangular graphene sheet is subjected to a lateral point load at the center and the deflection v_0 under the load is calculated. The flexural rigidity of the equivalent isotropic plate is then calculated from $D = \alpha P a^2 / v_0$, where the values of α are taken from the literature [7] and from it equivalent Young's modulus E in bending is found from $D = Eh^3/12(1-\upsilon^2)$ using h = 3.4 Å and the Poisson's ratio $\upsilon = 0.16$. The natural frequency from the classical theory for the isotropic rectangular plate can be calculated by $f_{ij} = \lambda_{ij}^2 \sqrt{D/\rho h} \,/ 2\pi a^2$ in Hz using the mass density of ρ = 2250 Kg m^{-3}. Indices i and j represent the numbers of half waves in a mode shape along horizontal and vertical axes, respectively. The values of λ_{ij} are readily available in [8] for different aspect ratios (b/a) and boundary conditions. The equivalent Young's modulus found in this manner can also be used along with the thickness and Poisson's ratio, if the FEM is chosen for the analysis of plates other than rectangular.

Numerical Examples. A wide range of length (a) and width (b) namely; $2.46 \text{ nm} \le a \le 30.03 \text{ nm}$ and $2.42 \text{ nm} \le b \le 60.39 \text{ nm}$ has been considered during the course of this study. The Young's modulus of elasticity is found to be settling down to the range of 1.03-1.04 TPa for the extensional condition and it is completely consistent with the results published by others. The same for the bending condition converges to 0.112 TPa. Study of the mass distribution was also done on the graphene sheet based on the number of carbon atoms in a particular case. The mass density converges to a value of 2250 which is equal to the mass density for graphite.

Table. Natural frequencies (THz) of rectangular SLGS clamped on all four sides.

(a = 4.92 nm and b=4.97 nm)

Mode Number	Extensional		Flexural	
	Lattice Structure	Continuum Plate	Lattice Structure	Continuum Plate
1	2.6114	2.5489	0.1633	0.1641
2	2.6184	2.5592	0.3287	0.3325
3	3.4158	3.2215	0.3368	0.3366
4	3.8986	3.7799	0.4903	0.4925
5	4.3117	4.2423	0.5877	0.5959
6	4.6838	4.4650	0.6069	0.6061
7	4.7411	4.4928	0.7407	0.7472
8	4.7503	4.7206	0.7528	0.7531
9	5.2961	5.1895	0.9356	0.8446
10	5.3504	5.2050	0.9685	0.8480

Table above shows the values of the first 10 natural frequencies of a rectangular graphene clamped on all four sides. The frequencies for the extensional modes are given in columns 2 and 3 obtained by the lattice structure and continuum plate theories respectively. Columns 4 and 5 show the corresponding frequencies in flexural modes. Figures 1 and 2 show the in-plane and out-of-plane mode shapes for the frequencies presented in the table. The symmetry and anti-symmetry with reference to horizontal and vertical axes and also the two diagonals of the rectangular graphene are distinctly observed. This particular graphene sheet is relatively small in size and that is why the discrepancy between the frequency values from the two methods is distinctly noticeable. When the overall size increases, this discrepancy decreases rapidly and the results from the two methods show excellent agreement.

Concluding Remarks. The lattice structure method is highly desirable, as it includes in modeling the very details at the atomic level and renders accurate results. However, the computation can be impeded if the graphene size increases even small to medium. Therefore, an alternate method in which the static analysis is performed by the lattice structure method and assuming thickness h = 3.4 Å and the Poisson's ratio υ = 0.16 to get two equivalent values of the Young's modulus. These are: 1.04 TPa and 0.112 TPa for the extensional and flexural modes which can be used in the classical plate equations to get very accurate results.

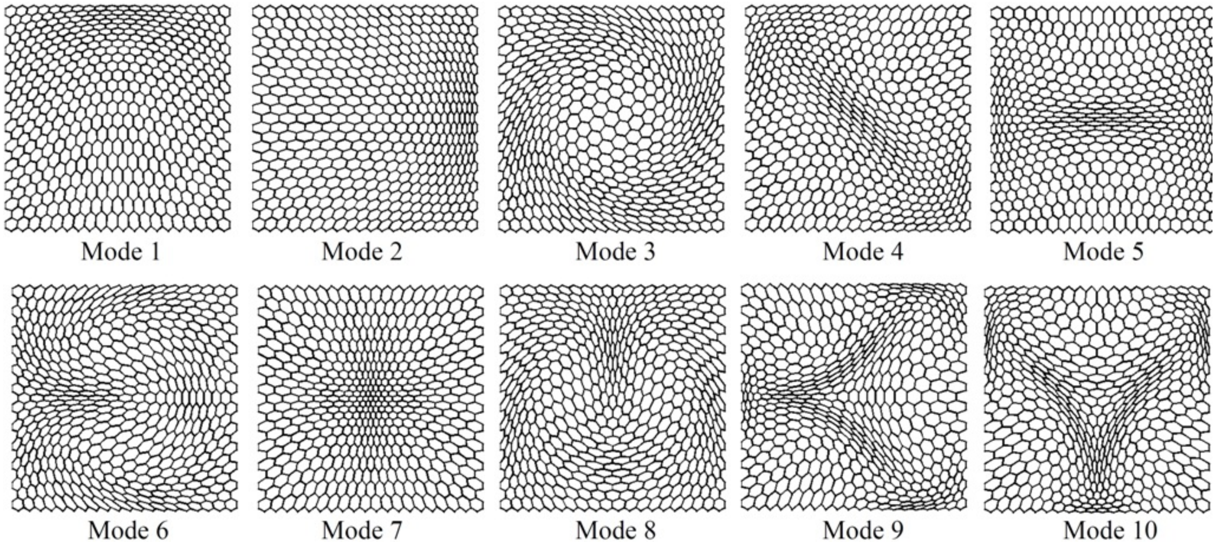

FIG. 1. First 10 in-plane mode shapes of a nearly square SLGS (4.92 nm×4.97 nm), CCCC

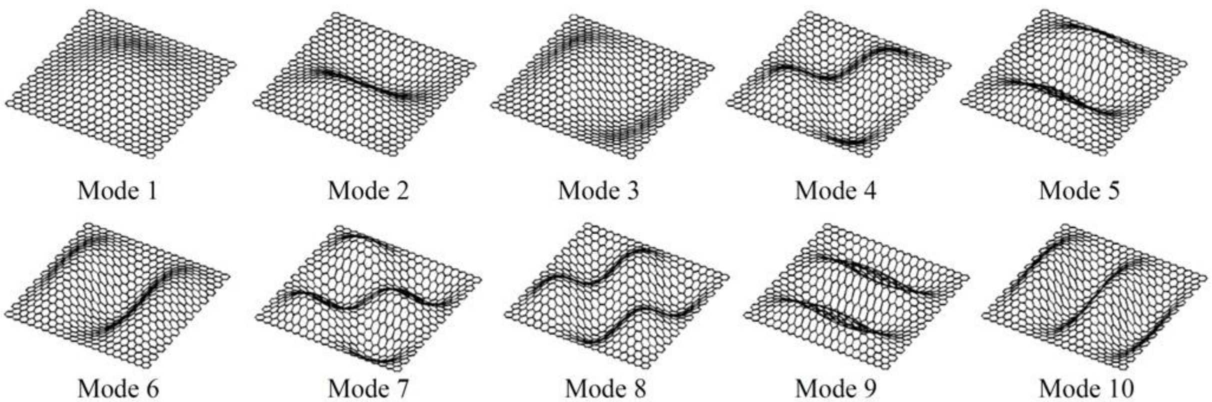

FIG. 2. First 10 out-of-plane mode shapes of a nearly square SLGS (4.92 nm×4.97 nm), CCCC.

References

[1] Novoselov, K. S., Jiang, D., Schedin, F., Booth, T. J., Khotkevich, V. V., Morozov, S. V., and Geim, A. K., 2005, "Two-Dimensional Atomic Crystals," The Proceeding of the National Academy of Sciences of the United States of America, **102**(30), pp. 10451-10453.
[2] Geim, A. K. and Novoselov, K. S., 2007, "The Rise of Graphene," Nature Mat., **6**, pp. 183-191.
[3] Li, C., and Chou, T. W., 2003, "A Structural Mechanics Approach for the Analysis of Carbon Nanotubes," Int. J. Solids Struct., **40**(10), pp. 2487-2499.
[4] Singh, A. V. Arghavan, S., 2010, "Vibrations of Carbon Nanoscale Structures: A Critical Review," Computational Technology Reviews, **1**, pp. 281-314.
[5] Arghavan, S. and Singh, A. V., 2011, Free vibration of single layered graphene sheets: Lattice Structure vs. continuum plate theories, ASME Journal of Nanotechnology in Engineering and Medicine, in press.
[6] Arghavan, S. and Singh, A. V., 2011, "On the Vibrations of Single-Walled Carbon Nanotubes," J. Sound Vib,330, 3102 - 3122.
[7] Timoshenko, S. and Woinowsky-Krieger, S., 1959, *Theory of Plates and Shells*, McGraw-Hill, New York, Second Edition.
[8] Blevins, R. D., 1979, *Formulas for Natural Frequency and Mode Shape*, Van Nostrand Reinhold, New York.

Discretization of structures using a negative stiffness approach in the context of structural optimization

Gottfried Spelsberg-Korspeter, Andreas Wagner

Dynamics and Vibrations Group, Technische Universität Darmstadt, Germany

1 Introduction

In many technical applications a goal for the design engineer is to achieve a certain dynamical behavior of a structure. Mathematically this can be achieved through eigenvalue optimization. In many cases one has to deal with an easy underlying structure which is to be modified such that a certain modal behavior is achieved. The question therefore arises on how to describe the modifications in a convenient manner. On the last ISVCS meeting Ilanko referred on the concept of negative stiffness and mass in the context of asymtotic modeling [1, 2, 3, 4, 6]. The purpose of this paper is to elaborate this approach in the context of structural optimization.

2 Demonstration of the approach with a simplistic example

The basic idea of the approach is that by using the concept of negative stiffness it is possible to discretize different parts of a structure in an adequate manner in a first step and to couple the discretizations in a second step.

As probably the easiest example consider the structural model of a longitudinal bar with different material parameters between L_1 and L_2 as shown in figure 1. The goal is to use one discretization

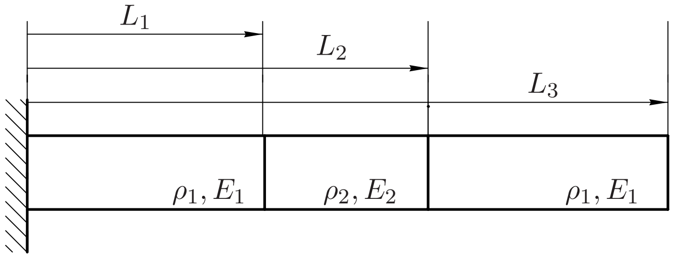

Figure 1: longitudinal bar with different sections

for the global rod and one for the distortion with different material parameters. The displacement field can be expanded in terms of shape functions

$$u(x,t) = \sum_i W_i(x) q_i(t)$$

yielding the discretized equations of motion

$$\boldsymbol{M}\ddot{\boldsymbol{q}} + \boldsymbol{K}\boldsymbol{q} = 0, \qquad m_{ij} = \int_0^L \rho A W_i W_j \mathrm{d}x, \qquad k_{ij} = \int_0^L EAW_i' W_j' \mathrm{d}x.$$

As shape functions one can either use global shape functions as for example $W_i(x) = \sin(i\frac{\pi}{L}x)$ or local shape functions

$$\begin{aligned} W_i(x) &= 1 + \frac{x - ih}{h} & (i-1)h \le x \le ih \\ &= 1 - \frac{x-(i+1)h}{h} & ih \le x \le (i+1)h. \end{aligned}$$

The area between L_1 and L_2 is taken into account using a separate discretization scheme and using negative stiffness and mass with the stiffness matrix $\boldsymbol{K}^-$ and the mass matrix $\boldsymbol{M}^-$.

In order to couple the two discretization schemes the degrees of freedom of both schemes have to be coupled by kinematic constraints. Assuming that the distortion between L_1 and L_2 is modeled with local shape functions the degrees of freedom of the nodes $\tilde{q}_i$ at the positions $\tilde{x}_i$ are constrained by

$$\tilde{q}_i = w(\tilde{x}_i, t) \qquad\qquad \tilde{\boldsymbol{q}} = \boldsymbol{Q}\boldsymbol{q}.$$

This has to be taken into account in the corresponding energy expressions

$$T = \frac{1}{2}\dot{\boldsymbol{q}}^T\boldsymbol{M}\dot{\boldsymbol{q}} - \frac{1}{2}\dot{\tilde{\boldsymbol{q}}}^T\boldsymbol{M}^-\dot{\tilde{\boldsymbol{q}}},$$
$$U = \frac{1}{2}\boldsymbol{q}^T\boldsymbol{K}\boldsymbol{q} - \frac{1}{2}\tilde{\boldsymbol{q}}^T\boldsymbol{K}^-\tilde{\boldsymbol{q}}.$$

The eigenvalue problem thus reads

$$[(\boldsymbol{M} - \boldsymbol{Q}^T\boldsymbol{M}^-\boldsymbol{Q})\lambda^2 + (\boldsymbol{K} - \boldsymbol{Q}^T\boldsymbol{K}^-\boldsymbol{Q})]\boldsymbol{v} = 0.$$

Using the parameters

$$\rho_1 = 7850\,\mathrm{kg/m^3} \qquad \rho_2 = 7850\,\mathrm{kg/m^3} \qquad E_1 = 2.06\,10^{11}\,\mathrm{N/m^2} \qquad E_2 = 0.206\,10^{11}\,\mathrm{N/m^2}$$
$$L_3 = 1\,\mathrm{m} \qquad L_1 = 0.4\,\mathrm{m} \qquad L_2 = 0.65\,\mathrm{m}$$

where $E_2 = 0.1\,E_1$ we perform three numerical experiments. In one calculation we use 12 global shape functions for the discretization of the rod and for the second one we use 80 local ones. The area of the distortion is approximated with 40 local shape functions. The results in the following table show that all results are in good agreement:

	global shape functions	local shape functions
ω_1	7274	7229
ω_2	21625	21533
ω_3	37188	36921
ω_4	51544	51286
ω_5	65326	64753

Performing the same calculation using $E_2 = 0$ reveals a very different result:

	exact solution	global shape functions	local shape functions
ω_1	20117	6487	19938
ω_2	45981	24033	45535
ω_3	60350	33043	59863
ω_4	91962	52321	91208
ω_5	100580	70399	99927

It is seen that the convergence of the approach with global shape functions is rather poor. The convergence for the approach with local shape functions is acceptable, however we note that the approximations do not yield an upper bound for the eigenfrequencies as for a standard Ritz-Galerkin approach. A couple of approximately zero eigenvalues corresponding to the nodes in the distortion have been discarded in the table. The reason for the poor convergence with global shape functions lies in the fact that now the left and the right part of the rod are not connected whereas the shape functions couple both parts. A look at the approximation of the first eigenforms shows that it is very poorly approximated with the global shape functions. Nevertheless in many applications the structure is not completely separated as in this case and a good convergence is to be expected also with global shape functions.

3 Structural optimization of a disc brake

It has been proved that breaking the symmetries of rotors in frictional contact helps to stabilize the system and to prevent squeal [5]. Therefore we try to optimize a bicycle disk brake such that no

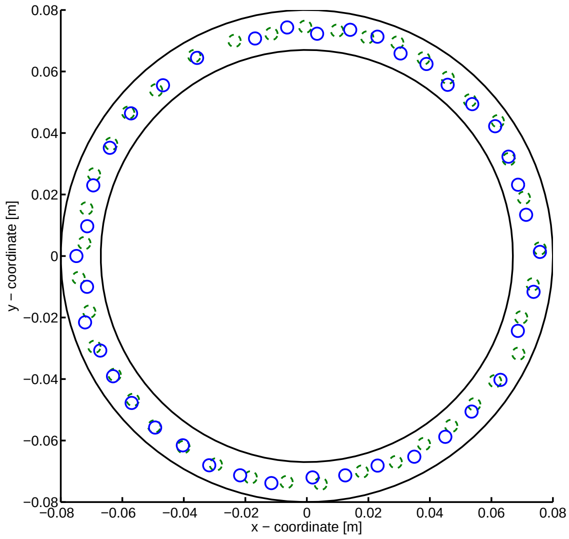

Figure 2: brake disk geometries

double eigenfrequency occurs by placing holes of given radius at variable positions. The disk has the inner radius $r_i = 67$ mm and outer radius $r_a = 80$ mm and is $h = 2$ mm thick. We give a random initial placement (green circles) for 40 holes with diameter 4 mm and optimize for their positions (blue circles). The objective function is to maximize the minimum distance between eigenfrequencies under the constraints that the disc stays statically balanced and holes do not intersect with each other or the boundary. The corresponding geometry is shown in figure 2 and a minimum splitting of the eigenfrequencies of around 60 Hz has been achieved. The major advantage of the method is that for plates and holes the same discretization can be maintained throughout the optimization and that only the matrix $\boldsymbol{Q}$ has to be build up in every step of the optimization.

4 Conclusions

The approach of using negative mass and stiffness operators suggested by Ilanko is not only useful in asymptotic modeling but also in structural optimization. It offers the opportunity to combine different discretization schemes which are suitable for a master structure and modifications. In this paper the method is applied to optimize a bicycle disk brake in order to prevent squeal. At the moment measures are taken to validate the results experimentally.

References

[1] Ilanko, S.: Existence of natural frequencies of systems with artificial restraints and their convergence in asymptotic modelling, *Journal of Sound and Vibration*, 255(5):883–898, 2002.

[2] Ilanko, S.: Introducing the use of positive and negative inertial functions in asymptotic modelling, *Proceedings of the Royal Society A: Mathematical, Physical and Engineering Science*, 461(2060):2545, 2005.

[3] Ilanko, S.; Dickinson, S.: Asymptotic modelling of rigid boundaries and connections in the Rayleigh-Ritz method, *Journal of Sound and Vibration*, 219(2):370–378, 1999.

[4] Ilanko, S.; Williams, F.: Wittrick-Williams algorithm proof of bracketing and convergence theorems for eigenvalues of constrained structures with positive and negative penalty parameters, *International Journal for Numerical Methods in Engineering*, 75(1):83–102, 2008.

[5] Spelsberg-Korspeter, G.: Breaking of symmetries for stabilization of rotating continua in frictional contact, *Journal of Sound and Vibration*, 322:798–807, 2009.

[6] Williams, F.; Ilanko, S.: The use of the reciprocals of positive and negative inertial functions in asymptotic modelling, *Proceedings of the Royal Society A: Mathematical, Physical and Engineering Science*, 462(2070):1909, 2006.

Computation of Lower Bound Eigenvalues using the Wittrick-Williams Algorithm

A. Watson, Loughborough University, UK & W. P. Howson, Cardiff University, UK

Abstract

The major strength of the Wittrick-Williams algorithm lies in its ability to solve transcendental eigenvalue problems that stem from exact solution of the governing differential equations. The algorithm was originally developed in the context of structural mechanics where the eigenvalues are positive numbers bounded below by zero. However, the authors show that in other disciplines, where eigenvalues can be negative, their existence does not impose a limitation on the algorithm. This is illustrated by a problem in mathematics in which negative eigenvalues can be calculated by first computing the eigenvalues when the problem is modified by the addition of a constant valued potential. Once these modified eigenvalues are computed, the required eigenvalues can be extracted by subtracting the original potential.

Section 1

Consider the classical second-order Sturm-Liouville (SL) equation, which can be written as

$$-\frac{d}{dx}\left(p\frac{dy}{dx}\right)+qy=\lambda wy \tag{1}$$

where p, q and w are all real valued, positive constants. For simplicity we allow *p*=*q*=*w*=1 to give

$$-\frac{d^2y}{dx^2}=\lambda y \tag{2}$$

Assuming an interval length of unity and left and right hand boundary conditions of $y = 0$ and $y' = 0$, respectively, the required eigenvalues are given by

$$\lambda_i=\left(\frac{(2i-1)\pi}{2}\right)^2 \qquad i=1,2,\ldots,\infty \tag{3}$$

If now the boundary conditions are changed, all the eigenvalues stemming from Eq.(3) would be modified. For example, suppose the right hand boundary condition is changed to

$$y'=-hy \tag{4}$$

where h is a real valued constant in the range $-\infty < h < \infty$. If now $h \geq 0$, then all eigenvalues are zero or positive. However, if $h<0$ negative eigenvalues are possible. The computation of a negative eigenvalue is more troublesome since the square root of the eigenvalue is imaginary. In order to overcome this we introduce a constant value potential, q, to Eq.(2). This will change the eigenvalues that are obtained from λ to λ^*, hence

$$-\frac{d^2y}{dx^2} + qy = \lambda^* y \qquad \Rightarrow \qquad -\frac{d^2y}{dx^2} = \left(\lambda^* - q\right) y \tag{5a, b}$$

The potential q needs to be sufficiently large so that the lower bound eigenvalue for the modified problem is shifted above zero. Once this is satisfied the modified eigenvalues can be computed using the normal approach. The original eigenvalue can then be recovered as

$$\lambda = \left(\lambda^* - q\right) \tag{6}$$

As an example, consider the case of $h = -2$. If a value of $q = 20$ is used in Eq.(5), the first eigenvalue of the modified problem is $\lambda^* = 16.3328$. This modified eigenvalue is not of interest as it is dependent upon the chosen value of q. The true eigenvalue is then recovered from Eq.(6) as $\lambda = -3.6672$.

Conclusions

The authors show, using an example from mathematics, how negative eigenvalues can be computed by solving a modified problem. In the current example, this was acieved through the introduction of a constant value potential into a second order Sturm-Liouville equation. However, such calculations are not restricted to the second order problem. The method described above can be adapted to extract negative eigenvalues from 4^{th} and higher order SL problems. More generally the computational procedure described has significant potential in all areas of science that require the calculation of negative eigenvalues with the only proviso being that the differential equation is soluble in closed form and that all the eigenvalues are real.

Acknowledgement

The authors are very grateful to Professor Pavel Kurasov of Lund University and Professor Marco Marletta of Cardiff University for their advice and helpful suggestions.

Reference

[1] F.W. Williams, W.P. Howson, A. Watson, “Application of the Wittrick-Williams algorithm to the Sturm-Liouville problem on homogeneous trees: A structural mechanics analogy”, Proceedings of the Royal Society series A: Mathematical, Physical and Engineering Sciences, 460(2045), 1243-1268, 2004.

Biosketches of Authors

Hao Bai

Associate Professor of Mechanical Engineering
Lakehead University
Thunder Bay, Ontario, Canada

I went to Peking University, Beijing, China, in 1982 and graduated in 1986. After that I went to University of Science and Technology of China, Hefei, China, to pursue my post graduate degree and I had my MSc in 1989. From 1992 to 1996, I had my Doctoral degree from Peking University. Later on I had my second PhD from the University of Manitoba, Winnipeg, Canada, from 1997 to 2002.

After receiving my Master's degree in 1989, I worked at Pingdongshan Institute of Technology in Henan, China, for three years. My main duty is teaching undergraduates. From 1995 to 1996, I worked as a research and development engineer in Beijing Institute of Control Engineering which belongs the China Academy of Aerospace in Beijing. After having my PhD from University of Manitoba, I worked as a research associate in Civil Engineering, University of Manitoba for one year. In 2003, I joined the faculty at Lakehead University in the Mechanical Engineering, where I have since remained. I am enjoying my research, teaching and living in Thunder Bay.

J.R. Banerjee

Professor of Structural Dynamics
City University London
London

My professional career spans 35 years of teaching and research experience within the technical areas of aeronautical and structural engineering. The main contributions to knowledge that I have made concern my new approaches to structural dynamics, aeroelasticity and related problems. In particular, the major activities of my research relate to (i) free vibration analysis of structures, (ii) dynamic stiffness formulation, (iii) response of metallic and composite structures to deterministic and random loads, (iv) aeroelasticity of metallic and composite aircraft, (v) a unified approach to flutter, dynamic stability and response of aircraft, (vi) aeroelastic optimisation and active control, (vii) application of symbolic computation in structural engineering research and (viii) development of software packages for computer aided structural analysis and design.

During the past 35-years, I have been able to combine the disciplines of aeroelasticity, composite materials, dynamic stiffness methods, symbolic computation and structural optimisation. The free vibration analysis of structures has been an ever-present research theme since I began my academic career. I provided the solutions of free vibration and response problems, which range from that of a simple single structural element to a large space platform with more than 21000 degrees of freedom, and a high capacity transport airliner capable of carrying more than 600 passengers. To provide these solutions, I resorted to an elegant, accurate, but efficient method, called the dynamic stiffness matrix method, which uses the so-called dynamic stiffness matrix of a structural element as the basic building block in the analysis. I have developed dynamic stiffness matrices of a large number of standard and non-standard structural elements with varying degrees of complexity, including those made of composite materials. The culmination of my research experience in free vibration and buckling analysis of structures resulted in the development of a FORTRAN computer program called BUNVIS (Buckling or Natural Vibration of Space Frames). This program received widespread attention and was further developed into BUNVIS-RG by NASA with my central involvement.

My main contributions in the Aeronautical Engineering field are, however, related to the solutions of problems in aeroelasticity concerned with metallic aircraft in early years, and in later years with composite aircraft. I developed a FORTRAN computer program called CALFUN (CALculation of Flutter speed Using Normal modes) for metallic aircraft during my doctoral studies and later extended it to cover aircraft built from composite materials. The associated theories for composite aircraft were developed by me and the allied problems of dynamic response to both deterministic and random loads were solved.

With the advent of advanced composite materials, my research interest turned to aeroelasticity of composite aircraft and then to optimization studies. New, novel and accurate methods have been developed with significant inroads made. I broke new ground by applying symbolic computation as an aid to the solution of structural engineering problems.

Piotr Cupial

Professor of Mechanical Engineering and Robotics
AGH University of Science and Technology
Cracow, Poland

I graduated in 1987 in the field of applied and computational mechanics. Still as a student, I was employed at the Institute of Physics of the Cracow University of Technology, working on the optimal design of circular plates subjected to nonconservative compressive loading. After three years, I moved to the Institute of Mechanics and Machine Design (now Institute of Applied Mechanics). In 1997 I obtained my PhD from the Cracow University of Technology in the field of the application of damping polymers in the vibration suppression of composite structures. Since March 2011 I hold a professor position at the Faculty of Mechanical Engineering and Robotics of the AGH University of Science and Technology in Cracow.

For several years now my main research activities have focused on the vibration analysis and control of electromechanical continuous systems. In 2008 I published a monograph "Coupled electromechanical vibration problems for piezoelectric distributed- parameter systems". My recent interests are also closely related to the field of adaptive and smart structures.

In 1991 I spent three months at Université de Technologie de Compiègne (France), within the European Union program TEMPUS, working on experimental modal analysis of large structures. During the years 1998-2001 I spent three years at the European Organization for Nuclear Research (CERN) in Geneva. For one year, starting in October 2000, I was appointed a position of scientific associate at CERN, a post granted to "researchers with established position in their field". At CERN I worked on the finite element analysis and dynamic measurements, in connection with the Large Hadron Collider (LHC) and the four particle physics experiments that are already taking data now. For almost three years, starting in 2008, I coordinated the participation of the Cracow University of Technology in the European project "EUROnu - A high intensity neutrino oscillation facility in Europe".

I am married to Gabriela and we have one son. In my free time I enjoy listening to different kinds of music and reading history books. I have always been fond of the mountains, hiking in the summer and skiing during winter. ISVCS8 will be my fourth symposium out of the eight held so far. I am looking forward to meeting the old and new colleagues and friends in the unique atmosphere of these symposia.

Stuart M. Dickinson

Professor Emeritus
The University of Western Ontario
London, Ontario, Canada

Stuart served an engineering apprenticeship with Ford Motor Company, Dagenham, UK, before attending the University of Nottingham, where he obtained his B.Sc. and Ph.D. in Mechanical Engineering and, perhaps more significantly, met his future wife, Rosemary. After spending three years as a lecturer at the University of Liverpool, he and Rosemary immigrated to Canada in 1969 where he took up a faculty position at The University of Western Ontario, becoming Professor Emeritus upon his early retirement in 1997. Whilst at Western, he had the opportunity of spending sabbatical leaves at the Institute of Sound and Vibration Research, Southampton, UK, the University of Canterbury, Christchurch, New Zealand, and Monash University, Melbourne, Australia.

His research interests were mainly in the vibration of beams, plates and shells, with brief excursions into acoustics. He enjoyed working with one or two graduate students at a time and found their contributions to his research invaluable. Most of the research was of a theoretical or numerical nature, primarily employing "classical" approaches, although some experimental work was conducted and, in the early years, some work was done on the development of finite element methods.

Over the years, his recreational interests, shared with his wife, have included curling, badminton, hiking and dinghy sailing. Several of these activities have been somewhat curtailed of late due to knee problems, also shared with his wife! Other interests include playing the euphonium (taken up a few years ago), travelling and wine making.

Stanley B. Dong

Professor Emeritus
University of California at Los Angeles
Los Angeles, California, USA

My entire college education occurred at the University of California at Berkeley, where I began in 1953 and completed in 1962 in the Department of Civil Engineering. I was quite fortunate to have Karl Pister as my advisor upon entering in my freshmen year. He remained my advisor throughout and was my doctoral dissertation supervisor, which dealt with various aspects of anisotropic mechanics with a primary emphasis on laminated anisotropic shells and plates.

After receiving my degree in 1962, I worked at Aerojet-General Corporation in Sacramento, California, with primary duties concerned with the analysis of filament-wound pressure vessels to be used as rocket motor cases in Polaris/Poseidon missiles. I was extremely fortunate to have some very distinguished co-workers, Leonard Herrmann and Edward Wilson. Our interactions (or more accurately, their tutelage) enabled me to learn to code in FORTRAN, and it was at Aerojet-General that I was able to develop my first finite element code for the analysis of laminated composite shells of revolution under axisymmetric loading. To mention that we worked on an IBM 7094 with 32K memory is a stark reminder of the digital Neanderthal period.

In 1965, I joined the faculty at UCLA in the then Engineering College, where I have since remained. This College (with only one department) was a brainchild of out late founding Dean L.M.K. Boelter, who was known for the *unified curriculum*. In 1970, the Engineering College was re-organized as the School of Engineering and Applied Science with seven departments based on technical disciplines rather than the conventional monikers of civil, mechanical, electrical, etc. In 1982, because of the confusion between these discipline names with the conventional departmental names, the School of Engineering and Applied Science regrouped itself into conventional departments. I was first affiliated with the Mechanics and Structures Dept., where I served as its Chair from 1973-76, and then with Civil and Environmental Engineering Dept., where I served another stretch as Chair from 1989-92. In 1994, the UC System offered an unusual and lucrative early retirement plan, which I (and about 10% of the entire UC faculty) opted for, and thus earning my present title as Professor Emeritus. My days in retirement have enabled me to pursue various topics at leisure.

Lorenzo Dozio

Assistant Professor of Aerospace Engineering
Politecnico di Milano
Milano, Italy

Lorenzo Dozio was born near Milan, Italy, on 1972. He received a M.S. degree in Aerospace Engineering in 1998 and a Ph.D. in Aerospace Engineering in 2002, both at the Politecnico di Milano. After two years as a post-doc, he won a position as Assistant Professor at the same University in 2004.

Since 2002 he has been involved in teaching activities concerning servosystems for aerospace applications, introduction to engineering experimentation and dynamics and control of aerospace structures.

His main research interests are vibration of structures, composite and smart materials, active and shunt piezoelectric control, structural-acoustic and real-time systems. He has been involved in many research projects in collaboration with industries on active noise reduction inside helicopter cabins, active control of instabilities in combustion chambers and design and implementation of real-time operating systems. Recently, he worked on control of vibration and noise radiation of plates with embedded passive and active periodicity. He is currently working on refined computational and analytical models for composite and smart structures.

He has authored 12 papers in international journals and over 40 conference papers. He has advised more than 20 graduate students at Politecnico of Milano. He served as a reviewer for, among others, Journal of Sound and Vibration, Journal of Vibration and Acoustics, Composite Structures and International Journal of Mechanical Sciences.

He is married to Letizia, and they have four children, two sons Paolo (9) and Tommaso (7), and two twin daughters Anna and Matilde (3). In his spare time, he loves playing acoustic and electric guitar.

Mark S. Ewing

Associate Professor of Aerospace Engineering
University of Kansas
Lawrence, Kansas USA

I grew up interested in science and mathematics, largely due to my fascination with the U.S. spacecraft I used to watch launch from Cape Canaveral—when I lived in nearby Orlando, Florida. I received my BS in Engineering Mechanics from the U.S. Air Force Academy, then began a 20-year career in the Air Force. I served for four years in turbine engine stress and durability analysis where I was an "early" user of finite element analysis for hot, rotating turbomachinery. I then served a two-year assignment in turbine engine maintenance and support, which was less technical, but eye-opening. During these early years—in my spare time—I earned an MS in Mechanical Engineering from Ohio State University.

With an MS in hand, I returned to the Air Force Academy to serve on the faculty as an Assistant Professor. After two years, I returned to Ohio State to complete a PhD. As a student of Art Leissa's, I focused on the combined bending, torsion and axial vibrations of "stubby" beams, thereby establishing my interest in the vibrations of continuous systems.

After returning to and teaching at the Academy for six years, I was assigned to the Air Force Flight Dynamics Lab, where I worked on two interesting projects. The first was the development of a structural design algorithm capable of, among other things, "maximizing" the separation of two natural frequencies. The utility of this endeavor was to allow the design of aircraft wings for which the bending and torsional natural frequencies are sufficiently separated (in frequency) to avoid flutter. The other interesting project was the analysis of the effect of convected aerodynamic loads on a missile.

I am now on the Aerospace Engineering faculty at the University of Kansas. My current research interests are in structural acoustics, which is a topic of increasing interest to aircraft manufacturers. In recent years, I have focused on the best way to characterize and estimate structural damping for built-up structures. All the test articles I've used to validate my work through experimentation are simple structural elements, namely beams and plates.

I have a great love of the outdoors, and of the mountains in particular. When Art Leissa asked me to help organize the first International Symposium on Vibrations of Continuous Systems—held in 1997—and he told me he wanted to meet in the mountains, I really got excited. I look forward to the 8th Symposium in Whistler as a time to visit with long-time friends and colleagues.

Peter Hagedorn

Professor Emeritus
Technische Universität Darmstadt
Darmstadt, Germany

I received most of my education in Sao Paulo, Brazil, where I obtained a degree in mechanical engineering and later a doctor's degree (in 1966) at the Escola Politecnica da Universidade de Sao Paulo. Later I did my 'Habilitation' (similar to a D.Sc. degree) at Karlsruhe in Germany. My main professional interests are vibrations and stability of discrete and continuous systems (such as beams, plates and cables), and vibration control. While my early work was more analytical (e.g. the converse of the Lagrange-Dirichlet theorem, differential games, etc.), during the last 30 years I have worked more and more also with problems related to industrial applications, including experimental work, the emphasis however usually being on producing practical mathematical models.

Recently I have been working with piezoelectric ultrasonic travelling wave motors, wind excited vibrations of overhead transmission lines (including CFD calculations), and with the dynamics and active noise control in disk brakes. I am the author of several books on linear and nonlinear vibrations as well as a three volume German textbook on elementary statics, strength of materials and dynamics. I have also organized several workshops dealing with the question of how we should teach engineering mechanics to our students today.

Since 2009 I am officially retired at the University. I am presently attached to AdRIA, a new institute dealing with active structures, affiliated to the University, where I still have a group of 5 PhD students and postdocs, and I am acting as an advisor to the Fraunhofer institute LbF.

I have been a visiting professor and research fellow at Stanford, Berkeley, Paris, Irbid (Jordan), Rio de Janeiro and Christchurch (New Zealand). At the University of Canterbury at Christchurch, New Zealand, I also hold the position of an Adjunct Professor, and we usually spend about a month there every year (also seeing the family and enjoying the grandchildren). My personal hobbies are travelling, reading, photography and hiking (mainly day hikes).

Shinya Honda

Assistant Professor of Human Mechanical Systems & Design
Hokkaido University
Sapporo, Japan

I am a faculty member of the Department of Human Mechanical Systems & Design in Faculty of Engineering, Hokkaido University. I graduated the Department of Mechanical Engineering in 2005, and obtained M. Eng. in 2007 from Hokkaido University. In 2009, I also obtained a PhD from Hokkaido University in the area of optimization of composite plates. My supervisor was Prof. Narita who is the editional chairman of 8^{th} ISVCS, and now I'm working with Prof. Narita in his laboratory.

The title of my doctor thesis is "Study on vibration design of fibrous composite plates with locally anisotropic structure". I wrote some articles about this topic, and got the Young Researcher Award from the Japan Society of Mechanical Engineering (JSME) in 2011.

Recently, I have an interest in a research field of smart structures, especially, vibration control of smart composite. I collaborate with Prof. Kajiwara who is also professor in Hokkaido University and specialist of smart structures. In 2010, I got the Excellent Presentation Award at the 53th Automated Control Conference (JSME).

I'm now eager to have a chance to study abroad, and looking for a professor who accepts me as a visiting researcher for about a year. If you can accept me, please contact me during the conference.

I was born and had grown up in Sapporo where I live in now with my wife Tomoko. We got married in 2009 and we are looking forward to having a baby in the near future. I like driving a car, going to gym and drinking beer.

Chiung-Shiann Huang

Professor of Civil Engineering
National Chiao Tung University
Hsinchu, Taiwan

Chiung-Shiann Huang's current position is a Professor in the Department of Civil Engineering, National Chiao Tung University, Taiwan. He received his Ph. D in 1991 at the Department of Engineering Mechanics at the Ohio State University. After that, he spent nine months as a postdoctoral research associate in the Department of Civil Engineering at the Ohio State University. The doctoral and postdoctoral research dealt with the use of singular corner stress functions to permit accurate solutions for free vibration frequencies of thin plates having sharp corners.

In 1992, he went back Taiwan and joined the research staff at the National Center for Research on Earthquake Engineering (NCREE). In addition to continue his serious interests on computational mechanics, he began to study the system identification of structures from monitoring earthquake responses of structures and the responses from various tests in field, such as ambient vibration test and forced vibration test.

After having stayed in NCREE for nine years, he joined the faculty of the Civil Engineering Department at National Chiao Tung University in 2000. His current main interests are vibrations of plates with stress singularities and system identification for structures using time series, neural network, and wavelet transform.

James R. Hutchinson

Professor Emeritus
University of California Davis
Davis, California, USA

Jim was born in San Francisco Ca. He graduated from Stanford University with a BS in Mechanical Engineering in 1954. Upon graduation he went to work for Westinghouse's Atomic Power Division in Pittsburgh Pa. While working at Westinghouse he earned his masters in Mathematics in 1958. He then went to work for Lockheed Missiles and Space Division in Palo Alto Ca. While working at Lockheed he went back to Stanford as a part time student, earning his Ph.D. in Engineering Mechanics in 1963. He stayed on at Lockheed for another year before taking an academic position at the University of California, Davis. He retired from UCD in 1993, but continued to teach on a recall basis for at least five more years.

His interest in vibrations began while he was working at Lockheed. His primary responsibility at Lockheed was in missile vibrations. When he arrived at Davis he was asked to teach the graduate course in Mechanical Vibrations. Many of his students were from Agricultural Engineering. They were interested in shaking fruit and nuts from trees. Of course, the solution methods were the same whether the vibrating body was a missile or a tree, and a number of cooperative projects took place on the study of tree vibrations. His early interest in continuum vibration also had its roots in missile applications.

Jim loves to sing and was very active in the Davis Comic Opera Company that mainly produced the works of Gilbert and Sullivan. He is still singing with the University Chorus. Last Spring he had the privilege of singing Berlioz "Te Deum" with an adult chorus of 125 and a children's chorus of 200. Jim is a former home-brewer and has dabbled in photography, stained glass, auto mechanics, and lately web design. He has become an avid golfer and even though he complains about his terrible scores, he still manages to play twice a week.

Jim does volunteer work with Citizens Who Care (a local non-profit agency dedicated to helping the elderly), and is presently president of the board of directors of that organization. Jim and his wife, Pat, are co-chairs of the CWC annual winter concert, which raises about $25,000 each year for the organization.

Jim and Pat moved into University Retirement Community, Davis (URC) three years ago. Both he and Pat have become very involved in URC activities. Pat is on the Resident Council, which is our main link to management. Jim is chair of the Facilities Committee, and this last April directed (and acted in) the entertainment for our "Foundation Dinner" a $125 a plate fundraiser. Everyone had a great time and we raised a lot of money.

Stanley Hutton, P.Eng.

Professor Emeritus of Mechanical Engineering
University of British Columbia
Vancouver, British Columbia, Canada

Dr. Hutton was born in England and completed his undergraduate degree at Nottingham University in 1963. He then worked for Taylor Woodrow (Int) as a site engineer on the construction of a nuclear power station at Wylfa, North Wales responsible for the design and quality control of the concrete used on the job. Subsequently he immigrated to Canada and pursued a MASc degree at the University of Calgary in the field of reinforced concrete design. After a weekend trip to Vancouver he took a job in Vancouver as a structural design engineer with H.A. Simons (Int) involved in the design of pulp and paper mills. Recognizing that a life as a design engineer was not for him he enrolled in a Ph D program at the University of British Columbia in the field of structural mechanics. His Ph D thesis (1970) was concerned with defining a clear mathematical basis for the finite element method. In 1971 he took a position at the University of Adelaide in Australia working on the dynamic response of bridges and tall buildings.

In 1979 he took a position in Mechanical Engineering at the University of British Columbia. Here he established a major research program designed to support the lumber industry of Canada. This work was primarily concerned with the vibration response of wood cutting band and circular saws. Of particular interest are the stability characteristics of such saws and their dependence on blade thickness, blade speed and feed speed. Currently his research is focused on the stability characteristics of guided circular saws.

Dr. Hutton has acted as a consultant to the wood cutting industry for the past 30 years. From 1980 to 2000 Dr. Hutton also acted as a consultant to the Canadian Navy on matters involving ship and submarine vibrations. During this same period Dr. Hutton has acted as an expert witness in approximately 20 law cases pertaining to rotor vibration issues.

Dr. Hutton took early retirement in 2001 from administrative and teaching responsibilities but has continued to support graduate students up to the present. He has wide sporting interests that include: golf, skiing, hiking, and cycling.

Sinniah Ilanko

Associate Professor of Engineering
The University of Waikato
Te Whare Wananga o Waikato
Hamilton, New Zealand

e-mail: Ilanko@Waikato.ac.nz
www URLs: http://sci.waikato.ac.nz/staff/engg/ilanko
http://www.geocities.com/ilanko/vibration.htm
http://www.geocities.com/ilanko/eng.html

Ilanko was born in the north of Sri Lanka (Jaffna) in1957, and according to the common Tamil practice, he does not have/use a family name. Ilanko is his given name and Sinniah is his late father's given name.

He graduated from the University of Manchester (U.K) with a BSc in civil engineering and also obtained an MSc from the same university under the supervision of Dr S.C. Tillman. His move to England at an early age was the result of his late brother Senthinathan's foresight on the Sri Lankan political situation. After working as an assistant lecturer at the University of Peradeniya in Sri Lanka for about two years, he commenced doctoral studies at the University of Western Ontario under the supervision of Professor S.M. Dickinson. Soon after completing his PhD, he worked as a postdoctoral fellow at the UWO for about six months until he joined the University of Canterbury in 1986. He continued his academic career at Canterbury for nearly 20 years, in various positions, as lecturer, senior lecturer and associate professor until he joined the University of Waikato in 2006. He has also served as the Head of Mechanical Engineering Department at Canterbury for a year (2001-2202) and worked as a visiting professor at the Annamalai University (India) and Technical University of Hamburg-Harburg during his study leaves. In 1997, he was awarded the Erskine Fellowship and visited several universities in Australia, Canada, Singapore and the U.K.

His research areas include vibration and stability of continuous systems, numerical modelling and adaptive mechanisms. Since January 2009, he is serving as the Subject Editor for Journal of Sound and Vibration, for analytical methods for linear vibration.

He is also interested in computer-aided learning and has developed and used several interactive lectures and tutorials for teaching Mechanics of Materials and Vibration, as well as computer tutorials and games for learning/teaching Tamil language. He maintains a "vibration resources homepage" (see the second URL above), which at present contains some interactive simulation programs for calculating natural frequencies and modes of some structural elements.

He is married to Krshnanandi and they have two daughters, Kavitha and Tehnuka. Ilanko's birth family is scattered across the globe (Australia, Canada, New Zealand, the U.K. and the U.S.A.) because of the civil war in Sri Lanka.

David Kennedy

Professor of Structural Engineering
Cardiff University
Cardiff, United Kingdom

David Kennedy obtained a First Class Honours degree at the University of Cambridge in 1978 and a PhD in the area of efficient transcendental eigenvalue computation from the University of Wales, Cardiff in 1994.

From 1978 to 1983 he was employed as an Analyst/Programmer for the computer services company Scicon Ltd, where he worked on the development of the Mathematical Programming software SCICONIC/VM. In 1981 he was awarded a 2-year BP Venture Research Fellowship in Non-linear Optimization, supervised by the late Professor Martin Beale.

In 1983 he was appointed as a Research Associate in the University of Wales Institute of Science and Technology, which was merged into Cardiff University in 1988. Working under the supervision of Professor Fred Williams and funded under a collaborative agreement with NASA, he coordinated the development of the space frame analysis software BUNVIS-RG which was released by NASA to US users in 1986/87. Further collaboration with NASA and British Aerospace (now BAE Systems) led to the development and successive releases, starting in 1990/91, of VICONOPT, a buckling and vibration analysis and optimum design program for prismatic plate assemblies. Both of these programs use analysis methods based on the Wittrick-Williams algorithm.

He was appointed to a Lectureship in the Cardiff School of Engineering in 1991, promoted to Senior Lecturer in 2000, Reader in 2005 and Professor in 2009. He has continued to manage the collaborative development of VICONOPT, successfully co-supervising 14 PhD students and holding Research Council grants on parallel computing, aerospace panel optimization, local postbuckling and mode finding. He has visited NASA Langley Research Center several times, and in 2007 he undertook a 6-month secondment to Airbus UK, funded by a Royal Society Industry Fellowship. In 2010 he was appointed as a Deputy Director of the Cardiff School of Engineering with responsibility for staff matters.

As Deputy Director of the Cardiff Advanced Chinese Engineering (ACE) Centre, Professor Kennedy has assisted in the development of research agreements with leading Chinese universities, including Tsinghua University, Dalian University of Technology and Shanghai Jiao Tong University.

Professor Kennedy is the author of 140 publications of which approximately 50% are in refereed journals of international standing.

He lives with his wife Helen and enjoys choral singing, organ playing and hill walking. Having been a keen cross-country and road runner at student level, he has tried to emulate this success as a veteran (50+) by competing 3 times in the Cardiff Half Marathon.

Yukinori Kobayashi

Professor of Human Mechanical Systems & Design
Hokkaido University
Hokkaido, Japan

Yukinori Kobayashi is a professor of the Division of Human Mechanical Systems and Design, Graduate School of Engineering, Hokkaido University. He received all of his degrees in mechanical engineering from Hokkaido University: Bachelor '81, Master '83 and Doctor '86. Professors Toshihiro Irie and Gen Yamada were his supervisors. The title of his dissertation was "Vibration and Response of Thin Shells" in which he analyzed linear vibration problems of a variety of shells using the Ritz method and transfer matrix method. He was a visiting scholar of the Ohio State University from 1991 to 1992 and started on research about the nonlinear vibration of plates and shells under supervision of Professor A. W. Leissa.

His current research interests include the nonlinear vibration of continuous systems and the vibration control of continuous systems. He is a member of the Japan Society of Mechanical Engineers, the Society of Instrument and Control Engineers, the Robotics Society of Japan. He has published over 80 papers on vibration of continuous systems and application of control theory for flexible structures. He teaches vibration engineering and control theory to students of department of mechanical engineering.

He was a member of a ski club when he was a university student and climbed mountains in Hokkaido many times. He now lives in a suburb of Sapporo near the Sapporo Art Park with his family.

Arthur W. Leissa

Professor Emeritus – Ohio State University
Adjunct Professor – Colorado State University

After earning two degrees in mechanical engineering, with a strong interest in machine design, I decided to seek better understanding of stress and deformation of bodies, so I got my Ph.D. in engineering mechanics (from Ohio State University in 1958). My dissertation research was in the theory of elasticity. I then stayed on as a faculty member.

Working part-time for two aircraft companies (Boeing and North American Aviation) made me very interested in vibrations. In 1965 I approached NASA to support me with research funds to collect the literature of the world in plate and shell vibrations, and summarize it in two monographs. They did, and the two books were published in 1969 and 1973. They were out of print for a long time. But in 1993 they were reprinted by The Acoustical Society of America and are currently available from them.

After gaining considerable knowledge in writing the two books, I continued to do extensive research on vibrations of continuous systems, including laminated composites, turbomachinery blades, and three-dimensional problems. Approximately 150 published papers and most of the 40 dissertations I supervised were in this field.

I always intended to update the "Vibration of Plates" monograph. Indeed, more than 20 years ago I had a graduate student collect the more recent literature. This consisted of 1500 additional references dealing with free vibrations. But I never could find the time needed to undertake the writing.

In June of 2001 I formally retired from Ohio State University after having been on its faculty for 45 years. In July 2002 Trudi and I moved to Fort Collins, Colorado, approximately 60 miles north of Denver, and close to the mountains. I am now an Adjunct Professor in the Department of Mechanical Engineering of Colorado State University. Having no serious responsibilities there, I continue my editorial functions with AMR, and still collaborate somewhat with others on research.

My serious interest in the mountains began as a boy, reading books about Mallory and Irvine on Everest, and others. In 1962 when I could first afford it (with a family) I began climbing mountains, which I pursued strongly for decades. Now being 79, I can no longer climb them, but I still enjoy greatly being in the mountains – hiking, skiing, and snowshoeing. They restore one's vitality and one's peace.

In 1995 Mark Ewing, who was in Colorado then, agreed to help me organize the first International Symposium on Vibrations of Continuous Systems, held in 1997 in Estes Park, Colorado. It was well received, and so it has continued every two years in marvelous mountain locales worldwide. I look forward to taking part again, this time in Canada in the mountains of Whistler.

Shinichi Maruyama

Associate Professor of Mechanical System Engineering
Gunma University
Japan

Shinichi Maruyama is an associate professor of the Department of Mechanical System Engineering in Graduate School of Engineering, Gunma University, Japan.

He was born in Takamatsu and had been lived in Chiba, suburb area of Tokyo, until he graduated university. He obtained Master of Engineering and Doctor of Engineering in 1999 and 2002, both from Keio University. Since 2002, he has been taking an academic position in Gunma University and working with Professor Ken-ichi Nagai.

His research interests include nonlinear and chaotic vibrations of mechanical systems, and analyses and experiments on dynamics of thin elastic structures.

He is a member of the Japan Society of Mechanical Engineers. Since 2010, He has been the chair of the Technical Section on Basic Theory of Vibration in the Division of Dynamics, Measurement and Control in JSME.

Luis E. Monterrubio

Postdoctoral Research Fellow
University of California San Diego
San Diego, California, USA

I was born in Mexico City and grew up in Merida, a smaller city in the Yucatan Peninsula, before I started my B. Eng. in Mechanical Engineering at the UNAM (the National University of Mexico located in Mexico City). I graduated in 1996 and worked for an automotive company for almost two years. Then, I moved to Canada to start my M.A.Sc. at the University of Victoria in BC, Canada graduating with a M.A.Sc. in Dec. 1999. In year 2000 I took training in Mechatronics in Japan. During 2001-2005 I went back to work for the automotive industry in Mexico City and Barcelona, Spain. After that I moved to Hamilton, New Zealand to pursue a Ph.D. at the University of Waikato working under the supervision of Dr. Ilanko. During my Ph.D. studies (2006-2009), I solved vibration and buckling problems of structural elements using the Rayleigh-Ritz method together with the penalty method to model constraints. The investigation of the penalty method included adding positive or negative penalty terms to either the elastic stiffness matrix or the geometric stiffness matrix or the mass matrix of the structure. I am currently in my second year as a Postdoctoral Research Fellow at the University of California San Diego (UCSD) working for Dr. Krysl in bioacoustics.

My hobbies are movies, music and sports. After graduating from the University of Waikato I spent a few months training to take part in the 2009 Ironman (triathlon) in Cozumel, Mexico. San Diego is also a fantastic place to train for triathlons and I especially enjoy swimming at La Jolla Cove with seals, leopard sharks, stingrays and dolphins.

Ken-ichi Nagai

Professor of Mechanical System Engineering
Gunma University
Japan

Ken is a professor of the Department of Mechanical System Engineering in Graduate School of Engineering, Gunma University.

He graduated from the national college of technology in Fukushima in 1967. During the student, he received academic interest from the book "Mechanics" written by Den Hartog. He wanted to devote himself to research and education. He received his B. Eng. in 1970 from Ibaraki University. He obtained M. Eng. and Dr. Eng. in 1972 and 1976 from Tohoku University, respectively. Main research subject was nonlinear vibrations of plates and dynamic stability of plates and cylindrical shells, under his supervisor Professor Noboru Yamaki.

Since 1976, he has been taking an academic position in Gunma University. From 1990 to 1991, he was a visiting fellow at Cornell University in U.S.A. During the stay in U.S.A., Professor Leissa in the Ohio State University gave him nice advises in research area. Then, he also visited Technische Hochshule Darmstadt in Germany to the labo. of Professor Hagedorn. Furthermore, he visited Polish Academy of Sciences in Poland.

He is a Fellow of the Japan Society of Mechanical Engineers. He has been a consultant to ministry, local government and automobile industry.

He is now devoted in the research filed of nonlinear vibration, dynamic stability and chaotic oscillations of structure such as beam, arch, plate and shell. Recently, he published the book of "Dynamic system Analysis -Energy Approaches from Structural Vibration to Chaos-" and “Dynamics of Nonlinear Systems –Introduction to Analysis of Nonlinear Phenomena-”.

His personal interests include hiking. He feels spiritual happiness as walking in fields and facing to new phenomena of chaotic vibration generated from thin elastic structures.

Yoshi (Yoshihiro Narita)

Vice Dean of Faculty of Engineering
Hokkaido University
Sapporo, Japan

First of all, I would like to start by expressing my deepest thanks to the friends in ISVCS community. After the worst earthquake took place on 11th March in Japan, I received many e-mails to worry about my family and people in Japan. Fortunately, our city Sapporo is far enough to avoid the damage due to the earthquake itself and my family was all safe. Please pray for Japan so that we can overcome the devastating tsunami damages and settle down the nuclear crisis still going on.

As for myself, seven years have passed since I moved to Hokkaido University (HU), and I am still enjoying teaching young students and working with graduate students who are capable of excellent research studies. The only problem is that I have quite limited time for research now, since I became Vice Dean of Faculty of Engineering.

I started my research on vibration of continuous systems when I was a graduate student under adviser Prof.Irie of HU in 1976, and had a chance to study one year in 1978-1979 under Prof.Leissa at the Ohio State University. I have kept the same topic thirty years. I combine the vibration and buckling of plates and shells with optimization.

Recently, I was pleased with a small good news. My university library is promoting the electronic documentation from publications by the researchers in the university. When they sent me the number of downloads of my doctoral dissertation "Free Vibration of Elastic Plates with Various Shapes and Boundary Conditions", I realized that my dissertation was downloaded 243 times, and 93 percent is from outside Japan, including 151 times from United States. If you have time to kill, please access: URI: http://hdl.handle.net/2115/32630

I am very happy that I could have joined all the ISVCS's, including ISVCS-I(Estes Park, USA), II(Grindelwald, Switzerland), III(Grand Teton, USA), IV(Keswick, UK), V(Berchtesgarden, Germany), VI (Squaw Valley, USA) and VII(Zakopane, Poland). These visits are full of good memories. In the present ISVCS-8, I look forward to meeting old and new friends in the research community of applied mechanics.

Let's enjoy!

Francesco Pellicano

Associate Professor of Mechanical and Civil Engineering
University of Modena and Reggio Emelia
Reggio Emelia, Italy

Francesco Pellicano was born in Rome, Italy on 1966. He received a M.S. degree in Aeronautical Engineering in 1992 and Ph.D. in Theoretical and Applied Mechanics in 1996, both at the University of Rome "La Sapienza," Dept. of Mechanics and Aeronautics.

He was Researcher at the University of Modena and Reggio Emilia, Faculty of Engineering, Dept. of Mechanical and Civil Engineering, 1996-2003.

He is currently Associate Professor at the same University since January 2004.

He was involved in investigations concerning: nonlinear vibrations of structures; nonlinear normal modes; axially moving systems; nonlinear vibration of shells with fluid structure interaction; gears modeling; non-smooth dynamics; Chaos; Nonlinear Time Series Analysis; Forecasting Methods in Oceanography.

He cooperated with Prof. Vestroni, Prof. Sestieri and Prof. Mastroddi of the University of Rome "La Sapienza" and with: Prof. Païdoussis (Mc Gill Univ. Canada); Prof. Vakakis (Univ. of Illinois at Urbana Champaign; recently National Technical Univ. of Athens, Greece); Prof. Amabili (Univ. of Parma, Italy).

The teaching activity regards: Vibrations of Discrete and Continuous Systems; Signal Processing; Machine Theory and Machinery.

He was coordinator of an international NATO CLG-Grant project on Nonlinear Dynamics of Shells with Fluid Structure Interaction and was the local coordinator of an Italian project on Shells Vibrations.

His research activity regards also industrial problems; he cooperated for research and consultancies with several companies about: vehicle stability; experimental vibrations; clutch instabilities and failures.

He was reviewer for the following international journals: SIAM Journal of Applied Mathematics, Nonlinear Dynamics, ASME Journal of Vibration and Acoustics, J. of Solids and Structures; J. of Sound and Vibration, Computer Methods in applied Mechanics and Engineering, Int. J. of Systems Science; and reviewer for the foundations: FCAR (Fonds pour la Formation de Chercheurs et l' Aide à la Recherche) Québec, CANADA; Natural Science and Engineering Research Council of Canada.

He is Associate Editor of the journals: *Mathematical Problems in Engineering, Hindawi; Chaos, Solitons and Fractals, Elsevier; moreover,* he takes part *to* the international advisory editorial board of the journal: *Communications in Nonlinear Science and Numerical Simulation, Elsevier.*

He published a Book, 35 Journal papers and more than 60 conference papers.

Wolfgang Seemann

Chair for Dynamics and Mechanatronics
Institut für Technische Mechanik, Universität Karlsruhe (TH)
Karlsruhe Institute of Technology
Karlsruhe, Germany

I was born on 31 March, 1961 in Keltern (Germany, Baden-Württemberg). After school I studied mechanical engineering at the University of Karlsruhe from 1980 to 1985. After civil service (1985-1987) I began as a PhD student working at the Institute of Applied Mechanics at the University of Karlsruhe. The PhD was finished in 1991 with a thesis on 'Wave propagation in rotating or prestressed cylinders'. In 1992 I joined the group of Peter Hagedorn at Darmstadt University of Technology to work in a post-doc position until 1998 when I got a professorship on machine dynamics in Kaiserslautern. In 2003 I got an offer to go back to the University of Karlsruhe on the chair of Applied Mechanics.

My previous and current research interests are in ultrasonic motors, nonlinear vibration, ultibody

dynamics, vibration of continuous systems, active materials, nonlinear phenomena in piezoelectric materials, humanoid robots, dynamics of human motion, mechatronic systems, road-vehicle interaction, rotor dynamics and wave propagation.

Besides I am responsible for the French-German cooperation of our university.

Anand V. Singh

Professor of Mechanical and Materials Engineering
University of Western Ontario
London, Ontario, Canada

I was born on July 05, 1948 in the village Rahimpur of Monghyr district, Bihar, India. I completed my elementary and secondary educations from Monghyr Zila School and was directly admitted to the Bihar Institute of Technology in Sindri. I graduated in 1968 with B.Sc. Engineering and joined the school of graduate studies at the University of Ottawa a year later. I began my research work with the derivation of the constitutive equations from the first principles for the free axisymmetric vibration of sandwich spherical shells under the noble supervision of Professor S. Mirza and subsequently received M. A. Sc. and Ph. D. degrees. These equations were developed in the spherical coordinate system and had solutions in Legendre functions of complex order which in itself became a research project as I had to derive many new equations and also to program those. During this study I also used energy methods to deduce the equations of motion for the free vibration of isotropic and sandwich plates and shells.

After the Ph. D., I joined Defence Research Establishment Suffield (DRES) near Medicine Hat Alberta and worked there as a defence scientist from January 1978 to April 1981. Following this I accepted a design-engineer position in the Civil Design Department of Ontario Hydro in Toronto and remained there until December 1984. There I mainly worked on the finite element analyses of large nuclear power plant structures and also on the seismic response of such structures. I came to the University of Western Ontario to teach machine component design and the finite element methods. Professor Stuart Dickinson was the chair of the Mechanical Engineering at that time and he is the one who hired me. Over the years at UWO, I taught graphics and engineering drawings, dynamics, kinematics and dynamics of machines, the theory of modern control systems, theories of plates and shells in addition to the two courses mentioned above. I worked with some remarkable students in the field of computational solid mechanics dealing with the linear and nonlinear vibrations of plates and shells. Currently, my research activities are involved with the vibrations of nano-scale structures and piezoelectric embedded composites.

On the personal note, I got married to Bimla in March of 1968 and have two adult children, the son Bidhi and daughter Shikha. Both are graduates of the University of Western Ontario and also have education from the University of Michigan and Michigan State University. Bimla and I attended all of the ISVCS except the very first one. We like to travel; have camped in the past with our children; enjoy walking in the park and on the beaches; and wish to live lives to the fullest as long as there is wellness.

Gottfried Spelsberg-Korspeter

Research Assistant
Technische Universität Darmstadt
Darmstadt, Germany

On August 13th 1978 I was born in Dortmund Germany. I grew up in Dortmund, Düsseldorf and Ludwigsburg where I finished high-school (Abitur) in 1998. After completion of the compulsory military service I started studying at TU Darmstadt in 1999.

In 2001 I finished my preliminary diploma in industrial engineering and in mechanical engineering and decided to pursue my mechanical interests in the applied mechanics department with main focus on dynamics. Taking part in an exchange program of the industrial engineering department I spend the fall semester 2002 and the spring semester 2003 at the University of Illinois at Urbana Champaign where I mainly worked in the area of operations research.

In 2004 I finished my masters degree in applied mechanics with a thesis related to mechanical modelling of ultrasonic motors and went back to the University of Illinois to write my master thesis in industrial engineering in the area of operations research. After completion I joined the research group of Professor Hagedorn in January 2005. In 2007 I completed my Ph.D. work with a thesis on self excited vibrations in gyroscopic systems. Since then I have been teaching classes on nonlinear vibrations, multibody dynamics and vibrations of continuous systems for masters students and engineering mechanics for bachelor students.

My hobbies are hiking, climbing and other sports.

Andrew Watson

Lecturer of Aerospace Structures
Department of Aeronautical and Automotive Engineering
Loughborough University, United Kingdom

Andrew Watson obtained an Upper Second Class degree from Cardiff University in 1993 and a PhD in the stability analysis and optimisation of prismatic thin walled structures in 1998.

Since then he stayed at Cardiff for five further years and worked as a postdoctoral researcher on two EPSRC funded projects. The first of these was in the initial and advanced postbuckling behaviour of optimised aerospace panels. This work was collaborative with the University of Bath and Airbus (UK). Throughout his PhD and first research project he has made contributions to and extended the computer programme VICONOPT, which is used by Airbus and NASA for the analysis and optimisation of aerospace panels. His work in this area has resulted in him now being a senior member of the American Institute of Aeronautics and Astronautics.

His second EPSRC research project saw him search for inter disciplinary applications of the Wittrick-Williams algorithm. He identified the area of spectral theory in mathematics and has published, with his collaborators, two Royal Society Series A journal publications.

After leaving Cardiff at the end of 2003 Andrew joined the Department of Aeronautical and Automotive Engineering at Loughborough University as the Lecturer in Aerospace Structures. His current research covers buckling and postbuckling of aerospace panels; vibration of beams and quantum graph theory. These areas are all eigenvalue problems and in general can be solved by using the Wittrick-Williams algorithm.

Andrew regularly reviews papers submitted to a wide range journals for publication. He has published over 30 journal and conference papers.

In his spare time he likes to keep up with current affairs and to keep fit he enjoys cycling and open water swimming.